Technical Review

No. 3 · 1987

Windows to FFT Analysis (Part I)

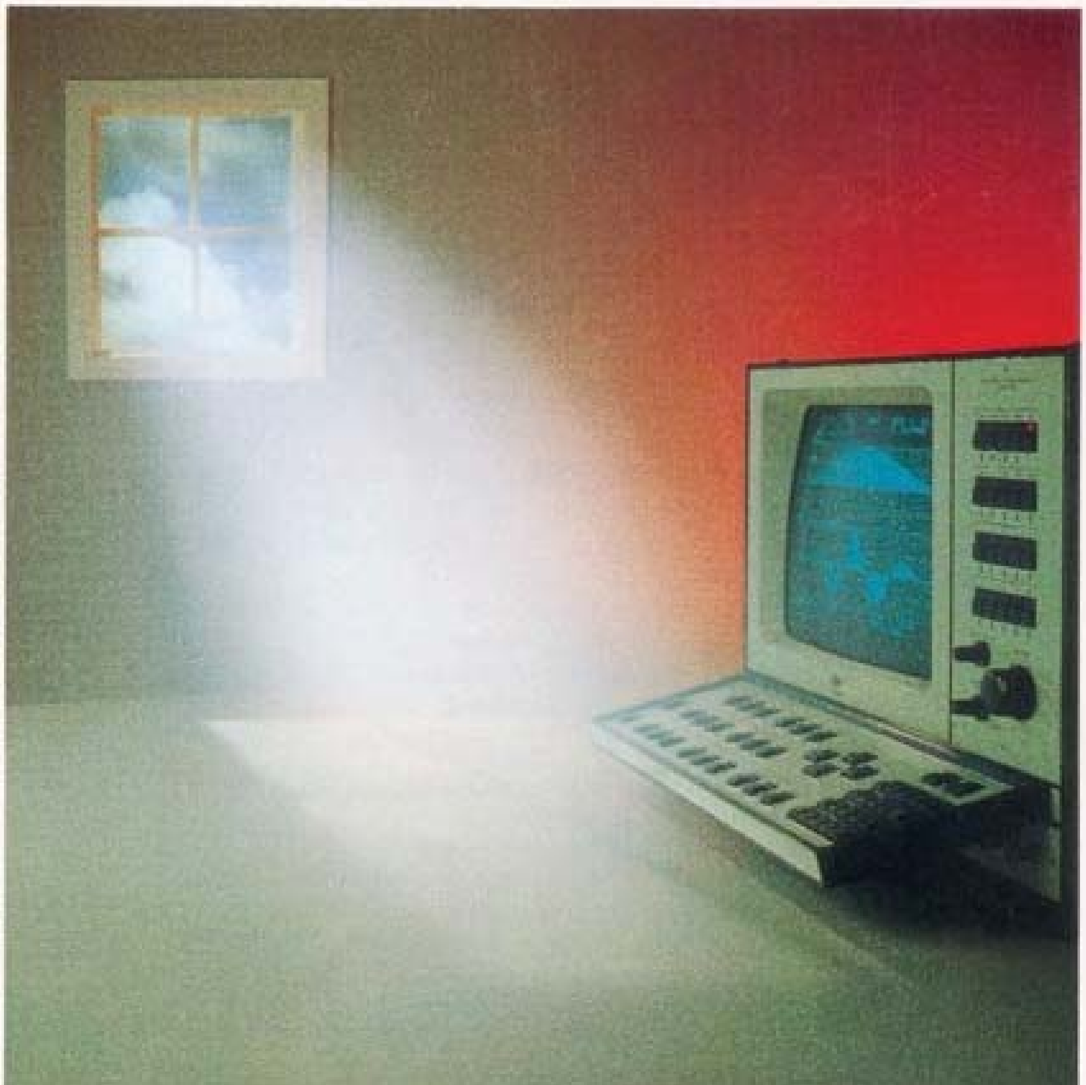

Brüel & Kjær

Previously issued numbers of Brüel & Kjær Technical Review

2-1987	Recent Developments in Accelerometer Design
	Trends in Accelerometer Calibration
1-1987	Vibration Monitoring of Machines
4-1986	Field Measurements of Sound Insulation with a Battery-Operated Intensity Analyzer
	Pressure Microphones for Intensity Measurements with Significantly Improved Phase Properties
	Measurement of Acoustical Distance between Intensity Probe Microphones
	Wind and Turbulence Noise of Turbulence Screen, Nose Cone and Sound Intensity Probe with Wind Screen
3-1986	A Method of Determining the Modal Frequencies of Structures with Coupled Modes
	Improvement to Monoreference Modal Data by Adding an Oblique Degree of Freedom for the Reference
2-1986	Quality in Spectral Match of Photometric Transducers
	Guide to Lighting of Urban Areas
1-1986	Environmental Noise Measurements
4-1985	Validity of Intensity Measurements in Partially Diffuse Sound Field
	Influence of Tripods and Microphone Clips on the Frequency Response of Microphones
3-1985	The Modulation Transfer Function in Room Acoustics
	RASTI: A Tool for Evaluating Auditoria
2-1985	Heat Stress
	A New Thermal Anemometer Probe for Indoor Air Velocity Measurements
1-1985	Local Thermal Discomfort
4-1984	Methods for the Calculation of Contrast
	Proper Use of Weighting Functions for Impact Testing
	Computer Data Acquisition from Brüel & Kjær Digital Frequency Analyzers 2131/2134 Using their Memory as a Buffer
3-1984	The Hilbert Transform
	Microphone System for Extremely Low Sound Levels
	Averaging Tiroes of Level Recorder 2317
2-1984	Dual Channel FFT Analysis (Part II)
1-1984	Dual Channel FFT Analysis (Part I)
4-1983	Sound Level Meters - The Atlantic Divide
	Design principles for Integrating Sound Level Meters
3-1983	Fourier Analysis of Surface Roughness
2-1983	System Analysis and Time Delay Spectrometry (Part II)
1-1983	System Analysis and Time Delay Spectrometry (Part I)
4-1982	Sound Intensity (Part II Instrumentation and Applications)
	Flutter Compensation of Tape Recorded Signals for Narrow Band Analysis

(Continued on cover page 3)

Technical Review

No. 3 · 1987

Contents

Use of Weighting Functions in DFT/FFT Analysis (Part I) …....... 1
by Svend Gade and
Henrik Herlufsen

Signals and Units 29
by Svend Gade and
Henrik Herlufsen

Use of Weighting Functions in DFT/FFT Analysis (Part I)

by Svend Gade and
Henrik Herlufsen

Abstract

This article demonstrates how the analogy between DFT/FFT (Discrete Fourier Transform/Fast Fourier Transform) analysis and filter analysis (analogue or digital) can be used to better understand the applications of different weighting functions used in DFT/FFT.

The filter characteristics of the most commonly used weighting functions (also called windows) are illustrated and discussed with respect to their use in various practical applications of system and signal analysis.

The mathematical formulations of the analogy as well as rigorous details of the article will be given in the Appendices in Part II of this article to be published in Technical Review No. 4-1987.

Sommaire

Cet article démontre comment l'analogie entre les analyses FFT ou DFT (Fast Fourier Transform et Discrete Fourier Transform) et les analyses par filtres (analogiques ou numériques) peut être utilisée pour mieux comprendre les applications des différentes pondérations utilisées en FFT ou DFT.

Les caractéristiques des filtres les plus couramment utilisés pour les fonctions de pondération (aussi appelées fenêtres) sont illustrées, et discutées en fonction de diverses applications pratiques, que ce soit en analyse de signaux ou de systèmes.

Les formules mathématiques de cette analogie, ainsi que les points de détail de cet article, seront donnés en appendice dans la seconde partie de ce même article, qui paraîtra dans Technical Review No.4-1987.

Zusammenfassung

Dieser Artikel demonstriert, wie die Analogie zwischen DFT/FFT (Discrete Fourier Transformation/Fast Fourier Transformation) -Analyse und Filteranalyse (analog und digital) benutzt werden kann, um die Anwendung verschiedener Bewertungsfunktionen (auch Zeitfenster) bei der DFT/FFT besser zu verstehen.

Die Filtercharakteristiken der gebräuchlich angewendeten Bewertungsfunktionen werden illustriert und bezüglich ihrer Anwendung in der System- und Signalanalyse diskutiert.

*Die mathematische Formulierung der Analogie sowie weitere Einzelhei-*ten werden im Appendix des zweiten Teils dieses Artikels beschrieben, der im Technical Reviev Nr. 4-1987 erscheinen wird.

Introduction

Whenever frequency analysis is performed, it is desirable that a choice of filter type should be available to suit the specific application. In acoustics there is a long tradition for using octave and one third octave-band filters, with standardized filter characteristics. For vibration analysis, narrow-band spectra based on constant-bandwidth analysis are usually preferred.

FFT/DFT

FFT/DFT (Fast Fourier Transform/Discrete Fourier Transform) analyzers produce narrow-band line spectra, in which each line represents the output of a filter/detector centered at the frequency of the line. The shape of the filter is determined by the chosen *weighting function.* The weighting function, also known as the *window,* is applied to the data record to be analyzed (i.e. the data is multiplied by the weighting function). The data record (block) is T s long and the filters are separated by $\Delta f = {}^{1}/T$ Hz. This filter spacing Δf is also called the line spacing, since the spectrum appears as a line spectrum on the analyzer. All the filters have the same characteristic on a linear frequency axis, which means that we obtain a constant bandwidth analysis with an FFT/DFT analyzer.

The analogy between filter analysis and FFT/DFT analysis is discussed in detail in **Appendix A** (found in Part II of this article). See also Refs. [1,2,4,7,8] which have a common approach for characterizing weighting functions.

In this article, the weighting functions and their spectra are treated as continuous, rather than discrete functions. This is to simplify the expressions and make interpretation easier.

Weighting Functions

The B & K Dual Channel Signal Analyzers Type 2032 and 2034 offer a choice of seven different weighting functions. The characteristics of four of these windows are fixed and three have user-definable characteristics.

The availability of different windows provides a choice of using filters with different characteristics in terms of *bandwidth, band-pass ripple* and *selectivity.*

The benefit of having different windows/filters available is that the user can select an optimum filtershape for a given application. The correct choice can minimize the measurement errors due to the fact that no filter is ideal.

Filter Analysis

A filter is a device that transmits a signal in such a manner that its output is the result of convolving the input signal with the impulse response function $h(t)$ of the filter. In the frequency domain this corresponds to a (complex) multiplication of the frequency spectrum of the signal, by the frequency response function of the filter $H(f)$. The filter is characterized by its impulse response in the time domain, and by its frequency response in the frequency domain. Both characterizations contain the same information about the filter and are related via the Fourier Transform:

$$H(f) = F\{h(t)\} \qquad (1)$$

The transmitted signal will have an amplitude spectrum equal to the product of the input signal amplitude spectrum and the amplitude of the filter frequency response $|H(f)|$ (the filter amplitude characteristic). Consequently the power spectrum, (or rather the mean-square spectrum) of the transmitted signal, is the product of the input power spectrum and the squared filter amplitude characteristic $|H(f)|^2$. This is illustrated in Fig. 1.

The output of the filter is fed to a detector which detects the power (the mean square) of the output signal, represented by the area under the amplitude spectrum squared, shown in Fig. 1 as the dotted curve. The square root of this, the root mean square (RMS), is the estimate of the amplitude spectrum of the input signal in that filter bandwidth. Frequency analysis is then performed by sweeping, or stepping, the filter through the frequency range of interest, or by using a bank of parallel filters. For more details see Ref. [1].

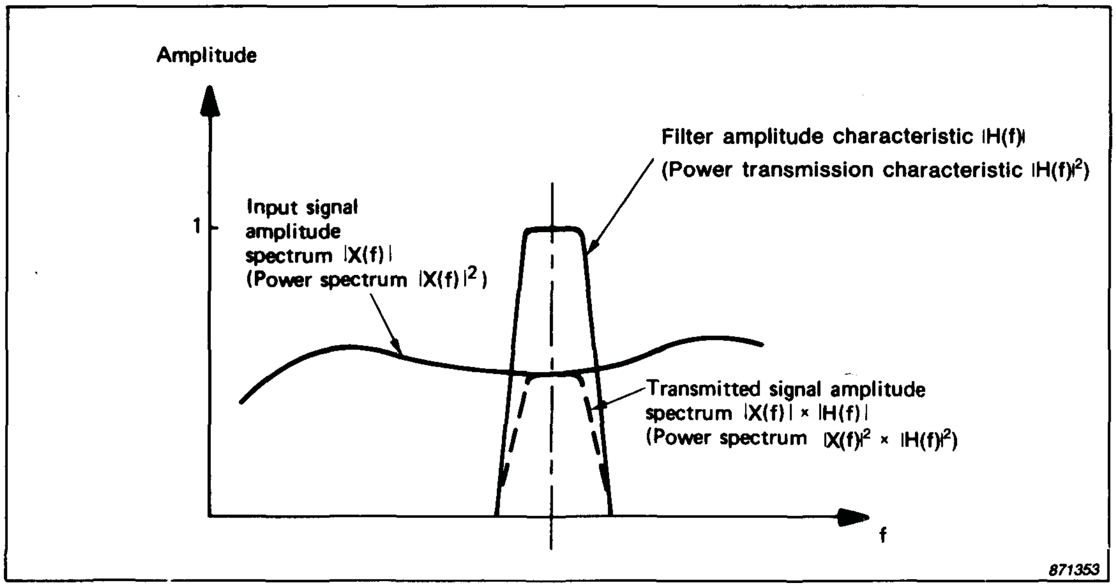

Fig. 1. Amplitude spectra for a filtered signal

Filter Characteristics

A filter is generally characterized in the frequency domain by four parameters; *centre frequency, bandwidth, ripple* and *selectivity.*

An ideal bandpass filter will transmit all components lying within its passband, of width B Hz, and completely attenuate all components at other frequencies (see Fig. 2).

The Centre Frequency f_o of a filter is defined as either the geometric, or the arithmetic mean value of the lower and upper frequency limits. Geometric mean is used for constant percentage bandwidth filters. Arithmetic mean is used for constant-bandwidth filters (see Fig. 2). The centre fre-

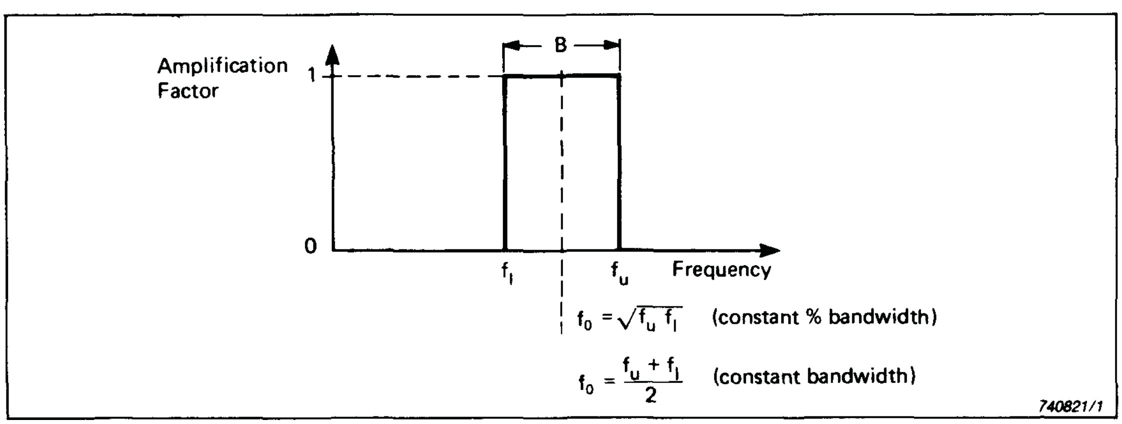

Fig. 2. An ideal filter

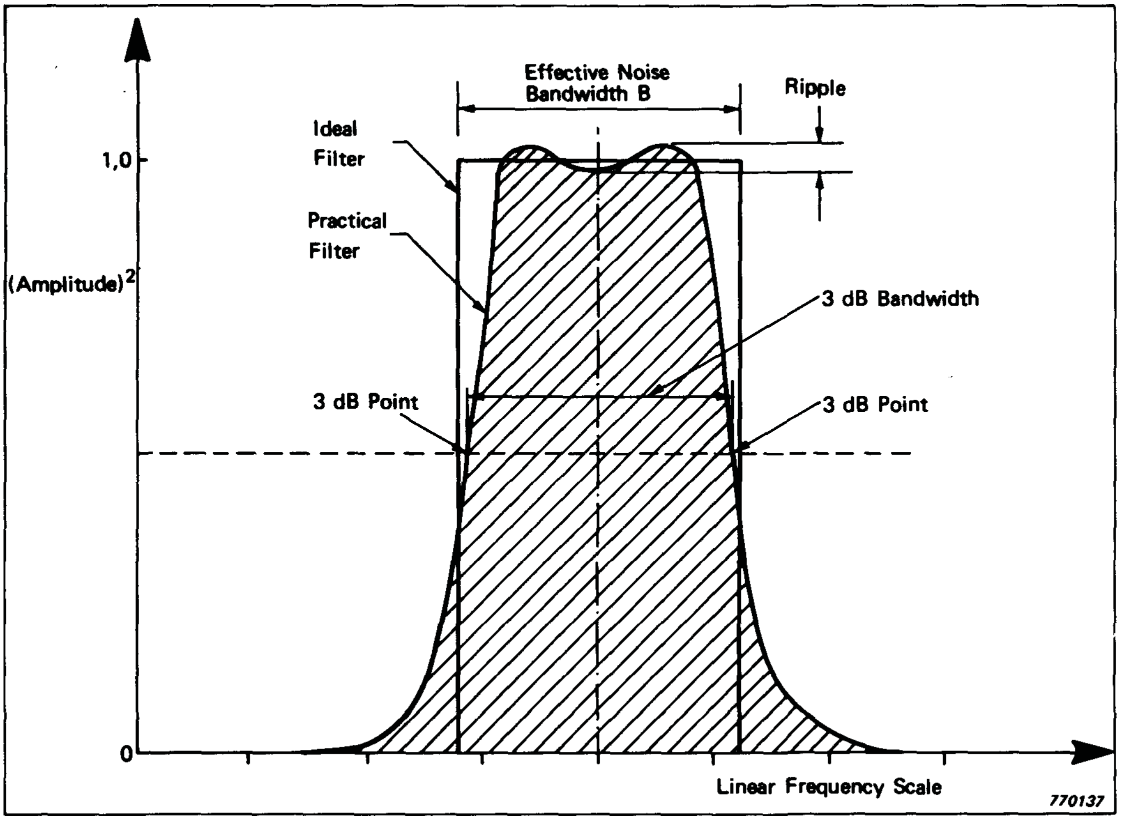

Fig. 3. Practical vs. ideal filter

quencies for DFT/FFT analysis are given by the choice of frequency range, or span, and the number of filters/lines in the analysis.

Practical filters deviate from ideal filters in several ways as illustrated in Fig. 3. The so-called *effective noise bandwidth* of a filter is defined as the width of an ideal filter which, with an identical reference-amplitude gain, would transmit the same power from a white noise source.

Another bandwidth associated with a filter is its 3 dB bandwidth, this is the difference in Hz or Rad/s between the half power points of the amplitude characteristic (i.e. the points where the level is 3 dB below the reference amplitude level). In most practical filters, the difference between the 3 dB bandwidth and the effective noise bandwidth is relatively small.

The 3 dB bandwidth is usually specified, in preference to the noise bandwidth, because it can easily be measured using a variable sine generator.

The bandwidth of a filter gives information about its ability to separate components of similar amplitudes, and thus determines the resolution of the analysis.

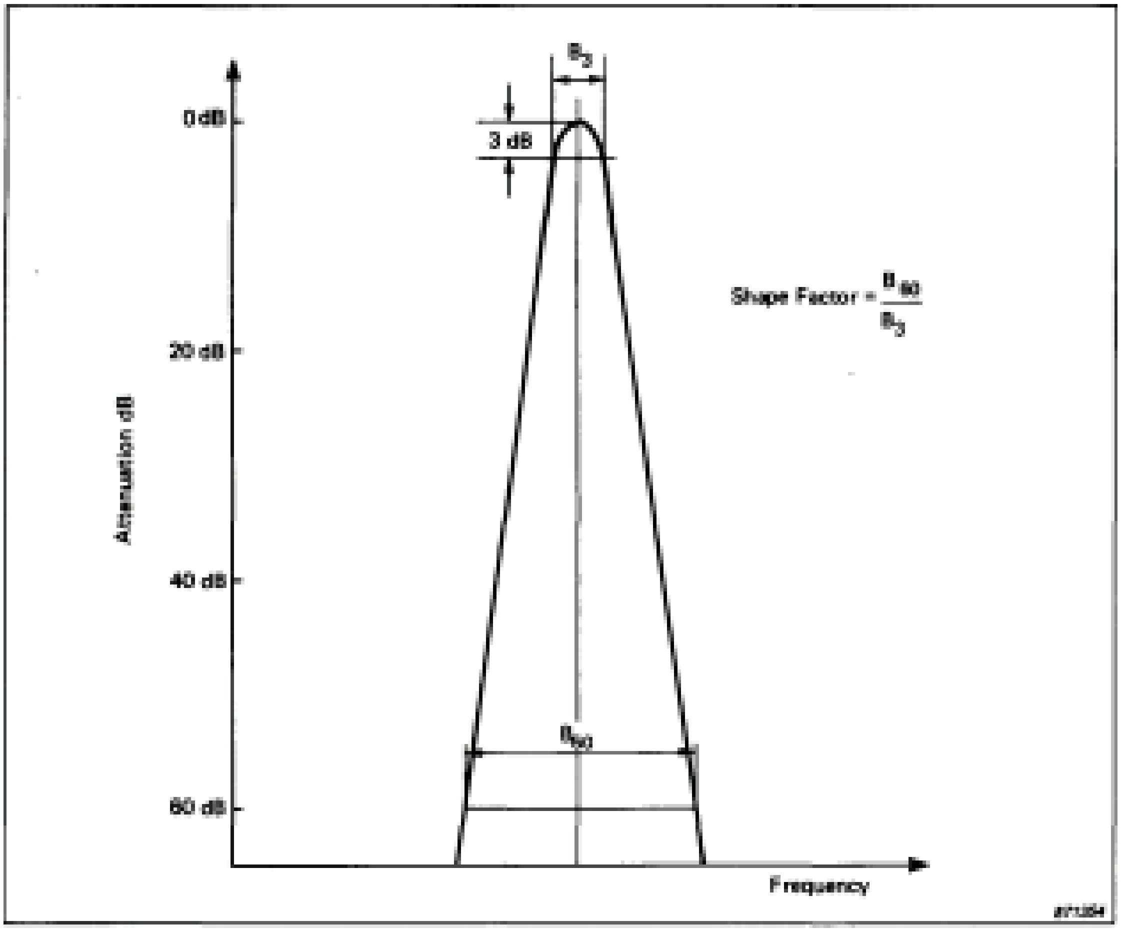

Fig. 4. Shape factor

Selectivity is a descriptor which indicates the ability of a filter to separate components of widely different levels. The basic parameter for selectivity is the *shape factor,* the ratio of the filter bandwidth at an attenuation of 60 dB, to its 3 dB bandwidth. Shape factor is normally used for constant-bandwidth filters, which have symmetrical characteristics on a linear frequency scale (see Fig. 4). For constant-percentage-bandwidth filters, which have symmetrical characteristics on a logarithmic frequency scale, it is more usual to use *octave selectivity,* which gives the attenuation of the filter characteristic one octave on either side of the centre frequency.

The amount of ripple in the passband of the filter, characterises the uncertainty with which the amplitude of a given signal can be determined (see Fig. 3).

Windowing

DFT/FFT analysis is made on blocks (time records) of data i.e. each DFT/FFT calculation is a transform of a time record of finite length. The signal is thus limited (truncated) by a the time-window. What happens to the signal before, and after, the time-window is not observed by the analyzer. Individual window types will emphasize parts of the signal in different ways, and thus give different results (spectra).

Time Windows

	Max. Amplitude	Min. Amplitude	Effective Duration
Rectangular	1	1	1 · T
Hanning	2	0	0,375 · T
Kaiser-Bessel	2,48	0	0,291 T
Flat Top	4,64	-0,33	0,175 · T

Table I. Time domain characteristics of weighting functions

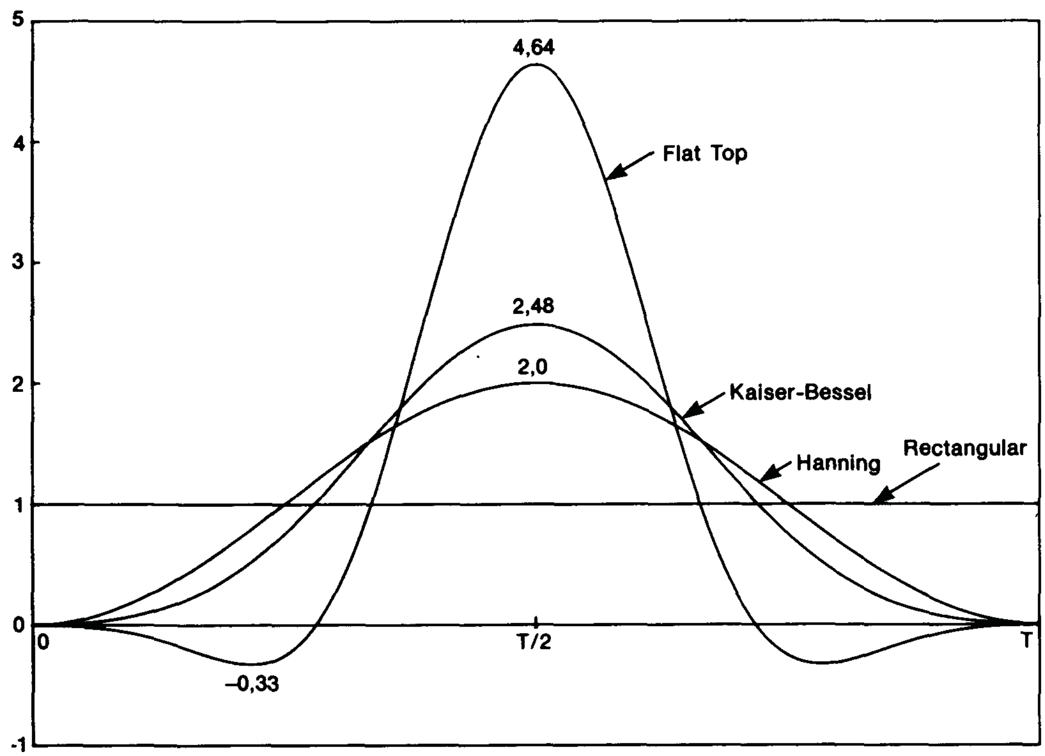

Fig.5. Rectangular, Hanning, Kaiser-Bessel and Flat Top weighting functions found in 2032/34

Table 1 lists and compares the various window functions (shown in Fig. 5) in the time domain, with respect to the following parameters:

1. Max. amplitude
2. Min. amplitude
3. Effective duration

Table 2 lists and compares the same window functions in the frequency domain, with respect to the following parameters:

1. Effective noise bandwidth
2. 3 dB bandwidth
3. Ripple in the passband. (The passband is defined here as the bandwidth A/centered around the centre frequency f_0. This is also the band between the crossover points of the filter with its two adjacent filters.)
4. Highest sidelobe
5. Sidelobe fall-off rate
6. 60 dB bandwidth
7. Shape factor

Parameters (4), (5), (6) and (7) are all used to characterize the selectivity of the window.

Window	Noise Band-width	3 dB Band-width	Ripple	Highest Sidelobe	Sidelobe Fall-Off rate per Decade	60 dB Band-width	Shape Factor
Rectangular	Δ f	0,89 A f	3,92 dB	-13,3 dB	20 dB	665 Δf	750
Hanning	1,5 Δf	1,44 Δf	1,42 dB	-31,5 dB	60 dB	13,3 Δf	9,2
Kaiser-Bessel	1,80 Δf	1,71 Δf	1,02 dB	-66,6 dB	20 dB	6,1 Δf	3,6
Flat Top	3,77 Δf	3,72 Δf	0,01 dB	-93,6 dB	0 dB	9,1 Δf	2,5

Table 2. Frequency domain characteristics of weighting functions

BT_{eff} per record	0%	50%	75%
Rectangular	1	0,660	0,363
Hanning	1	0,947	0,520
Kaiser-Bessel	1	0,989	0,628
Flat Top	1	1,000	0,995

T01596GB0

Table 3. Effective BT-product per filter, per record when overlap analysis is performed (theoretical values)

Table 3 lists the effective BT-product per filter per record, when 0%, 50% and 75% overlap is used in the analysis. The values in Table 3 have been verified experimentally. See **Appendix D.**

Formulae for calculating some of these parameters are given and discussed in **Appendix B.**

Rectangular Weighting

The Rectangular weighting, also called *Flat* or *Boxcar weighting,* is actually no weighting at all on the finite time record. It is defined as:

$$w(t) = 1 \quad \text{for} \quad 0 \leqq t < T$$

$$w(t) = 0 \text{ elsewhere} \qquad (2)$$

where T is equal to the record length (see Fig. 5).

The filter characteristic given by the integral Fourier transform of the Rectangular window is shown in Fig. 6. The filter has a mainlobe, which is twice the width of the line/filter spacing Δf, and an infinite number of

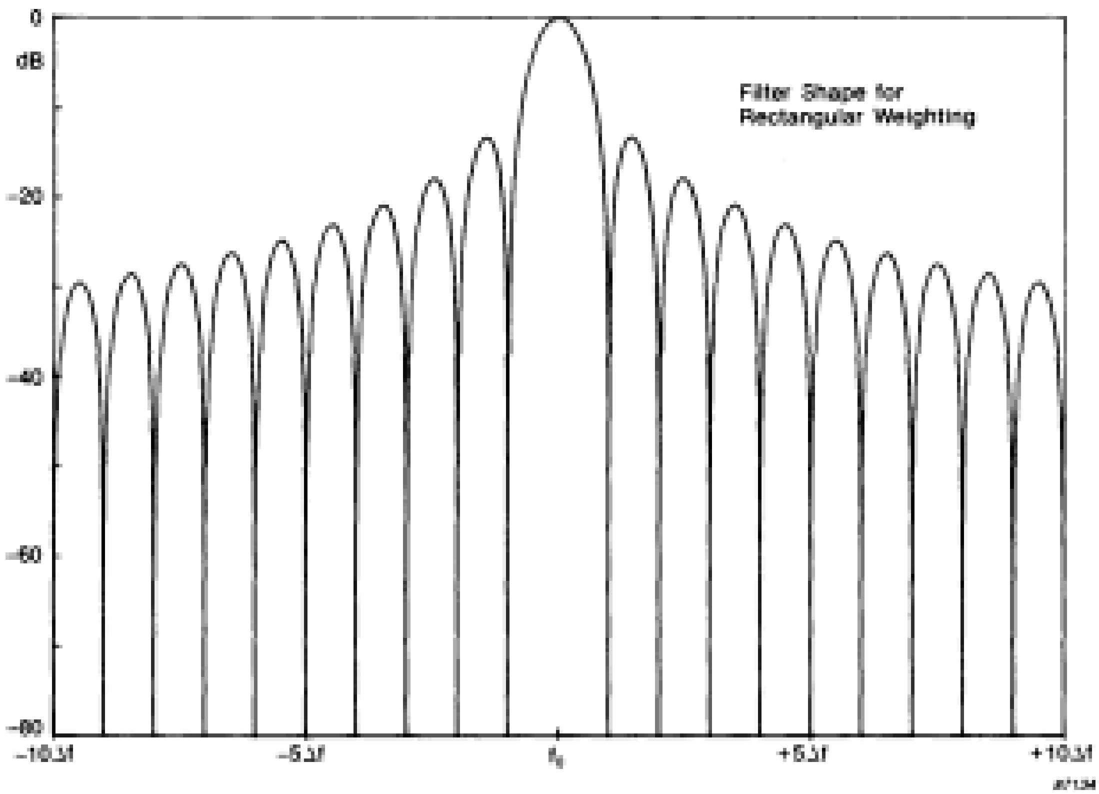

Fig. 6. Filter shape of the Rectangular Weighting function

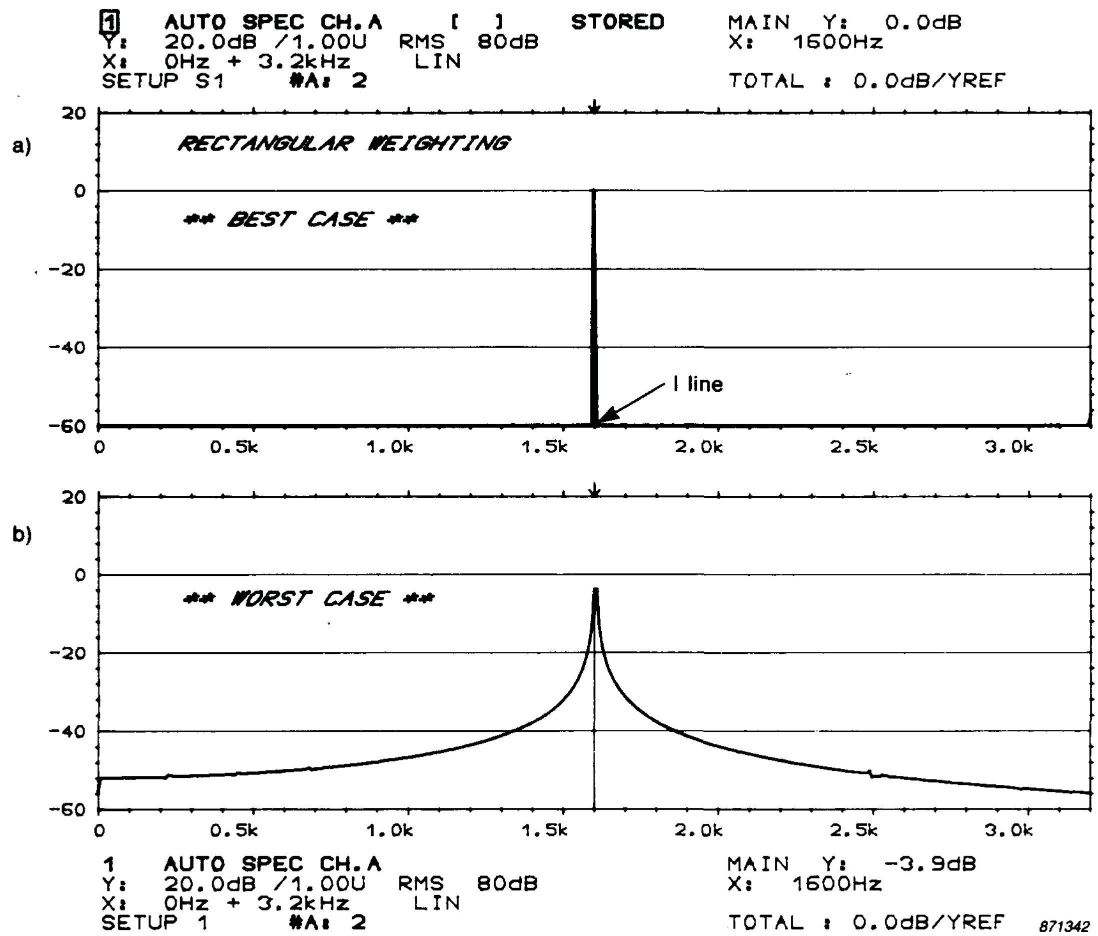

Fig.7. The "best case" and the "worst case", when analysing a sinusoid using Rectangular Weighting function

sidelobes with widths equal to the line/filter spacing. For the analysis of deterministic/harmonic signals this is a poor filter because it has:

1. A very poor selectivity, due to the wide 60 dB bandwidth.
2. A relatively large (3,9 dB) ripple in the passband.

At first sight, it would seem that the Rectangular window is a bad choice of window due to its poor filter characteristics.

On the other hand, if we analyze a sinusoid which has a frequency that coincides with the centre frequency of one of the filters we have the special, optimal, or "best case", situation where the frequency also coincides with a zero amplitude point for all of the other filters. Thus only one line, with the correct amplitude, will be displayed (see Fig. 7.a).

The "worst case" is when the frequency of the sinusoid coincides with a crossover frequency between two adjacent filters. The output of both filters will then be 3,9 dB too low, while all the other filters will give an output which corresponds to the maximum level in one of the sidelobes (see Fig. 7b). This effect is called leakage because energy, or power, appears to leak into all the filters/lines, instead of being concentrated into only one filter. Note, however, that the sum of the power/energy in all the filters will give the correct value (calculated and shown as Total in the cursor auxiliary information field, see Fig. 7a and b).

The practical use of the Rectangular window is for analyzing transients with shorter durations than the record length *T*. Due to the flat characteristic in the time domain all parts of the signal are equally weighted. In the frequency domain the bandwidth of the signal is greater than the bandwidth of the filters, because the signal is shorter than T, and therefore the filter characteristic will have no influence on the calculated spectrum of the transient signal.

When the spectral amplitude variations of a random signal are less than the variations of the filtershape, Rectangular weighting may be used for the analysis. This is exemplified in Fig. 10 a for a narrow band random signal, where only the relatively flat centre part of the spectrum is unaffected by the filter shape.

As explained, and shown in Fig. 7, the Rectangular window can only be used for analysis of sinusoids when their frequencies coincide exactly with the centre frequencies of the filters.

One such application is *order tracking,* used in the analysis of run-up/coast-down of machines, see Refs. [1, 2 and 11]. In this case external sampling is used to keep the sampling frequency in synchronism with the shaft speed. All components harmonically related to the shaft speed can then be arranged to coincide with centre frequencies of the filters (lines). It may be argued that Hanning weighting is a better choice when the speed variations are large. In this situation it may be difficult to track the signal, and the Rectangular weighting function would give more apparent leakage than the Hanning weighting function.

An application where Rectangular weighting is a "must", is in system analysis using a pseudo-random excitation signal, see Ref. [9]. A pseudo-random signal is a periodic signal with its period length adjusted to the record length *T* of the analysis. All the components of the pseudo-random signal will therefore coincide with the centre frequencies of the filters (lines) and the analysis will be free of leakage assuming Rectangular weighting is used (optimal situation or "best case").

Hanning Weighting

The Hanning weighting as shown in Fig. 5 is a smooth window function which is defined as:

$$w(t) = 1 - \cos 2\pi t/T$$
$$= 2\sin^2 2\pi t/T \quad \text{for } 0 \leqq t < T$$

$$w(t) = 0 \quad \text{elsewhere} \tag{3}$$

As can be seen, the window is a sum of a Rectangular window and one period of a cosine of equal amplitude (i.e. the sum of a DC and an AC component). The Hanning window can also be described as one period of a sine squared. In literature the Hanning window is often defined as a cosine squared, which is the case if the window starts at - $T/2$ rather than at time zero.

The window is shown in Fig. 5 and its filter characteristic in Fig. 8. The mainlobe is 4 Δf, double the width of the Rectangular window. The number of filters/lines excited will always be greater than or equal to three. The first sidelobe is much more attenuated, and the fall-off rate is much faster,

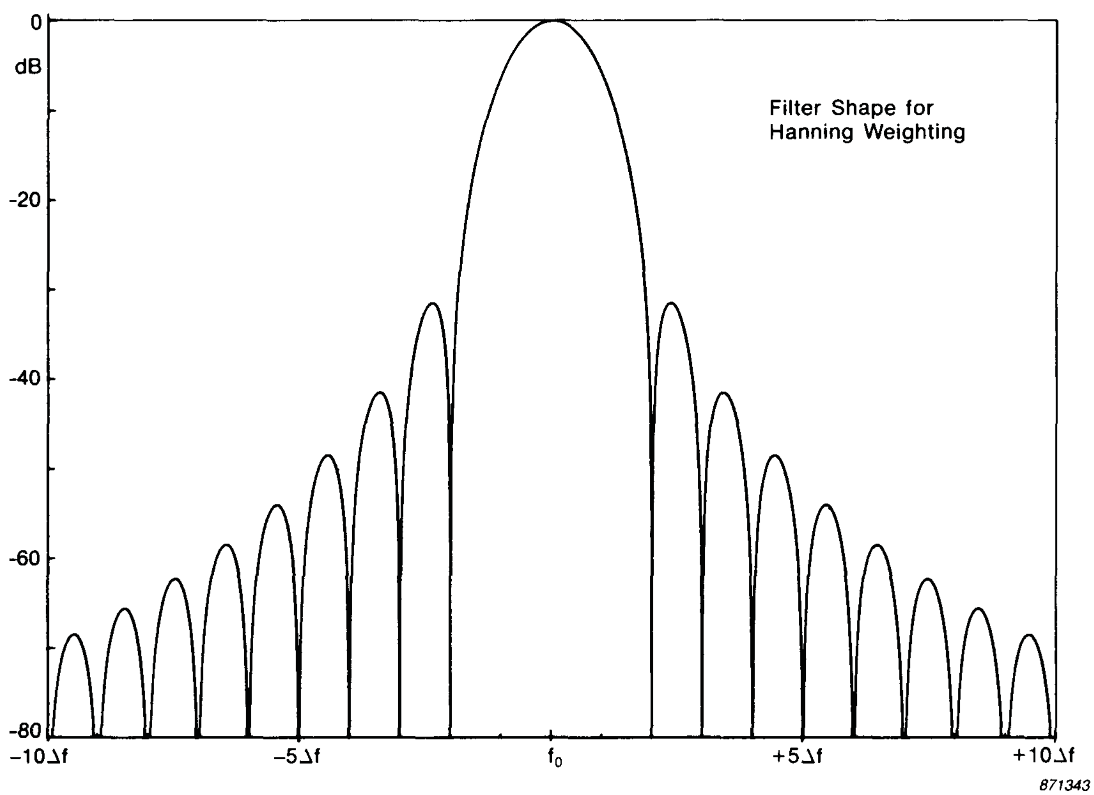

Fig. 8. Filter shape of Hanning Weighting function

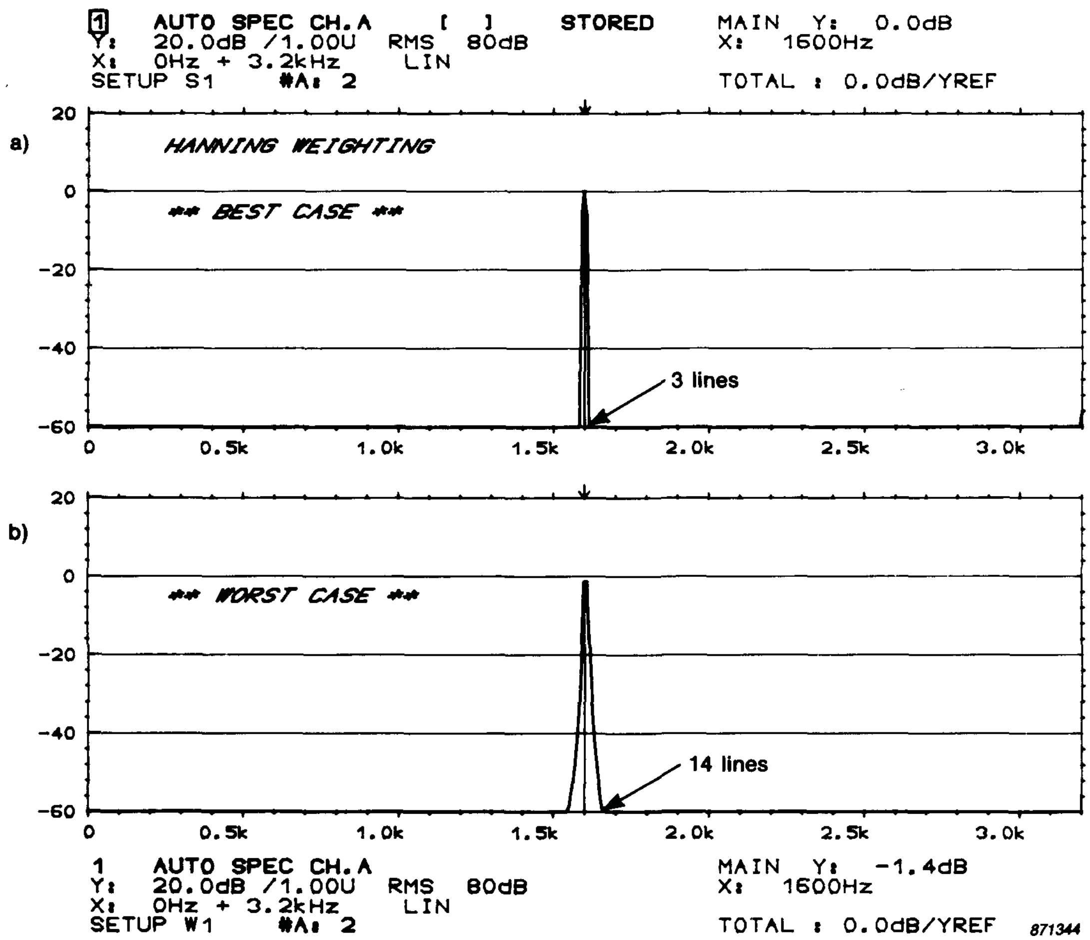

Fig. 9. The "best case" and the "worst case", when analysing a sinusoid using Hanning Weighting function

than for Rectangular weighting. This means that the 60 dB bandwidth is much narrower giving far better selectivity (see Table 2).

The maximum amplitude error, also known as the *picket fence effect* and given by the ripple in the passband, is only 1,4 dB for this window (see Fig. 9.b). In **Appendix** F the picket fence effect is discussed and it is shown how to compensate for it.

In comparison with Rectangular weighting, the noise bandwidth of Hanning weighting is 50% greater. Power spectrum values for broadband random signals will, therefore, be 1,5 times higher when analyzed using Hanning rather than Rectangular weighting. This correspond to a factor of $\sqrt{(1,5)} = 1,22$ for RMS readout, or $10 \log (1,5) = 1,76$ dB for readout in relative units, see Fig. 10. Correction of the noise bandwidth, to convert the power spectrum to the correct *power spectral density* (PSD) unit, should

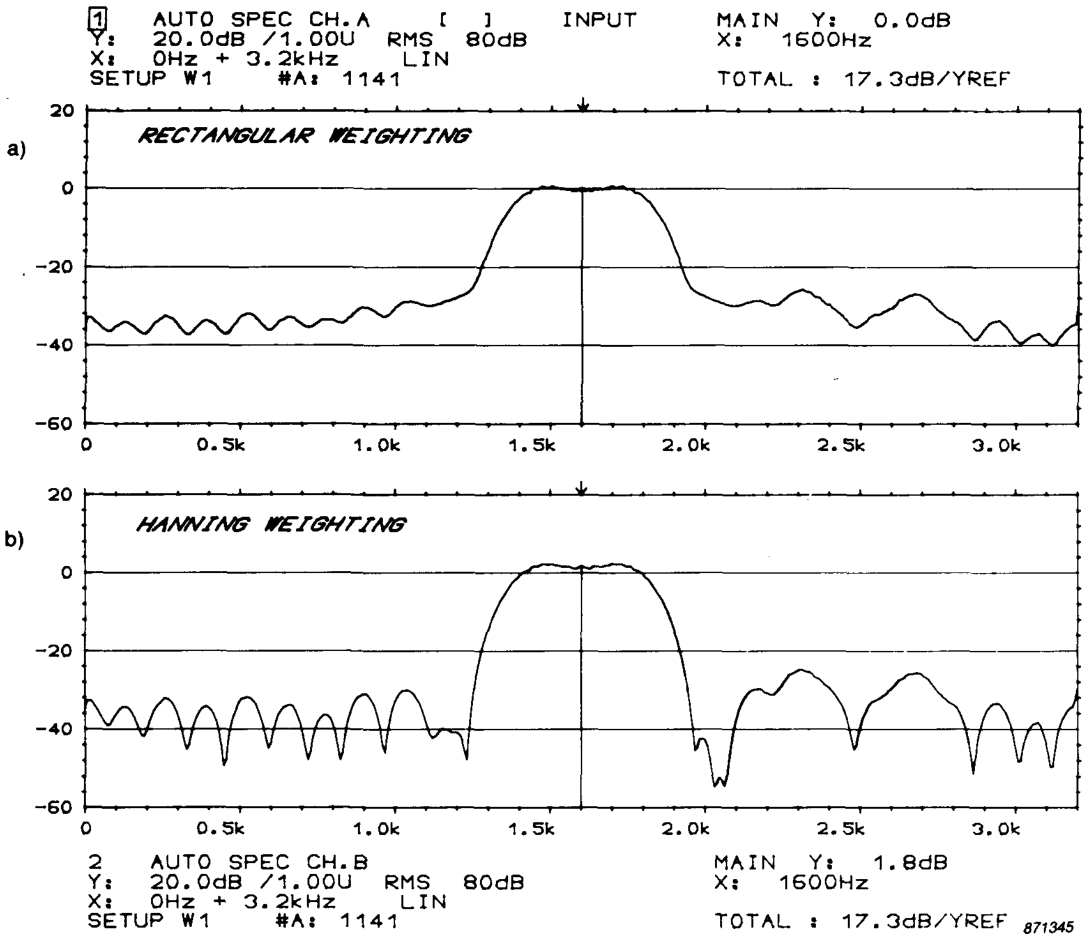

Fig. 10. The analysis of a narrow band random signal using Rectangular and Hanning Weighting

therefore be made by selecting PSD (rather than the RMS) in the display settings in Fig. 10. Note also that the total power across the full frequency range will be the same with either weighting, since the noise bandwidth is compensated for in this calculation. The Hanning window thus performs better than the Rectangular window with respect to selectivity, passband ripple and apparent leakage, and should be used in most cases where continuous signals are analyzed.

From Table 1 it can be seen that the effective duration is *3/8* of the record length *T*. An analysis using 50% overlap can therefore be made, giving results in half the time required with 0% overlap, without any significant loss of confidence in the results. (See Table 3).

Another feature of this window is that with linear averaging it gives an effective flat time weighting when 2/3 (66,67%) or 3/4 (75%) overlap is cho-

Real-Time Bandwidth (Display of Autospectrum)				
	Type 2032		Type 2034	
Window	**Single Channel**	**Dual Channel**	**Single Channel**	**Dual Channel**
Rectangular	17,7kHz	5,8 kHz	2,0 kHz	0,9 kHz
Hanning	16,6kHz	5,4 kHz	1,9kHz	0,9kHz
Kaiser-Bessel	10kHz	3,8 kHz	1,6kHz	0,8 kHz
Flat Top	10kHz	3,8 kHz	1,6kHz	0,8 kHz
User Defined	10kHz	3,8 kHz	1,6kHz	0,8 kHz

T01600GB0

Table 4. Real-Time bandwidth for the B & K Analyzers Type 2032 and 2034 using different weighting functions

sen (see **Appendix C** and Refs. [1 and 5]). The widest analysis bandwidth, in which a uniform weighting of the time signal can be obtained, is thus found to be with an overlap of 2/3. While 2/3 is not a practical overlap, since most DFT/FFT calculations use a transform length which is a power of two, the nearest value is good enough. For a transform size of 2048 samples, it is an overlap of 1365 samples.

In order to obtain results equivalent to a real-time analysis, where the overall weighting function must be uniform, the overlap has to be at least $^2/3$. This gives an effective real-time bandwidth which is 1/3 of the generally quoted Real-Time Bandwidth of an analyzer (based on analysis of adjacent blocks of data - i.e. 0% overlap). For the 2032 analyzer, this is 16,6 kHz/3 = 5,5 kHz in single channel mode. Table 4 shows the Real-Time Bandwidth of the 2032 and 2034 for the various windows.

Another use of the Hanning Window with, for example, 75% overlap is in the analysis of transients longer than the record length. With this technique, spectrum units of *energy spectral density* (ESD) must be chosen. The effective time-record length to use when scaling from PSD to ESD is, in the case of 75% overlap and n_d averages, given by $T \cdot n_d/4$ Refs. [1 & 5]. If a default value of T is used for the effective time-record length a further scaling (multiplication) of $n_d/4$ then has to be performed.

The Hanning window is also the best choice for system analysis (Frequency Response Function measurements) using a true random excitation signal. The relatively narrow mainlobe and low sidelobes give the lowest possible leakage (leakage causes underestimation of the peak value at resonance) Ref. [9].

The Hanning weighting function is a good overall, general purpose weighting function for continuous signals, it is easy to implement and gives a high real-time rate.

Kaiser-Bessel Weighting

The Kaiser-Bessel window as shown in Fig. 5 is calculated from

$$w(t) = 1 - 1{,}24 \cos 2\pi t/T + 0{,}244 \cos 4\pi t/T - 0{,}00305 \cos 6\pi t/T \quad \text{for} \quad 0 \leq t < T$$

$$w(t) = 0 \quad \text{elsewhere} \qquad (4)$$

The Integral Fourier Transform gives the filter characteristic of the window, shown in Fig. 11. This is superior to the other filters with respect to selectivity. The 60 dB bandwidth is only 6,1 times the line spacing. This is mainly due to the low level of the highest sidelobe, which is found to be at -67 dB.

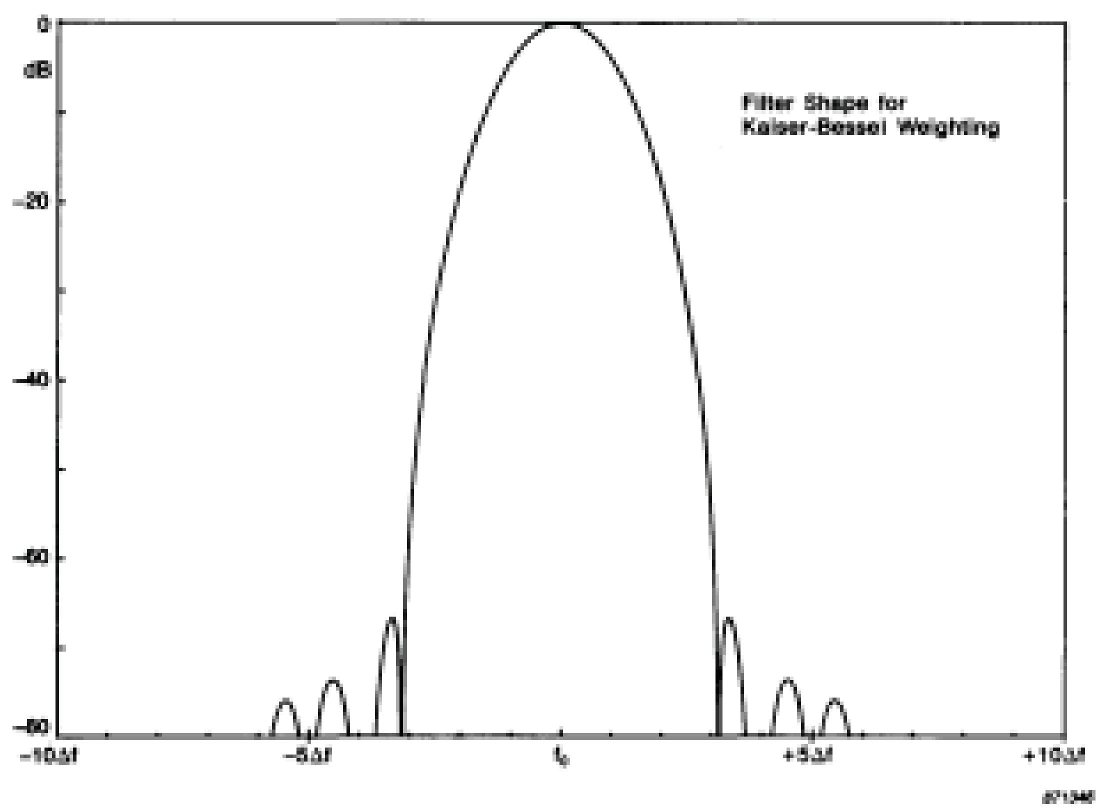

Fig. 11. Filter shape of Kaiser-Bessel Weighting Function

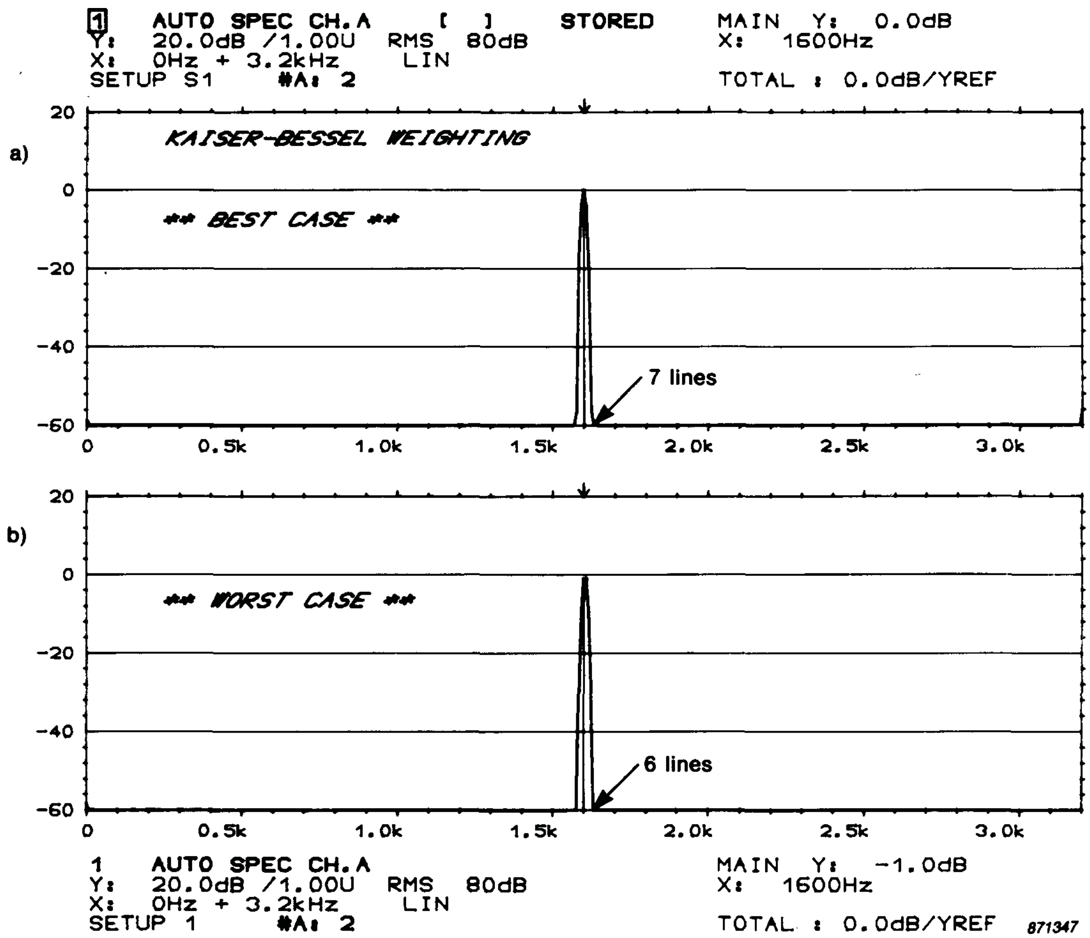

Fig. 12. The "best case" and the "worst case", when analysing a sinusoid using Kaiser-Bessel Weighting function

For analysing harmonic signals, the only difference between "best case" and "worst case" is, as shown in Fig. 12, the maximum amplitude error (ripple in the passband) of -1,0 dB.

Because it has good selectivity, the main use of the Kaiser-Bessel window is for two-tone separation of closely spaced frequency components with widely different levels. This is demonstrated in Figs. 13 and 14, where two "worst case" sinusoids, separated by a 40 dB difference in level and six times the line spacing in frequency, are analyzed using the four different standard weighting functions. Only the Kaiser-Bessel window can fully separate the two components over a dynamic range of 60 dB. Note that for the Rectangular Weighting the lower component is completely masked by the higher component.

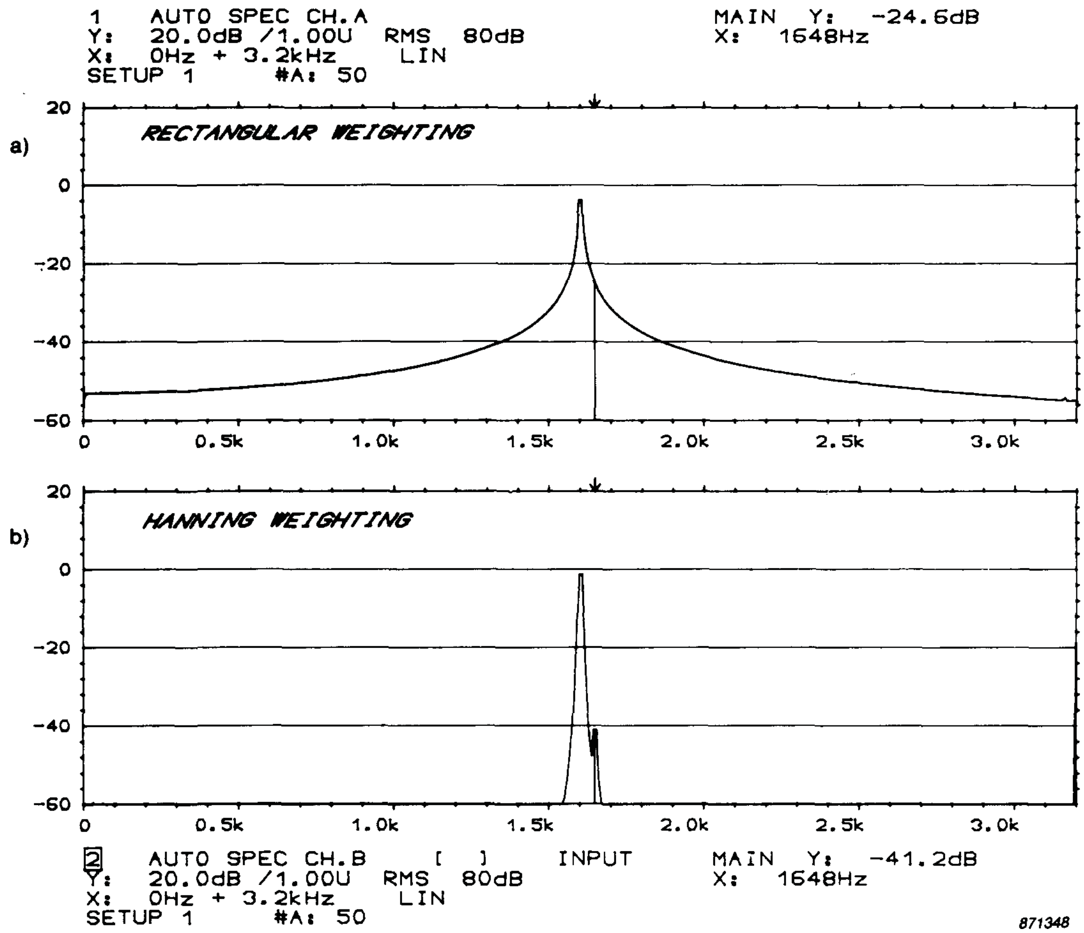

Fig. 13. Two-tone separation using Rectangular and Hanning Weighting. Level difference is 40 dB

For analysis of periodic signals the Kaiser-Bessel window is probably the best choice. Harris (Ref. [2]) states in his article: "This suggests that the Kaiser-Bessel or the Blackman-Harris window should be declared the top performer. My preference is the Kaiser-Bessel."

The only disadvantages, in comparison with the Hanning weighting function, are speed (Table 4) and that a uniform weighting of the time signal cannot be achieved by standard overlap analysis. Also note that, for system analysis using random excitation, this window will cause more leakage (than the Hanning window) at resonances and anti-resonances, due to its wider noise bandwidth.

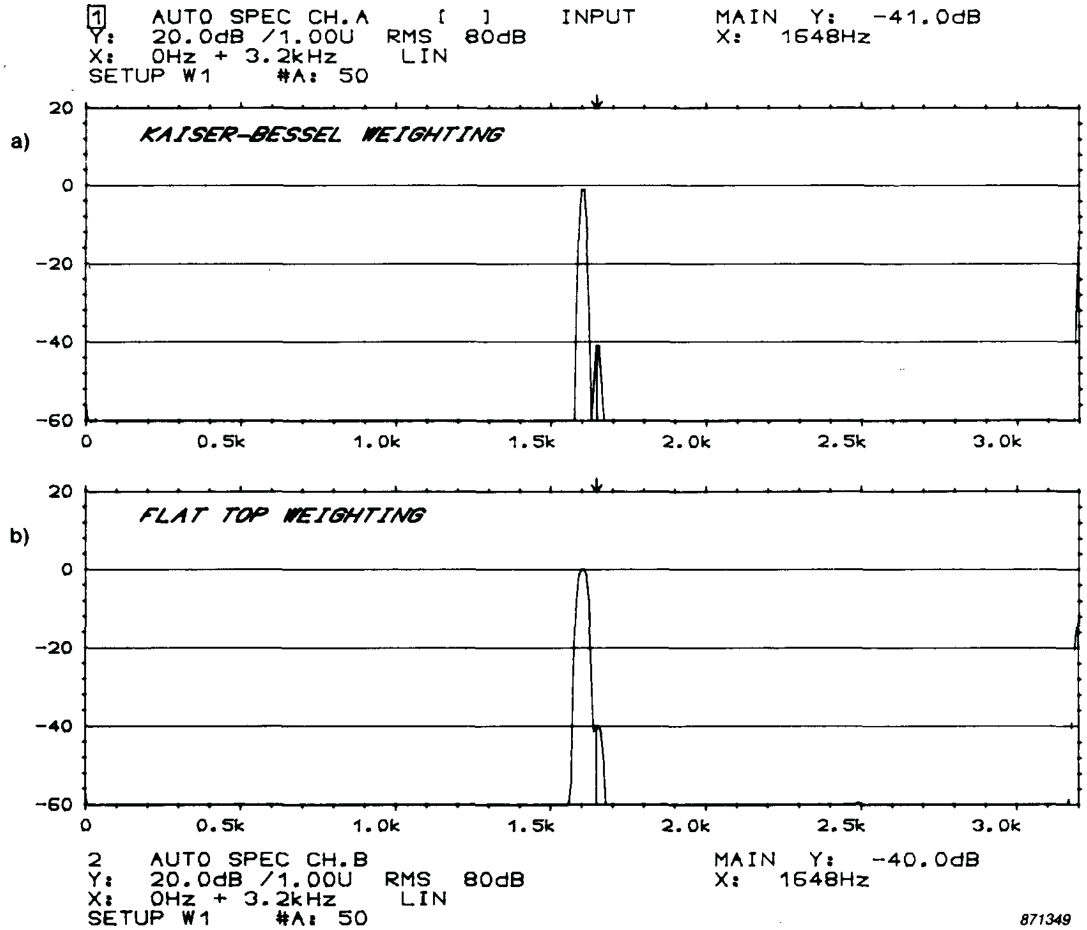

Fig. 14. Two-tone separation using Kaiser-Bessel and Flat Top weighting. Level difference is 40 dB

Flat Top Weighting

The Flat Top window as shown in Fig. 5 is calculated from

$$w(t) = 1 - 1{,}93\cos 2\pi\, t/T + 1{,}29\cos 4\pi\, t/T - 0{,}388\cos 6\pi\, t/T + 0{,}0322\cos 8\pi\, t/T \quad \text{for} \quad 0 \leqq t < T$$

$$w(t) = 0 \quad \text{elsewhere} \qquad (5)$$

and the filter shape is shown in Fig. 15. The name comes from the low ripple (< 0,01 dB) in the passband. The ripple is negligible and the amplitude error will be determined by the overall linearity of the analyzer. Thus the window is designed mainly for calibration purposes, although calibra-

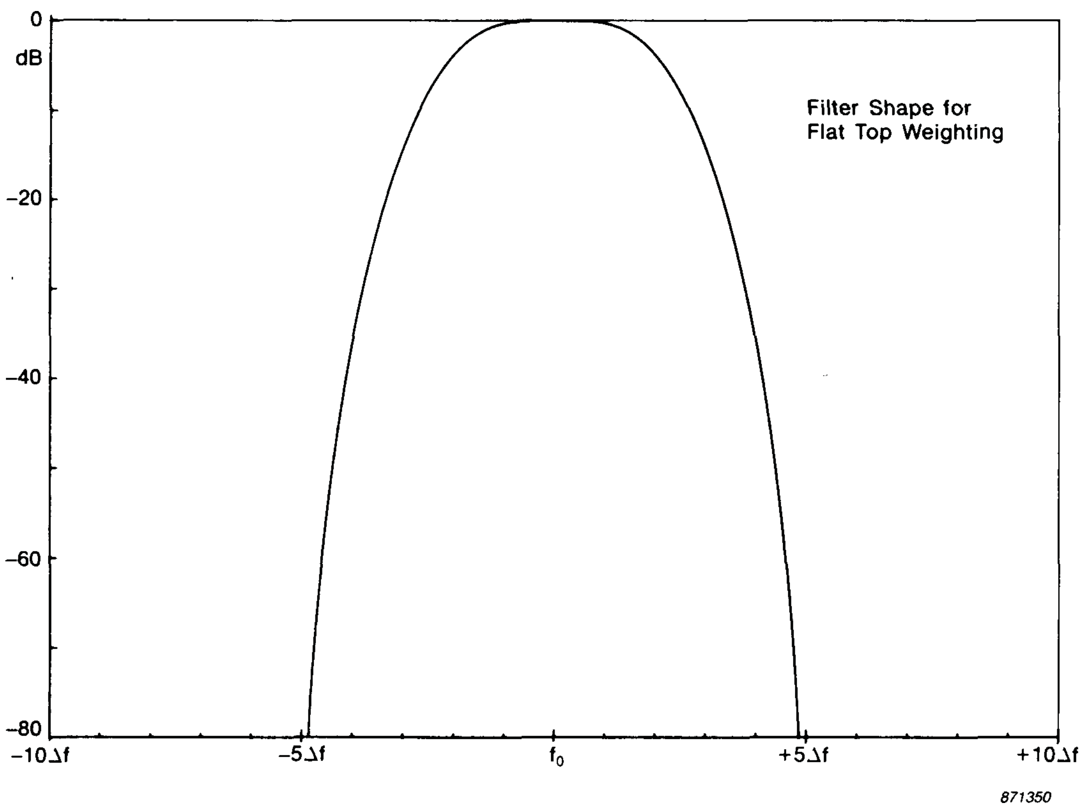

Fig. 15. Filter shape of Flat Top Weighting Function

tion could be made using the Hanning or Kaiser-Bessel windows and a readout of the total power (RMS), or power (RMS) in a delta band which included all the filters excited by the calibration signal (Fig. 9 and 12).

The selectivity is not as good as that of Kaiser-Bessel (Fig. 14). The shape factor is in fact lower which is an indication of the very steep filter skirts, but its 60 dB bandwidth is wider.

The Flat Top window is the FFT-filter which has a performance closest to that of an ideal filter with nearly identical 3 dB and Noise Bandwidths. It can be seen from Fig. 14 that it is also the only weighting function which measures the correct level of the lower amplitude component in the two-tone example.

In most applications one will probably prefer the Hanning weighting, to the Flat Top, for the following three reasons; it has a 2,5 times narrower bandwidth, it has a higher real-time rate, and it gives a uniform weighting achieved by simple overlap analysis.

The main use for the Flat Top window is for calibration, due to its negligible amplitude errors.

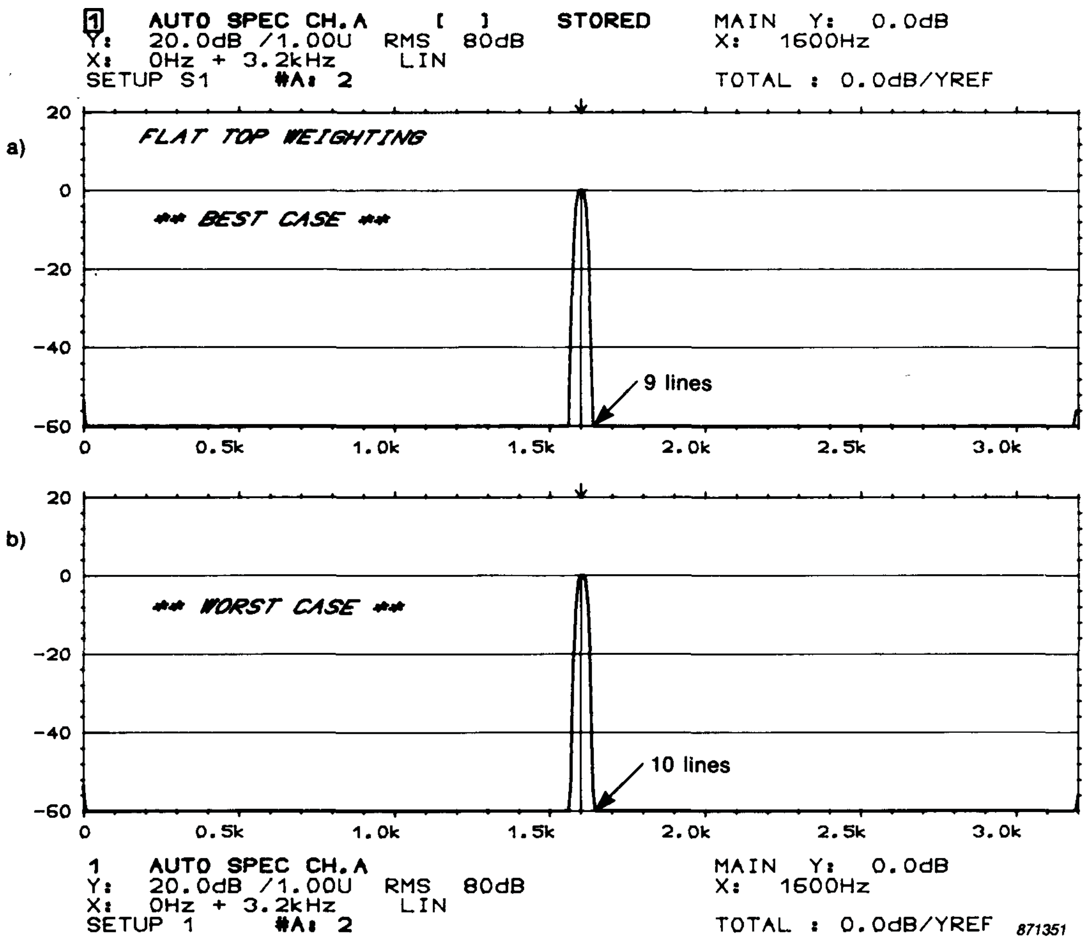

Fig.16. The "best case" and the "worst case" when analysing a sinusoid using Flat Top Weighting function

User Defined Weighting

The User Defined window is calculated from the general window formulation.

$$w(t) = a_0 - a_1 \cos 2\pi t/T + a_2 \cos 4\pi t/T - a_3 \cos 6\pi t/T + a_4 \cos 8\pi t/T \quad \text{for} \quad 0 \leqq t < T$$

$$w(t) = 0 \qquad \text{elsewhere} \qquad (6)$$

where the coefficients a_0, a_1, a_2, a_3 and a_4 can be defined using special parameters 10 to 15 in the 2032/34.

The effective noise bandwidth must also be defined and entered using special parameters 6 to 9, if readout of power spectral density (PSD) or energy spectral density (ESD), which are the proper units for random and transient signals respectively, are desired, Ref. [1 & 12]. The noise bandwidth is also needed for correct calculation of the overall power, or for power in a delta band as discussed earlier.

The Kaiser-Bessel and Flat Top windows are implemented as special versions of the User Defined window in 2032/34, and thus have the same real-time bandwidth (RTB) as defined in equation (7), independent of the number of coefficients used.

$$\text{RTB} = \frac{\text{No. of lines}}{\text{Calculation Time}} \tag{7}$$

where the *calculation time* is the effective time taken for the analyzer to make one average.
Examples of User Defined windows are shown in **Appendix E.**

Transient Weighting

The Transient window is similar in performance and use to the Rectangular window, but is shorter than the record length, thus giving a broader filter characteristic. The user can define both the starting point and the length of the Transient window, with respect to the measurement record. The samples outside the chosen time interval are set to zero, which improves the signal to noise ratio for analysis of short transients.

If smooth tapering is needed a leading and trailing half-cosine (half-Hanning) can be chosen using special parameters 16 and 17 in the 2032/34 (see Fig. 17 b).

As a visual feedback for correct positioning, the time weighting function or the weighted time signal can be viewed using special parameters 76 and 77 (Fig. 17 b and c).

The use of the Transient window is for the analysis of short transients, or for gating parts of a time signal contained in the input memory of the analyzer.

Exponential Weighting

The Exponential window is defined as

$$w(t) = e^{-(t-t0)/\tau} \quad \text{for} \quad t_0 \leqq t < T \qquad \text{and} \quad 0 \leq \tau < T$$

$$w(t) = 0 \quad \text{elsewhere} \tag{8}$$

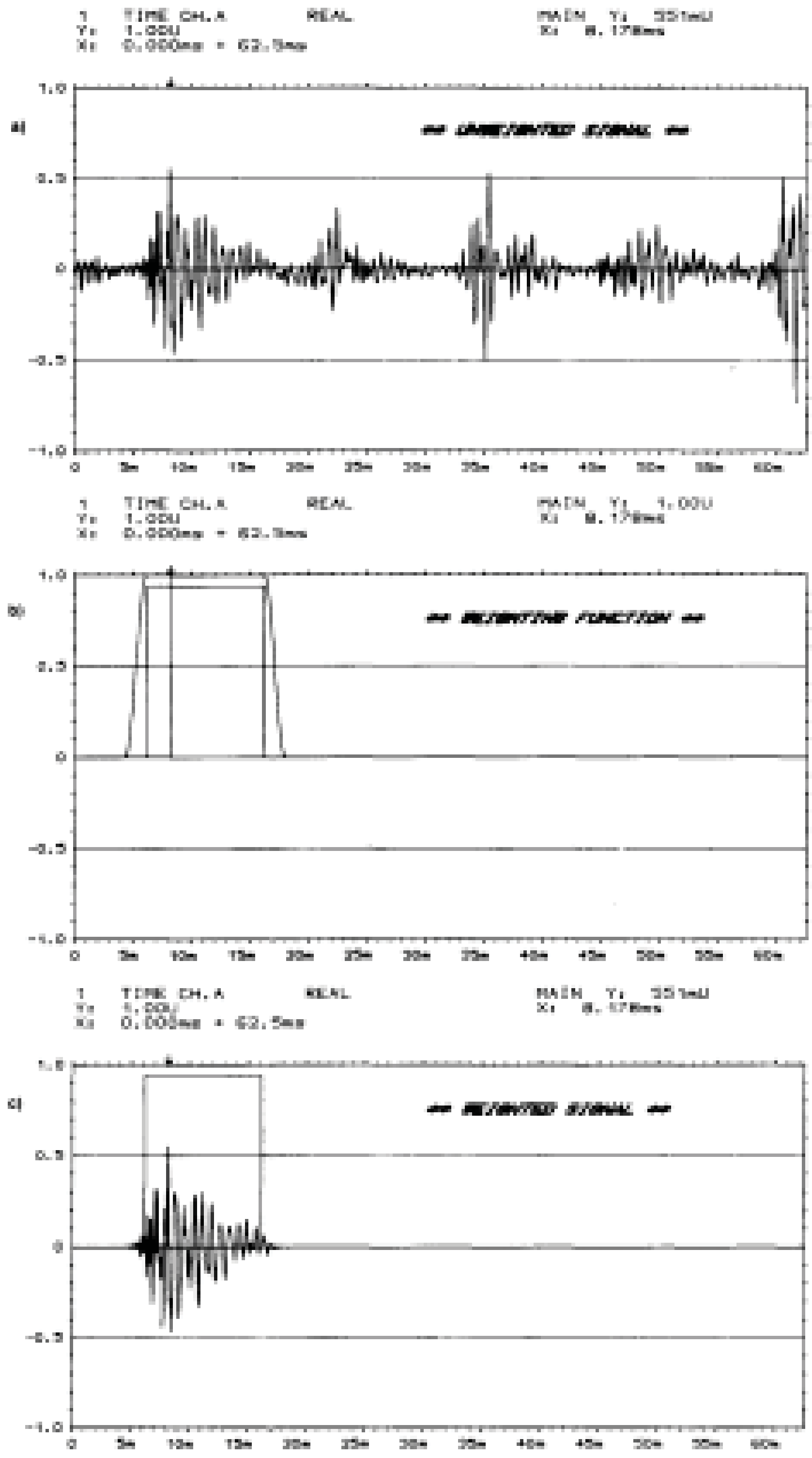

Fig. 17. Visual feedback when windowing time signals.
a) Unweighted signal. b) Weighting function. c) Weighted time signal

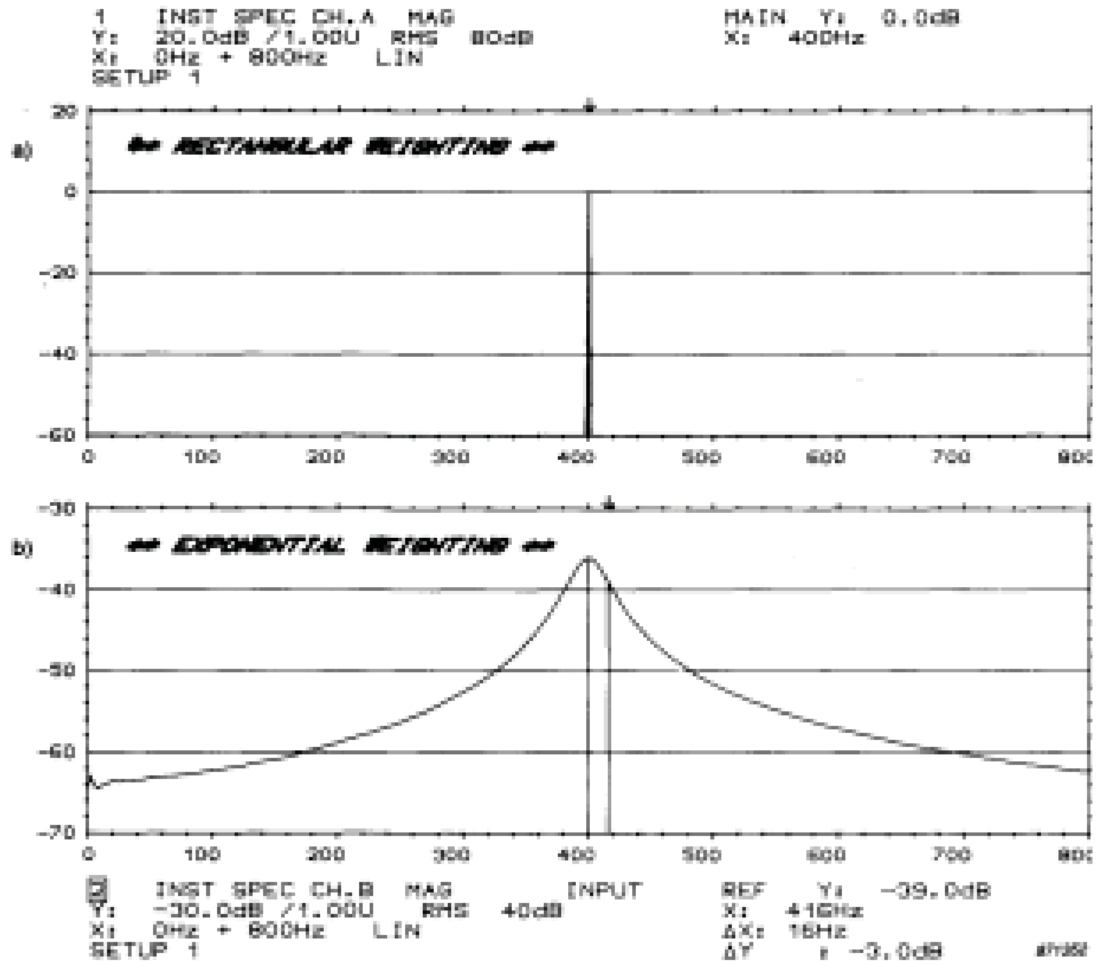

Fig. 18. A "best case" sinusoid analyzed with a) Rectangular Weighting b) Exponential Weighting, τ = 10 ms

where τ, the time constant, is selected as the length of the window and t_0 is the shift of the window. Thus the time signal is attenuated by a factor of $e = 2{,}71828$ or 8,69 dB per time constant.

The 3 dB bandwidth is given by 1/πτ Hz and the effective noise bandwidth is given by 1/2 τ Hz Ref. [I].

The filter characteristic (complex) given by the integral Fourier transform of the window is:

$$W(f) = \frac{\tau}{1 + j\,2\,\pi f \tau} \tag{9}$$

It is assumed here that the window is infinitely long, which means that the effect of the truncation at $t = T$ is neglected. This can only be done if the time constant τ is much shorter than T (at least a factor of 4). Otherwise the convolution of the filter characteristic (complex) of a rectangular window would have to be included in Eq. (9).

A leading half-cosine taper, as well as a delay from the end of the taper to the beginning of the exponential decay, can be chosen in special parameters 18 and 19 in 2032/34.

In Fig. 18 b, a "best case" sinusoid is analysed with an Exponential window using a time constant of 10 ms. Note that the 3 dB bandwidth of the spectrum is approximately 32 Hz ($1/\pi\,\tau$).

The main use of the Exponential window is for the analysis of transients longer than the record length. Signals, which exhibit an exponentially decaying amplitude as a function of time, should be weighted by this window. This is typically the case for the response of lightly damped structures when they are excited by an impact. If the signal is not sufficiently attenuated (40 dB is sufficient) at the end of the record, the truncation of the signal will produce an undesirable amount of leakage, resulting in ripples in the spectrum (Ref. [13]). By applying an exponential window, which forces the amplitude to be sufficiently attenuated at the end of the record, the amount of leakage is predictable and can be compensated for as shown in Eq. (10)

$$1/\tau_{signal} = 1/\tau_{measured} - 1/\tau_{window} \qquad (10)$$

which leads to the following simple relationship in the frequency domain

$$\Delta f_{3\text{ dB signal}} = \Delta f_{3\text{ dB measured}} - \Delta f_{3\text{ dB Window}} \qquad (11)$$

Implementation

All the time windows in the B & K Analyzers Types 2032 and 2034 are implemented as multiplications in the time domain. They could also have been implemented as convolutions in the frequency domain, but this would be inappropriate for the Transient and the Exponential windows.

The window parameters, and the choice of windows, can be changed after recording of the time signal has been completed by using special parameter 30 "Free Windows". This gives the user the ability to get a visual feedback so that the choice of an optimal window, and window parameters, can be made for a given signal.

Summary

For the analysis of *transients* the following windows should be used:

Rectangular Weighting for general purposes.

Transient Weighting for short impulses and transients, to improve the signal to noise ratio and for gating purposes.

Exponential Weighting should be applied for transients longer than the record length, e.g. exponentially decaying signals, which do not decay sufficiently within the record length.

Hanning Weighting with 66 2/3% or 75% overlap for transients much longer than the record.

For the analysis of *continuous signals* we have the following conclusions:

Rectangular Weighting should only be used when analysing special sinusoids, the frequencies of which coincide with the centre frequencies/ lines in the analysis. This is often the situation when pseudo-random types of signal are analysed, or when order tracking is applied.

Hanning Weighting is a general purpose weighting and should be used in most cases. Hanning window with *66 2/3%* or 75% overlap should be used when true real-time analysis is needed.

Kaiser-Bessel Weighting shows very good selectivity and should be used for two-tone separation of harmonic signals with widely different levels.

Flat Top Weighting is mainly designed for calibration and correct amplitude measurement.

For *system analysis,* that is *frequency response function* measurements, the following windows should be used (Refs. [9 and 10]):

Transient Weighting for the excitation signal when an impact hammer is used for excitation.

Exponential Weighting for the response signal of lightly damped systems, when an impact hammer is used for excitation.

It should be noted that for low frequency or zoom analysis where the record length *T* becomes long it will be advantageous to use random impact with the hammer in which case Hanning weighting should be used (Ref. [13]).

Hanning Weighting for both excitation and response signals when a random excitation signal is used.

Rectangular Weighting for both excitation and response signal when a pseudo-random excitation signal is used.

Conclusion

FFT analyzers are widely used today for frequency analysis of vibration signals. A careful choice with respect to weighting function or filtershape is required since no standard exists. This is in contrast to acoustic noise measurements, where there has been a long tradition for using standardized octave and 1/3 octave filter bands.

Even if an optimum FFT-filter shape is chosen the results must be scaled in the right unit according to the signal type (Ref. [12]). This is because the absolute bandwidth is also related to the chosen frequency range and the number of lines in the analysis.

Hopefully this article has enlightened and clarified some of the difficulties that exist in the choice of a proper weighting function for a given application using DFT/FFT analysis.

Acknowledgement

The authors wish to thank N. Thrane, E. Jørgensen and O. Døssing, Brüel & Kjær, for useful discussions.

References

[1] Randall, R.B. *"Frequency Analysis",* Brüel & Kjær, 1987

[2] Harris, F.J. *"On the Use of Windows for Harmonic Analysis with the Discrete Fourier Transform*", Proceedings of the IEEE, Vol. 66, No.1, January 1978, pp. 51-83.

[3] Welch, P.D. *"The use of Fast Fourier Transform for the estimation of power spectra: A method based on time averaging over short, modified periodigrams",* IEEE Trans. Audio Electro Acoust., Vol. AU-15, June 1967, pp.70-73

[4] Thrane, N. *"The Discrete Fourier Transform and FFT Analyzers",* B & K Technical Review, No.1-1979

[5] Thrane, N. *"Zoom FFT",* B & K Technical Review, No.2-1980

[6] Boyes, J.D. *"Effective Weighting of Overlapped Spectral Averaging",* B & K Internal Paper, 1980

[7] Brigham, E.O. *"The Fast Fourier Transform",* Prentice Hall Inc., New Jersey, 1974

[8] Papoulis, A. *"The Fourier Integral and its Applications",* McGraw-Hill Inc., New York, 1962

[9] Herlufsen, H. *"Dual Channel FFT Analysis, Part I",* B & K Technical Review, No.1-1984

[10] Herlufsen, H. *"Dual Channel FFT Analysis, Part* 2", B & K Technical Review, No.2-1984

[11] Herlufsen, H. *"Order Analysis using Zoom FFT",* B & K Application Note No. 012-81

[12] Gade,S., Herlufsen, H. *"Signals and Units",* B&K Technical Review No.3-1987

[13] Sohaney, R.C., Nieters, J.M. *"Proper use of Weighting Functions for Impact Testing",* B&K Technical Review, No.4-1984

Signals and Units

by Svend Gade and
Henrik Herlufsen

Abstract

The range of window functions available in DFT/FFT (Discrete Fourier Transform / Fast Fourier Transform) analyzers gives them the ability to analyze a wide variety of different signal types. The shape of the window function and the frequency span of the analyzer, determine the noise bandwidth of the filters and the analysis time for the signal. Consequently, it is important that the correct units are used to scale the frequency spectra. To obtain consistent results for some signals, the spectra have to be normalized with respect to the noise bandwidth and the measurement time.

Sommaire

La gamme de fonctions fenêtres des analyseurs DFT/FFT (Transformeé de Fourier discrète/rapide) permet d'analyser des types de signaux très divers. La forme de la fenêtre et la gamme de fréquence de l'analyseur déterminent la largeur de bande des filtres et le temps d'analyse du signal. En consequence, il est important de choisir des unités adaptées aux spectres de fréquence étudiés. Avec certains types de signal, il est nécessaire de normaliser les spectres en fonction de la largeur de bande et du temps de mesure afin d'obtenir des résultats cohérents.

Zusammenfassung

Für die DFT/FFT- (Diskrete Fourier Transformation/Fast Fourier Transformation) Analysatoren gibt es eine Reihe von Zeitbewertungsfunktionen, die die Analyse der verschiedensten Signalarten ermöglichen. Die Rauschbandbreite der Filter und die Analysenzeit für das Signal wird durch die Form der Zeitbewertung und den Frequenzbereich des Analysators bestimmt. Darum ist es wichtig, die Frequenzspektren in der richtigen Einheit zu skalieren. Bei bestimmten Signaltypen müssen die Spektren mit Bezug auf die Rauschbandbreite und Meßzeit normalisert werden, um reproduzierbare Ergebnisse zu erzielen.

Introduction

The analysis of different signal types requires not only that we use the appropriate weighting functions (Refs. [1 and 2]), but also the correct analysis parameters or units.

Fig. 1 illustrates the three basic types of signals. One fundamental difference is found in the duration of the signals, whether they are transients or continuous signals.

A transient is a signal which starts and ends at zero amplitude. In this case the complete signal should be analyzed in units of energy.

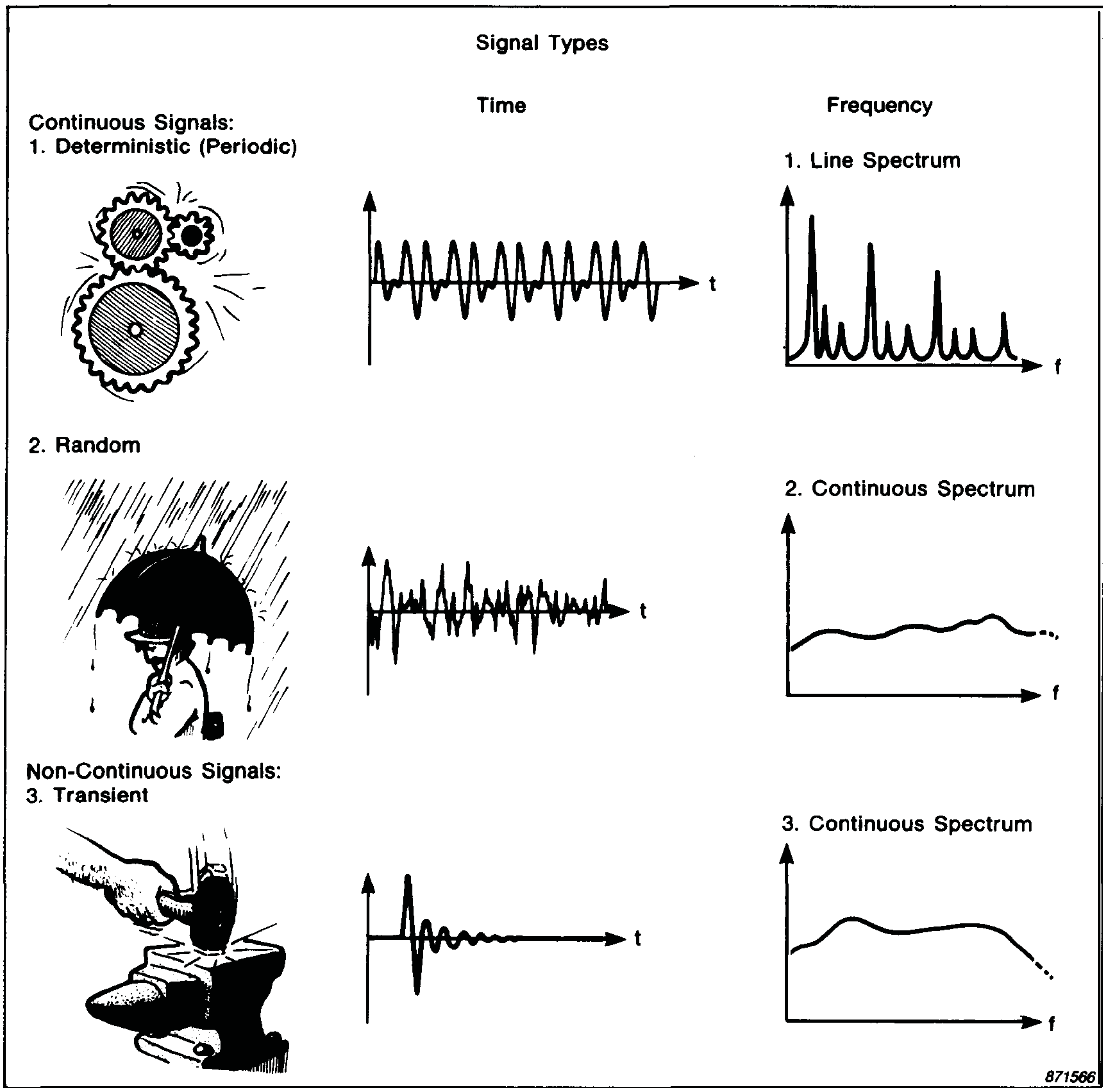

Fig. 1. Classifications of signals into deterministic, random and transient types

This is in contrast with stationary continuous signals, in which the amount of energy measured in is proportional to the observation time. These signals should be analyzed in units of power, energy per unit time.

Another basic difference between the signal types is found in the frequency domain, depending on whether they have line spectra or continuous spectra. Continuous spectra (like continuous signals, where the results are normalized with respect to unit time) should be normalized with respect to the frequency unit (i.e. Hz) to give Spectral Density. This is because the measured level (or amplitude) at a relatively flat part of the spectrum, is proportional to the filter/analysis bandwidth.

For line spectra, on the other hand, the measured amplitude is independent of the filter bandwidth, if the resolution of the analysis is sufficient to separate the individual frequency components.

Deterministic Signals

Stationary, deterministic (periodic) signals are made up entirely of sinusoids at discrete frequencies. The resolution of the frequency analysis is determined by the filter noise bandwidth used. The filter bandwidth should enable the analyzer to distinguish between the two most closely spaced frequency components (see Fig. 2). This means that only one sinusoid should lie within the filter passband at any one time, in which case the power transmitted by the filter is independent of the analysis bandwidth. The averaged frequency spectrum of a deterministic signal should, therefore, be scaled either in terms of mean square or power (PWR), in U^2

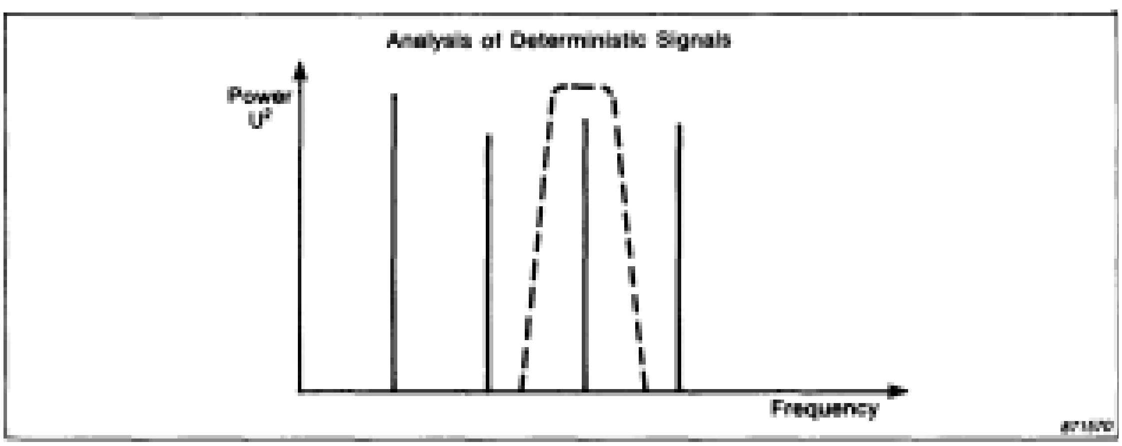

Fig. 2. For analysis of periodic, deterministic signals, the power or RMS amplitude transmitted by the filter in each frequency band should be measured in U^2 (PWR) or in U (RMS)

(units squared), or in terms of root mean square (RMS), in *U* (units). The unit *U* may be volts *(V),* or any of the physical units such as *Pascals,* m/s^2, *m/s, m, g, N* etc.

Fig. 3 shows the time record and the frequency spectrum for a deterministic signal analyzed on a Brüel & Kjær 2032/2034 Dual Channel Signal Analyzer. The "TOTAL" field gives the total power, or total RMS values, of the displayed frequency spectrum. Alternatively a delta cursor can be used, in which case the "ΔTOTAL" field gives the total power (or RMS) within the band selected by the delta cursor, and the "Δ/TOTAL" field gives the fraction of the total power (or RMS) within the selected band.

Each type of time-weighting function/filter produces a different number of frequency lines in the spectrum (see Ref. [2]). But in the 2032/34 the

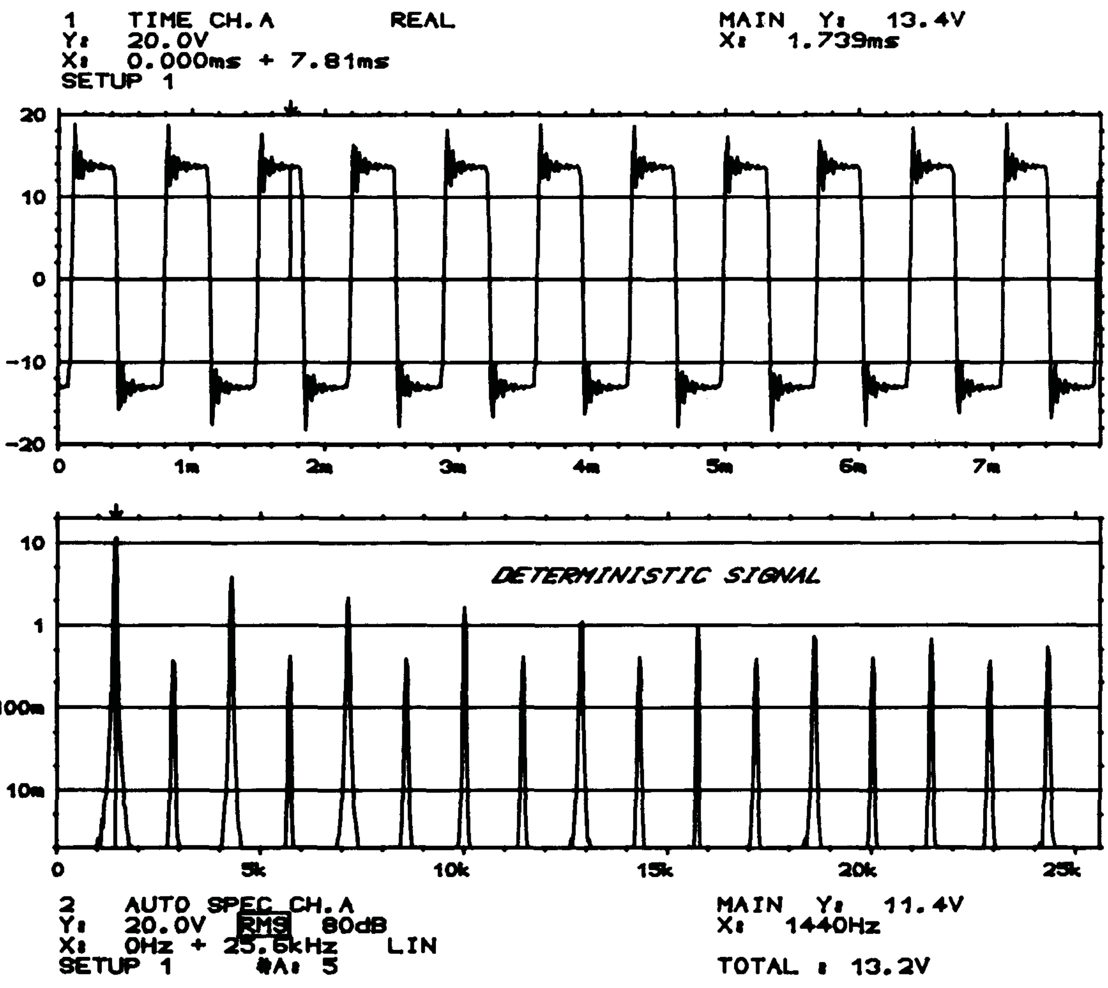

Fig. 3. Time record and frequency spectrum of a stationary, deterministic (periodic) signal. The frequency spectrum is scaled to the root mean square (RMS)

weighting functions are scaled so that the reference gain of the filter/lines is unity. This means that the amplitudes are correct power (PWR) or RMS spectrum amplitudes, except for possible picket fence effect errors due to the ripple in the passband of the filters. When the power in a user-defined (delta cursor) frequency band is calculated, by summing the power in the relevent lines, the correction for the noise bandwidth of the selected weighting function is automatically made.

Random Signals

Continuous, stationary random signals have spectra which are continuous functions of frequency (see Fig. 4). Consequently there is a continuous frequency distribution within the filter passband and the power transmitted by the filter depends on the filter bandwidth (the resolution of the analysis). In situations where the amplitude variations within the analysis bandwidth are relatively small, the influence of the filter bandwidth can be removed by dividing the transmitted power by the filter bandwidth. This process normalizes the result to a mean square spectral density, or Power Spectral Density (PSD) in U^2/Hz, which is a measure of the power per unit bandwidth. Sometimes the square root of PSD is preferred giving $U/\sqrt{\text{Hz}}$.

Fig. 5 shows the time record and the PSD frequency spectrum for a narrow band random signal. Note that read out using "TOTAL" or "Δ TOTAL" will be the power or mean square value of the selected band.

When using broadband analysis, such as the A-weighted, octave or one third octave analysis often used in acoustics, it is very seldom that the

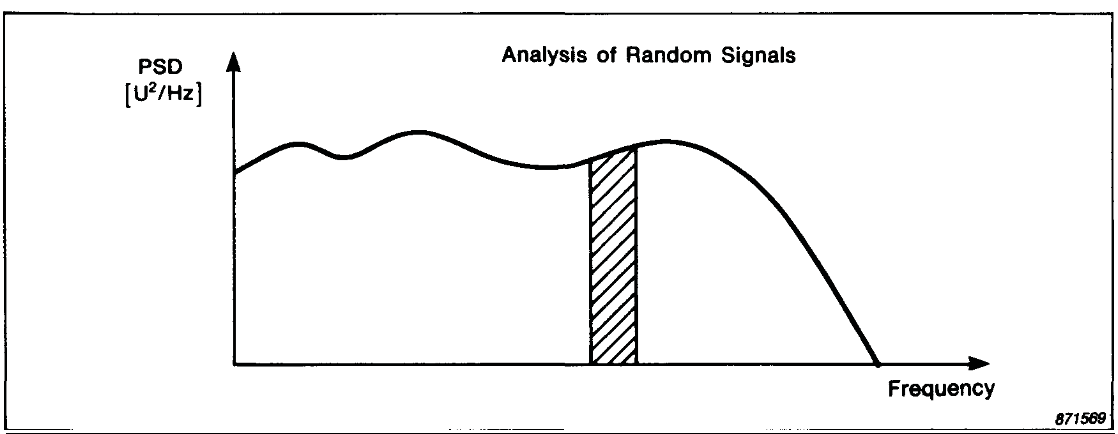

Fig. 4. For analysis of stationary random signals, the Power Spectral Density (PSD) should be measured, in U^2/Hz

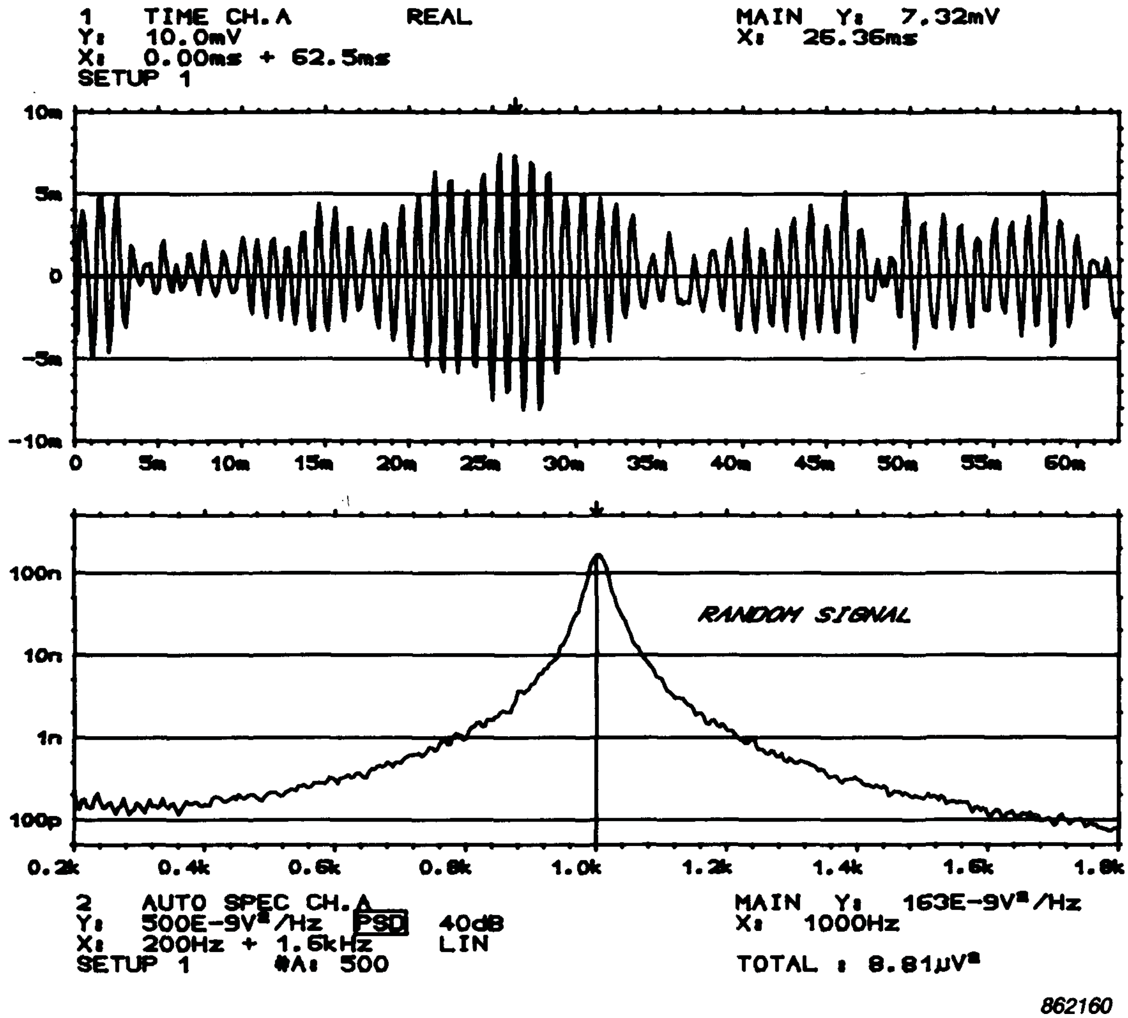

Fig. 5. Time record and frequency spectrum of a stationary, random process. The frequency spectrum is scaled as Power Spectral Density

results of analyzing stationary random signals are normalized to the bandwidth of the analysis/filters. This is because analysis using filters with standardized characteristics gives consistent results independent of the frequency range and averaging technique.

Transient Signals

Transient signals start and end with zero amplitude, and thus contain finite amounts of energy. They cannot, therefore, be characterized in terms of power which will depend on the record length (or averaging time). Ana-

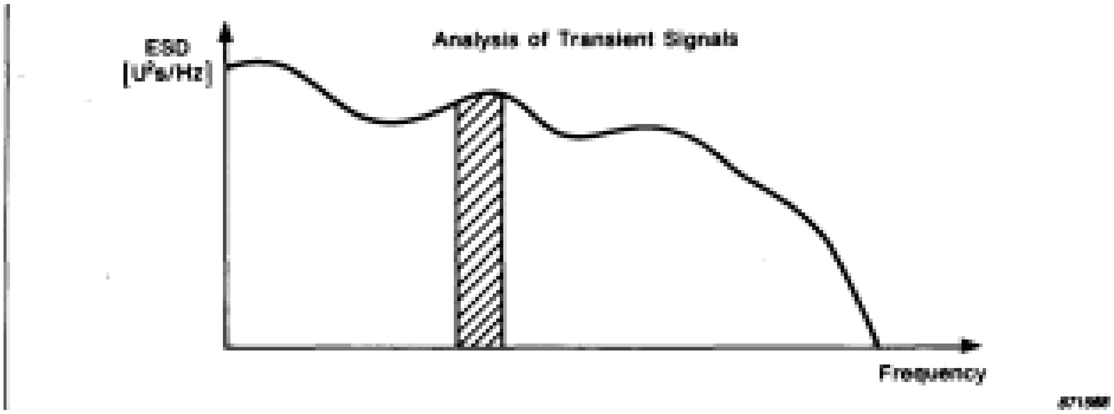

Fig. 6. For analysis of transient signals, the Energy Spectral Density (ESD) should be measured, in U^2s/Hz

lyzers detect power with reference to the record length *T,* or averaging time T_A (power is found by dividing the measured energy by *T* or T_A), thus the longer the time window - the lower the average power.

Transient signals also have spectra which are continuously distributed with frequency (see Fig. 6). Consequently, the transmitted energy per filter/line must be normalized with respect to the filter bandwidth, which results in units of energy per unit bandwidth, often termed energy spectra] density (ESD).

Fig. 7 shows the time record and the frequency spectrum (scaled in ESD), for a transient signal. Transients must be analyzed using an equal time-weighting function across the signal. To achieve this a Rectangular Weighting (no weighting), or a shorter Transient Weighting function, should be used depending on the length of the transients relative to the record length. An Exponential window or overlapping Hanning Windows can be used for transients which do not decay sufficiently within the record length (see Refs. [1 and 2]). Note that the read out, in "TOTAL" or "Δ TOTAL", will give the total energy in the selected band.

With standardized A-weighted, octave or one third octave filter analysis, compensation for the filter bandwidth is very rarely used (for the same reasons given for the analysis of stationary random signals). As already mentioned, it is necessary to compensate for the averaging time so that the results are consistent in terms of energy.

In acoustics this type of scaling for A-weighted sound pressure levels is called Sound Exposure Level (SEL), and it is used to express the amount of A-weighted energy in a transient.

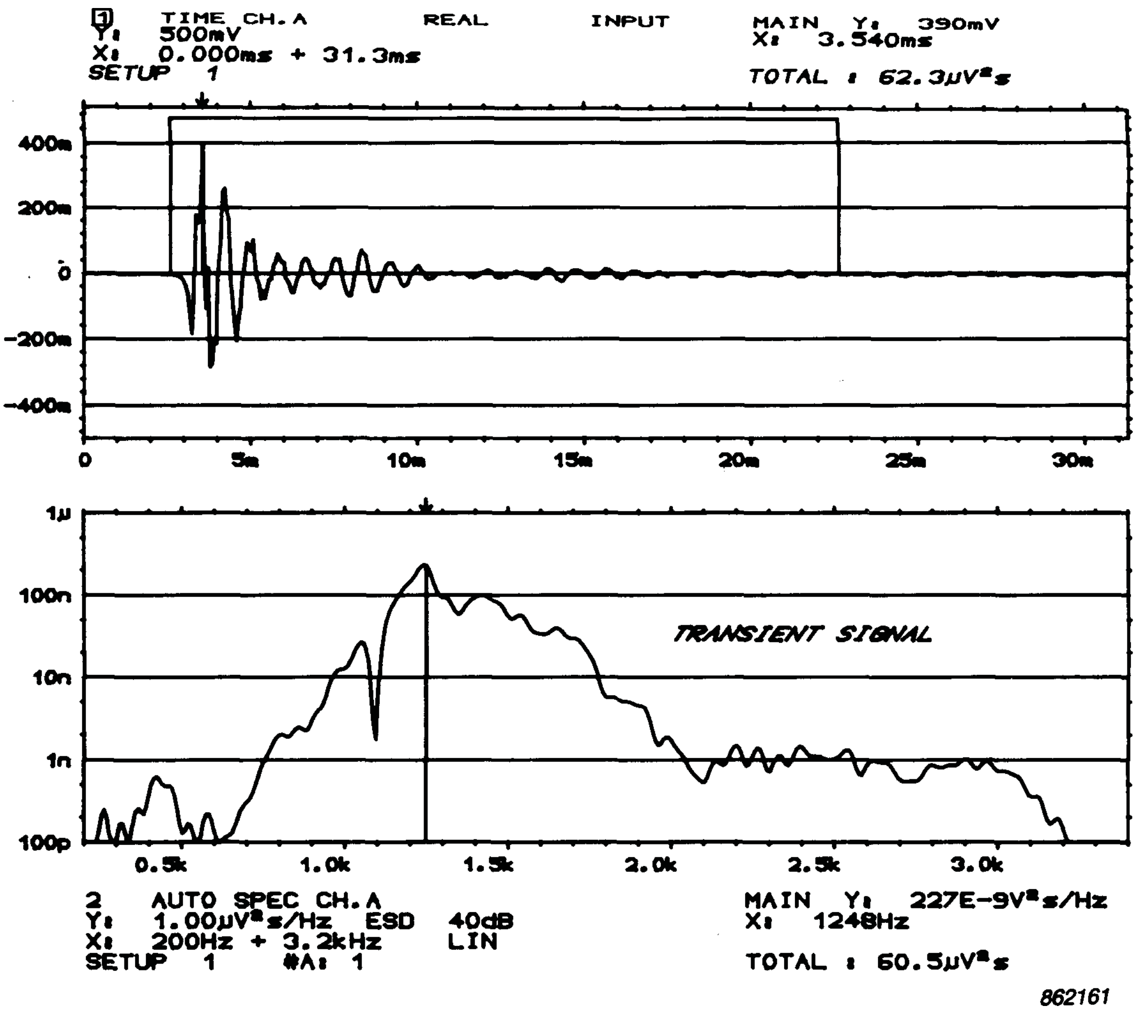

Fig. 7 Time record and frequency spectrum of a transient signal. A transient weighting function is applied to the time record, and the frequency spectrum is scaled as Energy Spectral Density

Conclusions

Analyzers normally detect the mean square (PWR) or the root mean square (RMS) of the filtered signal. Depending upon the type of signal to be analyzed, the results should be scaled properly by calculation of:

RMS:

$$\mathrm{RMS} = \sqrt{\mathrm{PWR}} \tag{1}$$

Power:

$$\mathrm{PWR} = \mathrm{RMS}^2 \tag{2}$$

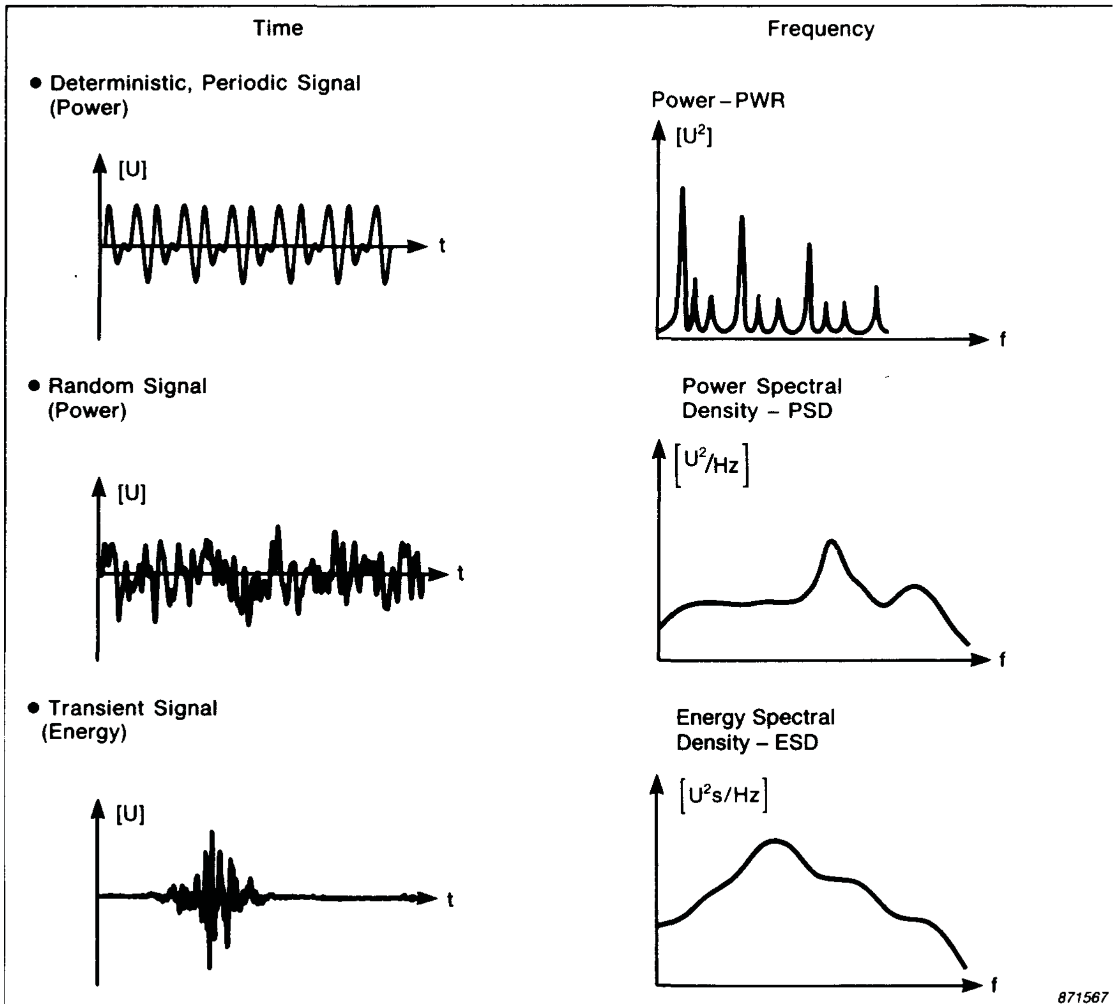

Fig. 8. Signal types and correct units

Power Spectral Density:

$$PSD = PWR/Bandwidth \quad (3)$$

Energy Spectral Density:

$$ESD = PSD \cdot Observation\ Time \quad (4)$$

It should be noted that "Power" is engineering units squared, it is not physical power because impedance is not taken into account.

As shown in Fig. 8 and summarized in Table 1:

1. Periodic, deterministic signals should be analyzed in terms of RMS or PWR spectrum units

Type of Signal	Spectrum Unit (Scaling)	Units	
		Absolute	**Relative**
Deterministic	RMS (Root Mean Square)	U	e.g. dB re 1 u
	PWR (Power)	U^2	e.g. dB re 1 u^2
Random	PSD (Power Spectral Density)	U^2/Hz	e.g. dB re 1 u^2/Hz
Transient	ESD (Energy Spectral Density)	U^2s/Hz	e.g. dB re 1 u^2s/Hz

T01643GB0

Table 1. A summary of the scaling units to be used with different signal types

2. Stationary, random signals should be analyzed in terms of PSD spectrum units
3. Transient signals should be analyzed in terms of ESD spectrum units

Correct scaling of the results is obtained by selecting the appropriate unit in the "Spectrum Unit" field for the type of signal to be analyzed.

In many practical situations where the signals are combinations of different types, for example periodic and random, RMS or PWR values should be used for scaling the sinusoidal components (individual lines in the spectrum) and PSD for the continuous part of the spectrum given by the random content of the signal.

References

[1] Gade, S. and Herlufsen, H. "*Use of Weighting Functions in DFT/FFT analysis.*", Brüel & Kjær Technical Reviews nos. 3 & 4, 1987

[2] Randall R.B. "*Frequency Analysis* ", Brüel & Kjær Book, 1987

Previously issued numbers of Brüel & Kjær Technical Review

(Continued from cover page 2)

3-1982 Sound Intensity (Part I Theory).
2-1982 Thermal Comfort.
1-1982 Human Body Vibration Exposure and its Measurement.
4-1981.1 Low Frequency Calibration of Acoustical Measurement Systems.
Calibration and Standards. Vibration and Shock Measurements.
4-1982 3-1981 Cepstrum Analysis.
2-1981 Acoustic Emission Source Location in Theory and in Practice.
1-1981 The Fundamentals of Industrial Balancing Machines and Their Applications.
4-1980 Selection and Use of Microphones for Engine and Aircraft Noise Measurements.
3-1980 Power Based Measurements of Sound Insulation.
Acoustical Measurement of Auditory Tube Opening.
2-1980 Zoom-FFT.
1-1980 Luminance Contrast Measurement.
4-1979 Prepolarized Condenser Microphones for Measurement Purposes.
Impulse Analysis using a Real-Time Digital Filter Analyzer.
3-1979 The Rationale of Dynamic Balancing by Vibration Measurements.
Interfacing Level Recorder Type 2306 to a Digital Computer.
2-1979 Acoustic Emission.
1-1979 The Discrete Fourier Transform and FFT Analyzers.
4-1978 Reverberation Process at Low Frequencies.
3-1978 The Enigma of Sound Power Measurements at Low Frequencies.

Special technical literature

Brüel & Kjær publishes a variety of technical literature which can be obtained from your local Brüel & Kjær representative.
The following literature is presently available:

○ Mechanical Vibration and Shock Measurements (English), 2nd edition
○ Modal Analysis of Large Structures-Multiple Exciter Systems (English)
○ Acoustic Noise Measurements (English), 3rd edition
○ Architectural Acoustics (English)
○Noise Control (English, French)
○ Frequency Analysis (English)
○ Electroacoustic Measurements (English, German, French, Spanish)
○ Catalogues (several languages)
○ Product Data Sheets (English, German, French, Russian)

Furthermore, back copies of the Technical Review can be supplied as shown in the list above. Older issues may be obtained provided they are still in stock.

Brüel & Kjær

DK-2850 Nærum · Denmark · Telephone: +45 2 80 05 00 · Telex: 37316 bruka dk · Fax.: 02 80 14 05

ISSN 007-2621
BV 0031-11

Printed in Denmark by Nærum Offset

Technical Review

No. 4 · 1987

Windows to FFT Analysis (Part II)
Acoustic Calibrator for Intensity Measurement Systems

Brüel & Kjær

Previously issued numbers of
Brüel & Kjær Technical Review

3-1987	Use of Weighting Functions in DFT/FFT Analysis (Part 1)
	Signals and Units
2-1987	Recent Developments in Accelerometer Design
	Trends in Accelerometer Calibration
1-1987	Vibration Monitoring of Machines
4-1986	Field Measurements of Sound Insulation with a Battery-Operated Intensity Analyzer
	Pressure Microphones for Intensity Measurements with Significantly Improved Phase Properties
	Measurement of Acoustical Distance between Intensity Probe Microphones
	Wind and Turbulence Noise of Turbulence Screen, Nose Cone and Sound Intensity Probe with Wind Screen
3-1986	A Method of Determining the Modal Frequencies of Structures with Coupled Modes
	Improvement to Monoreference Modal Data by Adding an Oblique Degree of Freedom for the Reference
2-1986	Quality in Spectral Match of Photometric Transducers
	Guide to Lighting of Urban Areas
1-1986	Environmental Noise Measurements
4-1985	Validity of Intensity Measurements in Partially Diffuse Sound Field
	Influence of Tripods and Microphone Clips on the Frequency Response of Microphones
3-1985	The Modulation Transfer Function in Room Acoustics
	RASTI: A Tool for Evaluating Auditoria
2-1985	Heat Stress
	A New Thermal Anemometer Probe for Indoor Air Velocity Measurements
1-1985	Local Thermal Discomfort
4-1984	Methods for the Calculation of Contrast
	Proper Use of Weighting Functions for Impact Testing
	Computer Data Acquisition from Brüel & Kjær Digital Frequency Analyzers 2131/2134 Using their Memory as a Buffer
3-1984	The Hilbert Transform
	Microphone System for Extremely Low Sound Levels
	Averaging Times of Level Recorder 2317
2-1984	Dual Channel FFT Analysis (Part II)
1-1984	Dual Channel FFT Analysis (Part I)
4-1983	Sound Level Meters - The Atlantic Divide
	Design principles for Integrating Sound Level Meters
3-1983	Fourier Analysis of Surface Roughness
2-1983	System Analysis and Time Delay Spectrometry (Part II)
1-1983	System Analysis and Time Delay Spectrometry (Part I)

(Continued on cover page 3)

Technical Review

No. 4 · 1987

Contents

Use of Weighting Functions in DFT/FFT Analysis (Part II) ....…..…….   1
by Svend Gade and
Henrik Herlufsen

Acoustic Calibrator for Intensity Measurement Systems ....…….. 36
by Erling Frederiksen

Use of Weighting Functions in DFT/FFT Analysis (Part II)

by Svend Gade and
Henrik Herlufsen

Abstract

Part II of the article "Use of Weighting Functions in DFT/FFT analysis" contains the following Appendices referred to in Part I of the article

A: Analogy between filter analysis and DFT/FFT analysis,
B: Windows and figures of merit,
C: Effective Weighting of overlapped spectral averaging
D: Experimental Determination of the BT product for FFT-analysis using different weighting functions and overlap,
E: Examples of User Defined Windows,
F: Picket Fence Effect

Sommaire

La deuxième partie de cet article, "Application des fonctions de pondération en analyse DFT/FFT", contient les appendices auxquels fait référence la première partie.

A: Analogie entre l'analyse par filtres et l'analyse DFT/FFT.
B: Caractéristiques des fenêtres.
C: Pondération effective des moyennes de spectres avec recouvrement.
D: Determination expérimentale du produit BT en analyse FFT, avec différentes fonctions de pondération et recouvrements.
E: Exemples de fenêtres définies par l'utilisateur.
F: Effet de barrière.

Zusammenfassung

Der zweite Teil des Artikels „Anwendung von Bewertungsfunktionen in der DFT/FFT-Analyse" enthält folgende Anhänge, auf die im ersten Teil Bezug genommen wird:

A: Analogie zwischen Filter-Analyse und DFT/FFT-Analyse

B: Fenster und mathematische Beschreibung
C: Effektive Bewertung bei spekraler Mittelung mit Überlappen
D: Experimentelle Bestimmung des BT-Produkts bei der FFT-Analyse mit verschiedenen Bewertungsfunktionen und Überlappungen
E: Beispiele für anwenderdefinierte Fenster
F: Lattenzauneffekt

Appendix A

Analogy between filter analysis and FFT/DFT analysis

In the time domain a linear filter is described by its impulse response function *h(t),* which is the response due to an infinitely short and infinitely high unit impulse (so-called Dirac Delta function δ *(t),* see Ref. [1]).

By considering any input signal x (t) to the filter as a sum of weighted and time shifted delta functions i.e.

$$x(t) = \int_{-\infty}^{\infty} x(\tau)\, \delta(t-\tau)\, d\tau \tag{A.1}$$

we find, under assumptions of linearity, that the output of the filter is

$$y(t) = \int_{-\infty}^{\infty} x(\tau)\, h(t-\tau)\, d\tau \tag{A.2}$$

or since h $(t) = 0$ for $t < 0$, that

$$y(t) = \int_{-\infty}^{t} x(\tau)\, h(t-\tau)\, d\tau \tag{A.3}$$

The output of a filter at a given point in time t_o is thus determined by the input time history up to time t_o weighted by the impulse response function inverted with respect to time and shifted to t_o i.e. $h(t_o - t)$. This is illustrated in Fig. A.1 for a simple lowpass filter with an exponential decaying impulse response function. The output at time t_o, y (t_o) is the integral (or the area) of the curve in Fig. A.1 d). Mathematically the calculation in eqn.

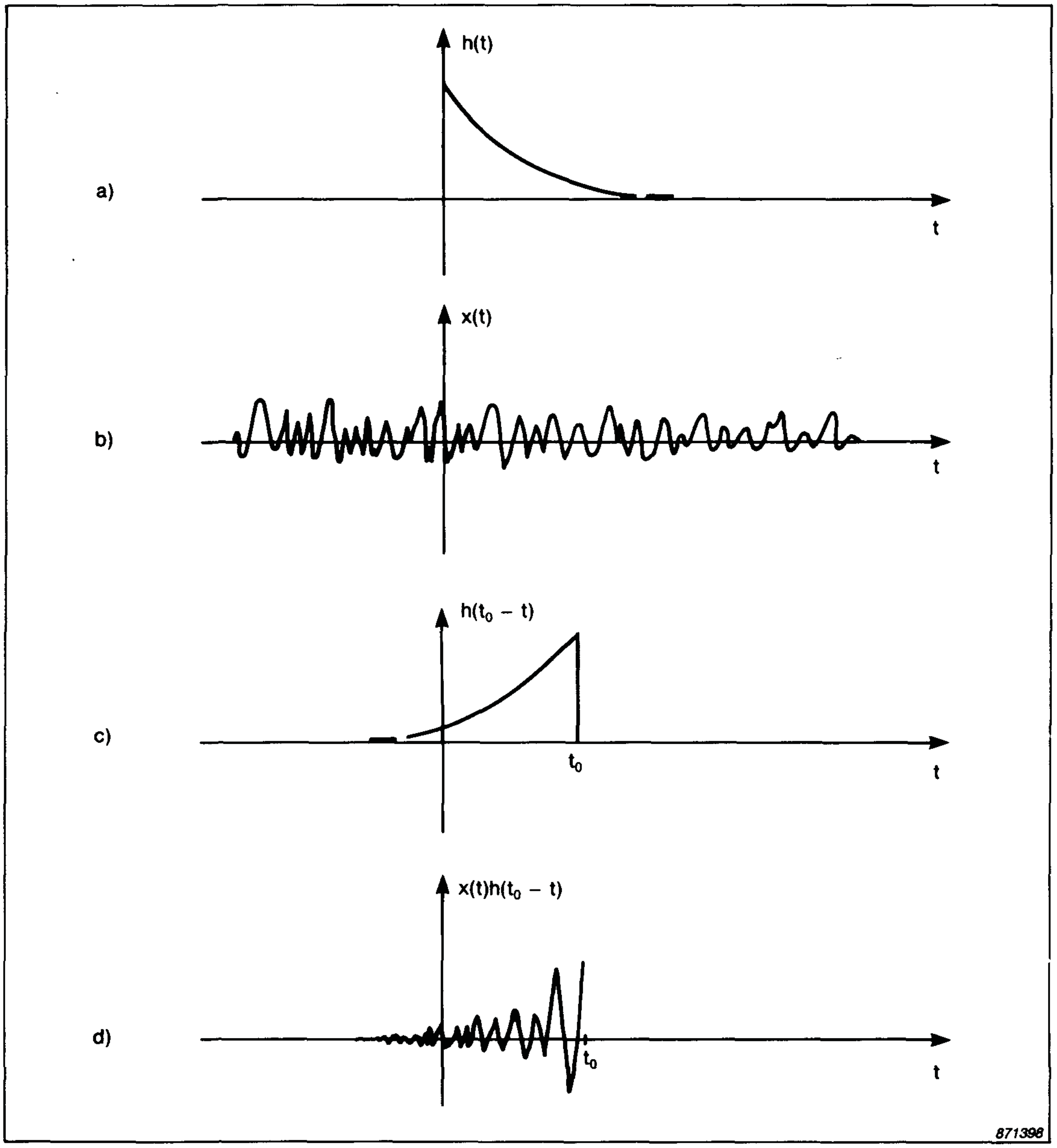

Fig. A.1. a) impulse response of a simple lowpass filter h(t),
b) input signal to be analysed x(t),
c) impulse response inverted and shifted $h(t_o - t)$,
d) weighted input signal to be integrated to give output at time t_o, $y(t_o)$

(A.3) is called convolution of $x(t)$ with $h(t)$ (denoted by $x(t) * h(t)$). Let us now have a look at the FFT/DFT calculation. To simplify the notation the integral formulation will be used instead of the discrete. The consequence of the discrete form and finite calculation time will be discussed later. Each Fourier spectrum is a transform of the input signal $x(t)$

applied with a proper weighting function $w(t)$. The transform is based on a time record of length T.

$$Y(f) = \int_{-\infty}^{\infty} x(\tau) w(\tau) e^{-j2\pi f\tau} d\tau = \int_{0}^{T} x(\tau) w(\tau) e^{-j2\pi f\tau} d\tau \qquad \text{(A.4)}$$

$Y(f)$ is the output of the transform at frequency f and at time T (neglecting for the time being the delay due to the calculation time T_{cal}). Considering this output at a certain frequency f_0 as a function of time $Y(f_0,t)$ or just $Y(t)$, we have

$$Y(t) = \int_{t-T}^{t} x(\tau)\, w\big(\tau-(t-T)\big) e^{-j2\pi f_o\left(\tau-(t-T)\right)} d\tau \qquad \text{(A.5)}$$

Rewriting this using

$$W_h(t) = w(-t+T) \qquad \text{(A.6)}$$

we get

$$Y(t) = \int_{t-T}^{t} x(\tau) w_h\big(-\tau+(t-T)+T\big) e^{j2\pi f_o\left(-\tau+(t-T)\right)} d\tau$$

or

$$Y(t) = \int_{t-T}^{t} x(\tau) w_h(t-\tau) e^{j2\pi f_o(t-\tau-T)} d\tau \qquad \text{(A.7)}$$

This is exactly the same equation as for a filter (eqn. A.3) and we can define an equivalent (complex) impulse response function $h_{\text{FT}}(t)$ for the Fourier Transform (FT) at frequency f_0 by

$$h_{FT}(t) = w_h(t)\, e^{j2\pi fo(t-T)} \qquad \text{for} \qquad 0 \le t < T \qquad \text{(A.8)}$$

$$h_{FT}(t) = 0 \qquad \text{elsewhere}$$

and (A.7) becomes

$$Y(t) = \int_{t-T}^{t} x(\tau) h_{FT}(t-\tau) d\tau \qquad \text{(A.9)}$$

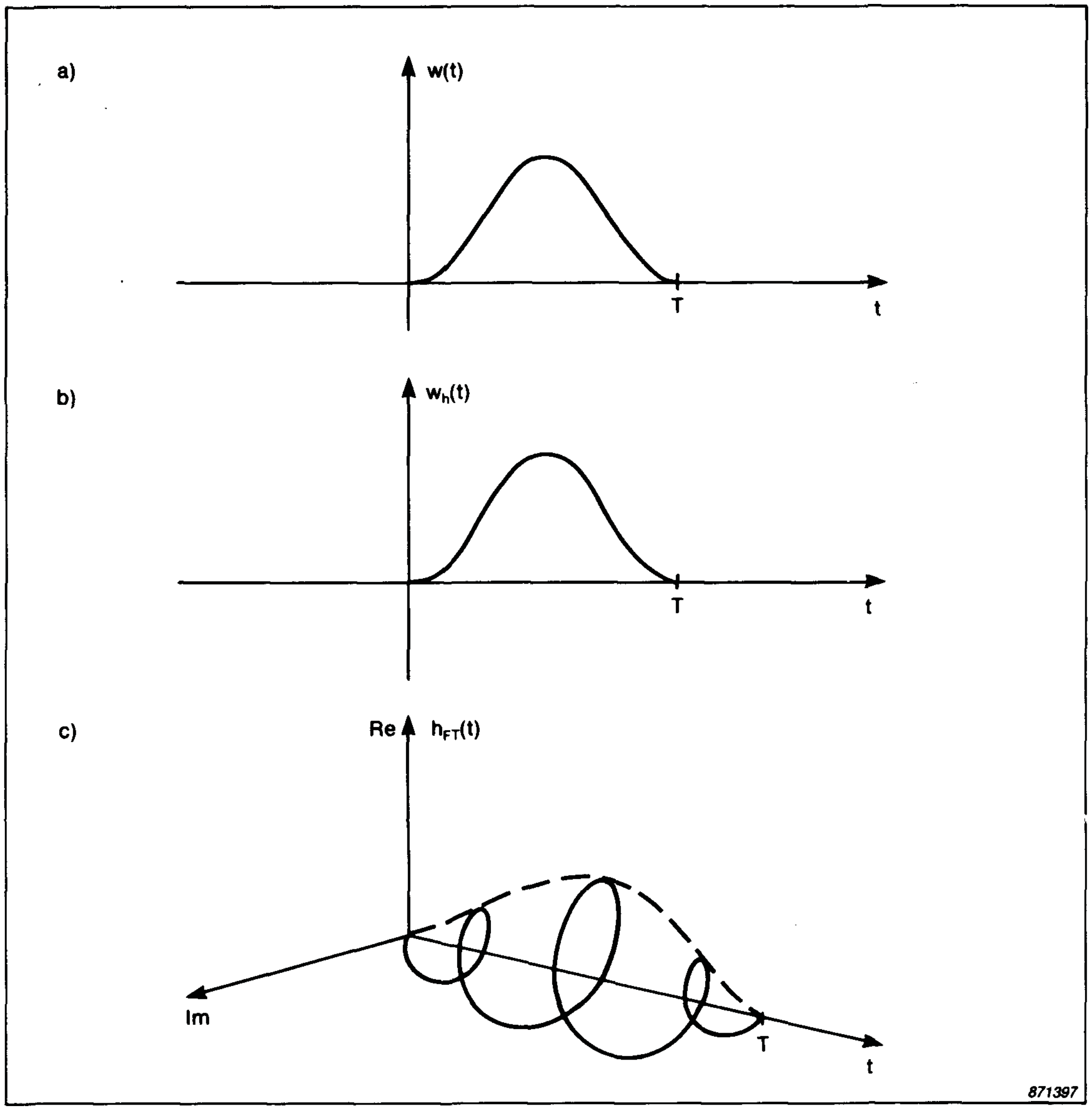

Fig. A.2. a) Hanning Weighting function w(t),
b) $w_h(t) = w(-t + T)$ *for the Hanning Weighting,*
c) complex impulse response function for filter/line at $f_0 = 4\ \Delta f$ *with Hanning Weighting*

This proves the analogy between the Finite Fourier Transform eqn. (A.9) and the filtering analysis eqn. (A.3). The impulse response h_{FT} (0 is complex and of finite length T and is determined by the weighting function $w(t)$ (equations (A.8) and (A.6)). Fig. A.2 shows an example of a weighting function and one of the corresponding complex impulse response functions.

Notice that for the commonly used weighting functions like Hanning, Rectangular, Kaiser-Bessel and Flat Top, $w\ (t) = w_h\ (t)$ since they are symmetrical around $t = {}^{T}/2$ (see also Appendix B eqn. (B.1) and table B.1).

So far we have used an integral formulation of the Fourier Transform. In practical calculations we will of course work with

a) sampled versions of the time signals and their spectra

b) finite calculation time T_{cal} of the transform

The transform which is discrete in both time and frequency domain is called the Discrete Fourier Transform (DFT). The Fast Fourier Transform (FFT) is a fast calculation of the DFT based on a certain algorithm.

re a): The time signals are sampled at time intervals $\Delta t = 1/f_s$, where f_s is the sampling frequency, and the transform will be of N samples which means that $T = N \cdot \Delta t$. The spectrum is computed at discrete frequencies $f_0 = k\ \Delta f = k\ {}^{1}/T$, where k is an integer and $0 \leq k < {}^{N}/2$. The transform is thus in its proper form written as:

$$Y(k) = {}^{1}/N \sum_{n=0}^{N-1} x(n)\, w(n)\, e^{-j2\pi\, kn/N} \qquad \text{(A.10)}$$

$x\ (n)$ is the n'th time sample in the record, $w\ (n)$ is the n'th time sample of the weighting function and $Y(k)$ is the spectral value at frequency $k\ \Delta\ f$. The factor ${}^{1}/N$ is just a scaling factor irrelevant for the discussion here.

re b): Since we have a finite calculation time T_{cal} which in most situations is much larger than the sample interval $\Delta\ t$ we will not get a continuous output as with an analog filter or a sample per sample output every $\Delta\ t$ as with a real time digital filter.

Every FFT represents a sample of the Fourier Transform filters (eqn. (A.8) and (A.9)), but the relatively long T_{cal} makes the analysis appear blockwise rather than continuous. In many applications, analysis of transients for instance, it is preferable to look at it as a transform of a data block with various trigger possibilities. This approach will be dealt with later.

In a situation where $T_{cal} \leq \Delta t$ (analysis of very low frequencies or analysis with very high zoom factors or much faster calculations than available today) the FFT will be indistinguishable from a bank of real-time digital FIR (finite impulse response) filters with (complex) impulse response functions as given in eqn. (A.8). The FFT is here assumed to work continuously i.e. with free run triggering, as a digital filter.

Since the filtering or FFT is only part of the analysis we will now look at the detector/averager.

The purpose of the detector in a filter analyzer is to measure the power (mean square) of the output signal of the filter $y\ (t)$, by time averaging of the squared signal $y^2(t)$. The averaging can be linear

$$\overline{y^2} = \frac{1}{T_a} \int_{T_a} y^2(\tau)\, d\tau \qquad \text{(A.11)}$$

or exponential

$$\overline{y^2}(t) = \frac{1}{\tau_0} \int_{-\infty}^{t} y^2(\tau)\, e^{(\tau - t)/\tau_0}\, d\tau \qquad \text{(A.12)}$$

which is a continuous running average. The bar indicates average values. For a complete discussion of this subject see Ref. [1].

The averaging in the FFT analyzer is the corresponding summation of the squared amplitudes $|\, Y(i)\, |^2$ of the output samples $Y(i)$, where i is the time or number index. Assuming a transform every T_{cal} we will have the i'th sample at time $t = t_i = i\, T_{\text{cal}}$.

This gives for linear averaging

$$|\overline{Y}|^2 = \frac{1}{N} \sum_{i=1}^{N} |\, Y(i)\,|^2 \qquad \textit{(see Footnote page 35)} \qquad \text{(A. 13)}$$

and for exponential averaging

$$|\, Y(i)\,|^2 = 1\ (\,|\, Y(i)\,|^2 + (^N/2 - 1)\ |\, Y(i-1)\,|^2) \qquad \text{(A.14)}$$

which is a discrete and recursive form of the analog version eqn. (A.12).

Notice that T_{cal} thus includes calculation of FFT as well as the averaging.

It could now be argued that in order to get a real-time analysis in the sense that all input time samples are equally weighted in the averaging process we need to fulfil the requirement.

$$T_{\text{cal}} \leqq \Delta t \qquad \text{(A.15)}$$

as for real-time recursive digital filtering.

The weighting of the input samples in each power (mean square) calculation $|\, Y(i)\, |^2$ is given by $|h_{\text{FT}}(t)|^2 = w^2_h\ (t)$, and $w_h(\text{t}) = w\ (t)$ for the weighting functions considered here as mentioned earlier.

In linear averaging this will result in an effective weighting function $w_{eff}(t)$ on the time data given by

$$w^2_{eff}(t) = \frac{1}{N}\sum_{i=1}^{N} w^2\left(t - iT_{cal}\right) \tag{A.16}$$

It turns out that if Hanning Weighting is used $w^2_{eff}(t)$ is uniform (flat) if $T_{cal} = {}^{T}\!/_{3}$, ${}^{T}\!/_{4}$, ${}^{T}\!/_{5}$, ..., i.e. if 66 $^{2}\!/_{3}$ % overlap, 75% overlap, ... can be performed. This is shown and discussed in **Appendix C.** "True" real-time analysis can thus be performed with Hanning Weighting if

$$T_{cal} \leqq {}^{T}\!/_{3}, \tag{A.17}$$

is fulfilled.

If Rectangular weighting is used no overlap would be required. This is however as discussed in the article, in general a poor choice of weighting function for continuous signals.

As an example, the B & K Analyzer Type 2032 has a $T_{cal} \approx 50$ ms in single channel mode with Hanning weighting. This gives the possibility of "true" real-time analysis (with either 66 $^{2}\!/_{3}$ % or 75% overlap) with a 3,2 kHz frequency span setting (i.e. $\Delta f = 4$ Hz, $T = 250$ ms).

After having discussed the analogy between filter and FFT analysis in the time domain and its limitations with respect to real-time operation we will now consider the analogy in the frequency domain.

The relation between input and output in the frequency domain for a filter is

$$Y(f) = H(f) \cdot X(f) \tag{A.18}$$

where $X(f)$ and $Y(f)$ are the spectra of the input and output signals respectively and $H(f)$ is the frequency response of the filter. This is a consequence of eqn. (A.3) and the convolution theorem for the Fourier Transform (Refs. [1,7,8]). $H(f)$ is the Fourier Transform of $h(t)$

$$H(f) = F\{h(t)\} \tag{A.19}$$

and is called the (complex) filter characteristic, containing both amplitude and phase information.

From eqn. (A.8) we thus find that the filter characteristic for the FFT at frequency f_0 is given by

$$H_{FT}(f) = F\{w(t)e^{j2\pi f_0(t-T)}\} \quad (A.20)$$

since $w_h(t) = w(t)$ for the weighting functions considered here.

Defining

$$F\{w(t)\} = W(f) \quad (A.21)$$

we have that

$$H_{FT}(f) = F\{w(t)\, e^{j2\pi f_0(t-T)}\} = W(f-f_o) \quad (A.22)$$

The filter characteristic for the filter/line at frequency f_0 is thus the Fourier Transform of the weighting function shifted to the relevant frequency f_0. The FFT can thus be considered as a bank of parallel, identical constant bandwidth filters with the amplitude characteristic $|W(f-f_0)|$ i.e. $|W(f)|$ I centered at the frequency f_0. This is the basis for the plots of the filter amplitude characteristics for the different weighting functions (Fig. 6, 8, 11 and 15) in Part I of this article.

For analog filters the characteristics are always complex conjugate symmetric about $f = 0$ i.e. $H(-f) = H^*(f)$. This is not true for $W(f - f_0)$, where $f_0 \neq 0$, and the FFT output $Y(i)$, for $f_0 \neq 0$, is in general complex.

The phase characteristic of the FFT filters is given by the phase of $W(f)$, $\angle W(f)$. For the weighting functions considered here which are symmetric about $t = {}^T\!/_2$ the phase is given by the time shift of ${}^T\!/_2$ as

$$\angle W(f) = -2\pi f T/2 = -\pi f T = -\pi f / \Delta f \quad (A.23)$$

or

$$\angle W(f - f_o) = -\pi (f - f_o) / \Delta f \quad (A.24)$$

The phase characteristic is linear with a shift of $-\pi$ for every Δf (filter/line spacing) see Fig. A.5 b). (A linear phase characteristic is often a main advantage in application of FIR filters).

As already mentioned another approach for the formulation of the FFT is very often used. This approach is based on the blockwise analysis and that the FFT line spectrum is considered as the Fourier Series of a periodic signal with the data block (record) being one period. The derivation of the FFT from the Integral Fourier Transform is given by the following steps:
a) time sampling, b) time multiplication - frequency convolution, c) frequency sampling. This is dealt with in detail in Refs. [4 and 7].

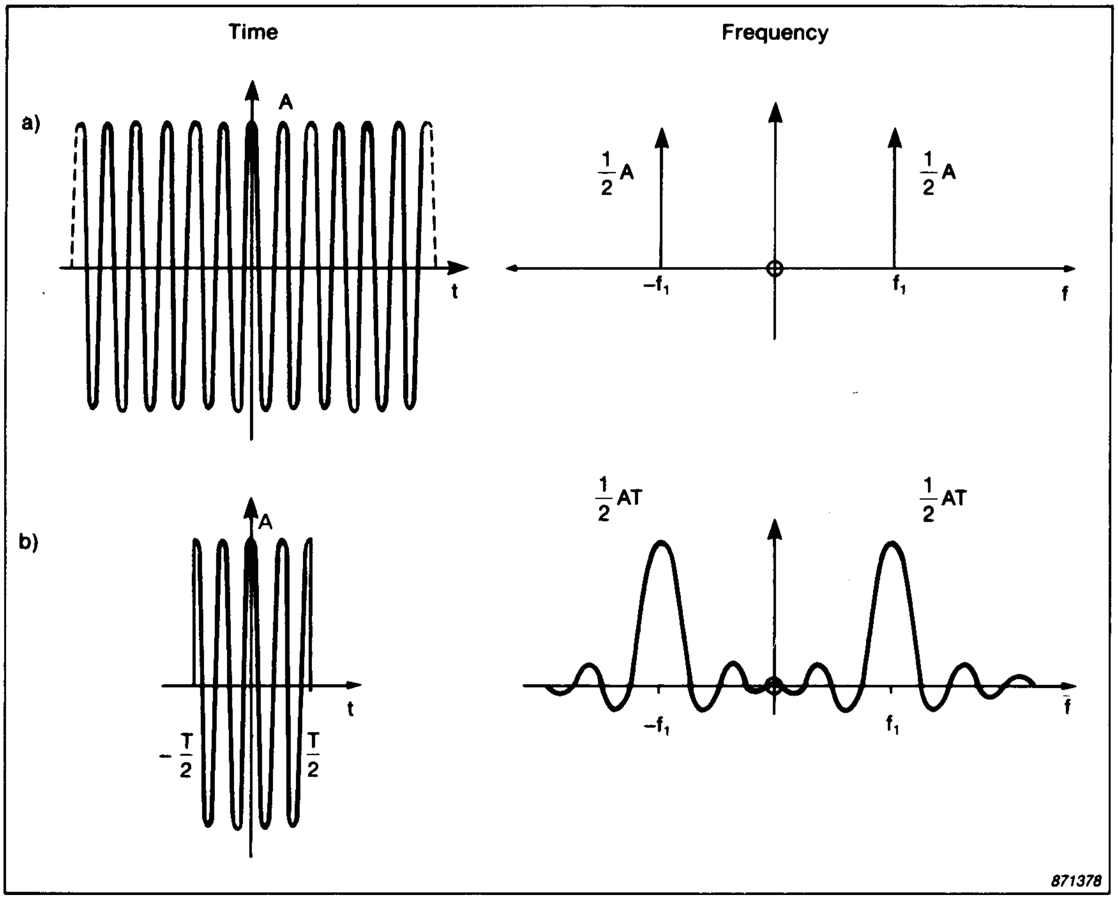

Fig. A.3. Frequency spectrum of a) a sinusoidal time signal and b) the tone burst produced by truncating the time signal in a)

Let us here take an example and see the differences and similarities of the two formulations. The signal to be analyzed is the cosine, $x(t) = A \cdot \cos(2 \pi f_1 t)$ with a Fourier Spectrum as shown in Fig. A.3.a).

Truncation of the signal by multiplication with Rectangular weighting of length T, produces the tone burst shown in Fig. A.3.b). The effect of this multiplication is a convolution in the frequency domain of the spectrum in Fig. A.3.a) with the spectrum of the Rectangular window $W(f) = T \frac{\sin(\pi f T)}{\pi f T}$ resulting in the spectrum shown in Fig. A.3.b). The convolution is written as

$$X(f) \star W(f) = \int_{-\infty}^{\infty} X(f') \cdot W(f - f') df' \qquad \text{(A.25)}$$

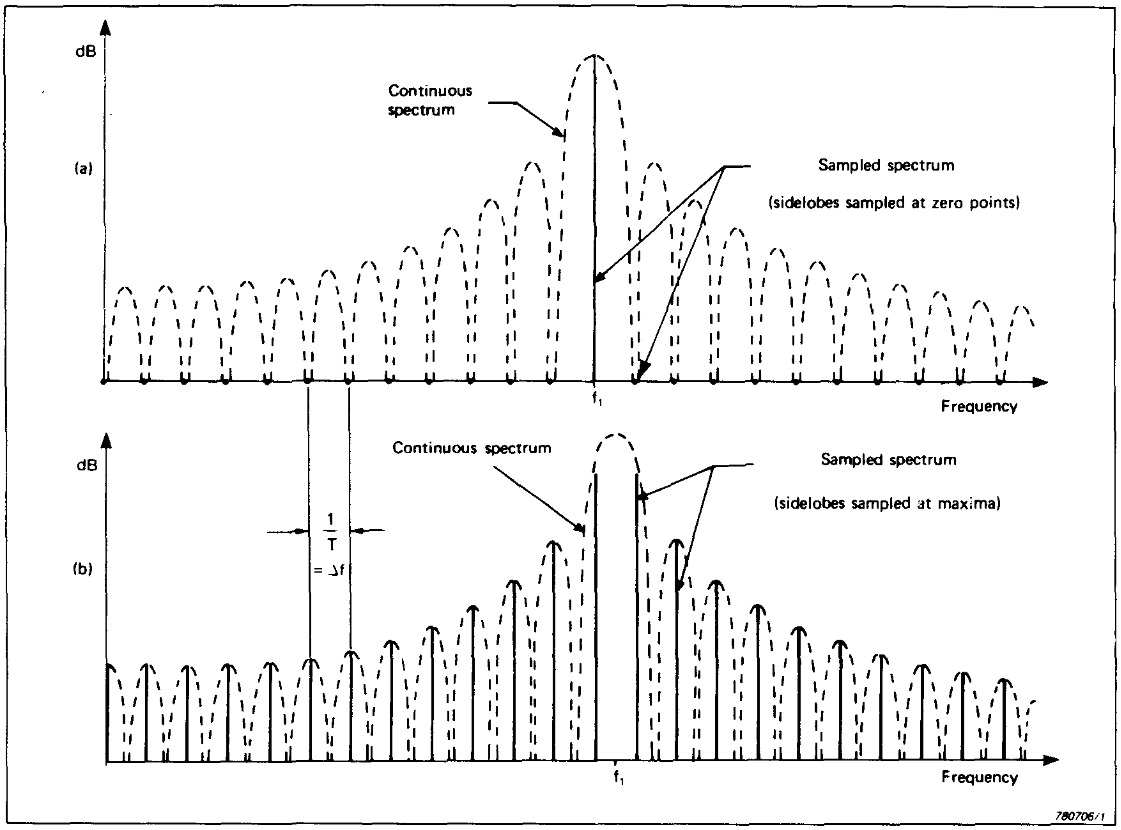

Fig. A.4. Frequency sampling of the continuous spectrum of the time limited sinusoid. Number of periods within the time window (record length) is a) integer (12) b) half-integer (12 $^1/_2$)

which can be interpreted as a swept filter analysis where $W(f_0 - f)$ is the filter characteristic.

The continuous spectrum is calculated i.e. sampled at the discrete frequencies $f = k\ \Delta f = k\ ^1/_T$. Depending upon the frequency f_1 we will get different results as exemplified in Fig. A.4. In Fig. A.4.a) f_1 coincides with one of the samples, here $f_1 = 12\ \Delta f$ (corresponding to 12 periods in the record length T), and we get only one line with the correct amplitude in the FFT spectrum. In Fig. A.4.b) however f_1 is in between two samples, here $f_1 = 12\ 1/2\ \Delta f$ (corresponding to 12 1/2 periods in the record length T) and all the side lobes will appear in the analysis and the maximum amplitude is too low. This is also referred to as leakage.

Returning to the filter analogy let us consider a bank of filters at $f_0 = k\ \Delta f$ with filter characteristics $W\ (f - f_0)(= W(f_0 - f))$ to give the same results as convolution and sampling. In Fig. A.5 it is shown how the output $Y(i)$ is found using the filter model (i is the time index as defined

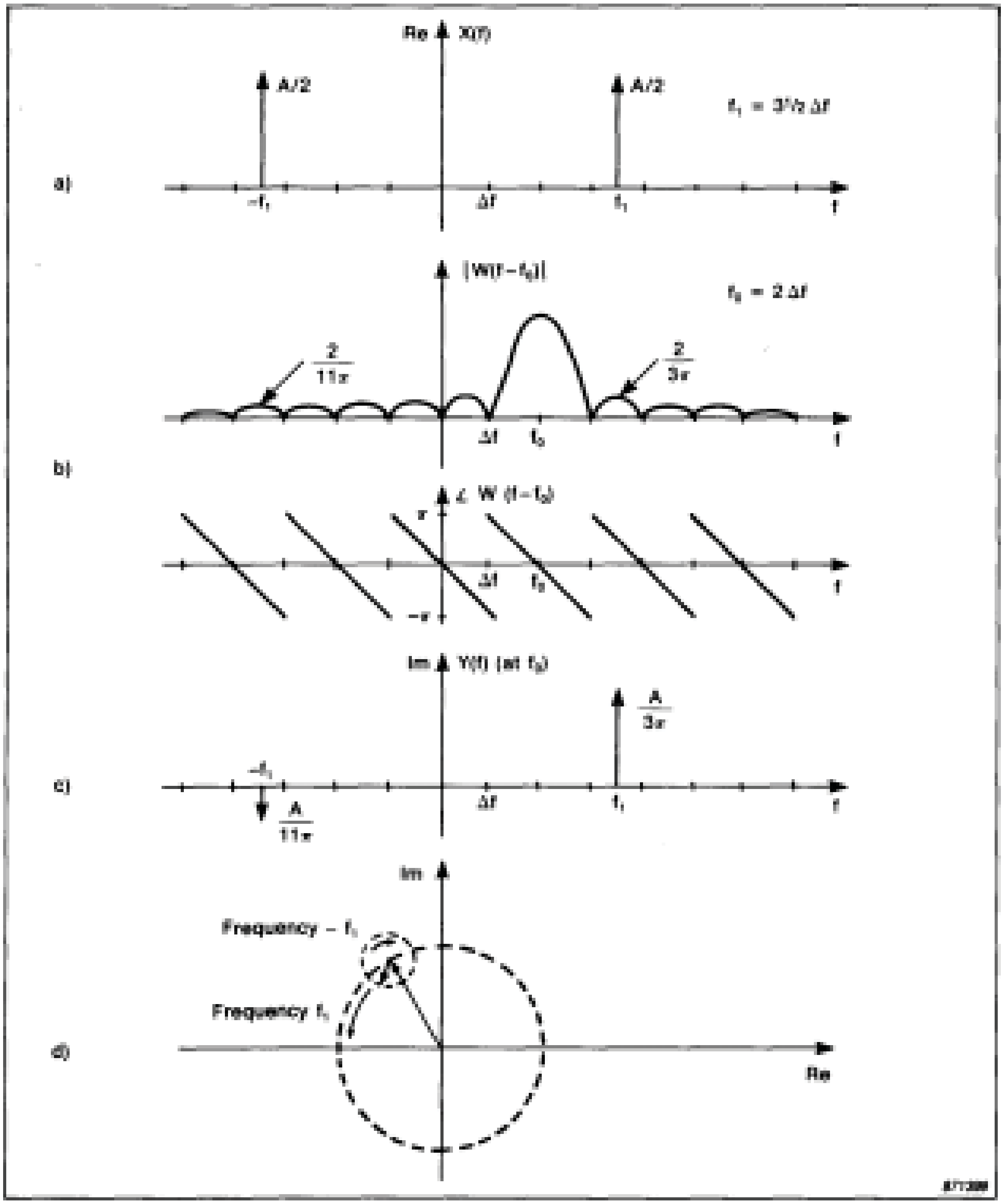

Fig. A.5. a) Spectrum of input time signal $x(t) = A \cos (2 \pi f_1 t)$, $f_1 = 3\ 1/2\ \Delta f$,

b) amplitude and phase characteristic of filter/line at $f_0 = 2\ \Delta f$, with rectangular weighting,

c) Spectrum of output signal for filter/line $f_0 = 2\ \Delta f$,

d) complex time output signal for filter/line $f_0 = 2\ \Delta f$ (sum of contra-rotating vectors with frequency of f_1 and $-f_1$ respectively) earlier). The input signal is in this example a cosine with frequency $f_1 = 3\ 1/2\ \Delta f$ and the filter considered is at $f_0 = 2\ \Delta f$ as shown in Fig. A.5 a) and b). The complex filter output at $f_0 = 2\ \Delta f$ in the frequency domain and in the time domain is shown in Fig. A.5 c) and d) respectively. $|Y(i)|$ will vary between

$$|Y(i)|_{max} = \frac{A}{3\pi} + \frac{A}{11\pi} \quad \text{and} \quad |Y(i)|_{min} = \frac{A}{3\pi} - \frac{A}{11\pi}$$

which means $\frac{|Y(i)|_{max}}{|Y(i)|_{min}} = 1{,}75$ (corresponding to 4,9 dB).

The maxima are found when the two contra-rotating vectors point in the same direction and the minima when they point in opposite directions.

This varying amplitude can be seen on the FFT analyzer when analyzing a sinusoid with free run trigger and Rectangular weighting (see Ref. [4] Fig. 8 for inst.).

In the other model this is explained by changing the phase of the input signal relative to the window, i.e truncating at different points in time. Truncating at a zero crossing of the sinusoid instead of at a maximum will give a different tone burst and a corresponding different spectrum than shown in Fig. A.3 b). The sidelobes of the sin *x/x* will add at low frequencies and subtract at high frequencies instead of subtract at low frequencies and add at high frequencies as in Fig. A.3 b). This is discussed in detail in Ref. [4].

Conclusion

The filter analogy of the FFT has been discussed and is a practical tool in many situations to better understand certain phenomena and is used extensively in this article. The limitation in the analogy with respect to real-time considerations has been pointed out as well and should be kept in mind.

The other formulation based on time multiplication - frequency convolution and sampling has proven to be a very convenient and a preferable model in several other applications of FFT.

It should be noted that these models or mathematical formulations are developed for understanding the FFT techniques. They are valid within their limitations and neither one should be considered superior to the other.

Appendix B

Windows and Figures of Merit

The mathematical formulation of the Weighting Functions used in the B & K Analyzers Types 2032 and 2034 is as follows:

$$w(t) = a_0 - a_1 \cdot \cos 2\pi\, t/T + a_2 \cdot \cos 4\pi\, t/T - a_3 \cdot \cos 6\pi\, t/T + a_4 \cdot \cos 8\pi\, t/T$$

$$= a_0 - \sum_{i=1}^{2} a_{(2i-1)} \cdot \cos 2\pi (2i-1)\, t/T + \sum_{i=1}^{2} a_{(2i)} \cdot \cos 2\pi (2i)\, t/T \quad \text{(B.1)}$$

for $0 \leqq t < T$

$w(t) = 0$ elsewhere

except for Transient and Exponential Weighting.

As can be seen the windows consist of a sum of a DC and four harmonic terms. The coefficients of the 4 standard windows implemented in the 2032 and 2034 are given in Table B.I.

	a_0	a_1	a_2	a_3	a_4
Rectangular	1	-	-	-	-
Hanning	1	1	-	-	-
Kaiser-Bessel	1	1,298	0,244	0,003	-
Flat Top	1	1,933	1,286	0,388	0,032

Table B.1. Window coefficients

Maximum Amplitude

The max. amplitude can be calculated from the sum of the window coefficients.

$$\textbf{Max}\ w(t) = \sum_{i=0}^{n} a_i \quad \text{(B.2)}$$

Another relevant quantity for windows, sometimes called the Coherent Gain, is

$$\text{Coherent Gain} = a_0/\text{Max } w(t) \tag{B.3}$$

This quantity indicates the reference amplitude gain of the filter characteristic if the maximum amplitude (Max. $w(t)$) was unity.

In 2032/34 all windows are scaled in such a manner that the "area" under the weighting function is equal to one ($a_0 = 1$). This corresponds to a reference gain of unity which ensures no power spectral bias error for a sinusoid with a frequency coinciding with one of the centre frequencies/ lines of the filters.

Effective Duration

The effective duration of the window is calculated from

$$T_{\text{eff}} = \frac{1}{(\text{Max } w(t))^2} \int_0^T w^2(t)\ dt \tag{B.4}$$

By use of (B.2) and Parseval's theorem, for the weighting function considered as a periodic function with period T, the effective duration can be calculated from the square of the window coefficients by

$$T_{\text{eff}} = \frac{a_0^2 + 2\sum_{i=1}^{n} \left(\frac{a_i}{2}\right)^2}{\left(\sum_{i=0}^{n} a_i\right)^2} \cdot T \tag{B.5}$$

The effective duration can be interpreted as a measure of the energy (integral of values squared) of the weighting function $w\ (t)$ normalized with the maximum amplitude Max. $w\ (t)$.

Effective Noise Bandwidth

The Effective Noise Bandwidth (ENBW) is defined as

$$\text{ENBW} = \frac{\int_{-\infty}^{\infty} |W(f)|^2\ df}{\text{Max } |W(f)|^2} \tag{B.6}$$

Using Parseval's theorem we find the definition in the time domain given by

$$\text{ENBW} = \frac{\int_0^T w^2(t)\, dt}{\left(\int_0^T w(t)\, dt\right)^2} \tag{B.7}$$

Again using Parseval's theorem for the weighting function considered as a periodic function with period T as previously we find, since

$$\int_0^T w(t)\ dt = a_0 T \tag{B.8}$$

that

$$\text{ENBW} = \frac{\left(a_0^2 + 2\sum_{i=1}^{n} \left(\frac{a_i}{2}\right)^2\right) T}{a_0^2 T^2} = \frac{a_0^2 + 2\sum_{i=1}^{n} \left(\frac{a_i}{2}\right)^2}{a_0^2} \cdot \Delta f \tag{B.9}$$

The reciprocal of ENBW is sometimes in the literature called the Processing Gain (PG), since an increased noise bandwidth permits additional noise to contribute to a spectral estimate, giving a lower signal to noise ratio, when detecting sinusoidal signals in noise.

Overlap Correlation

If windows are applied to non-overlapping partitions of a time sequence, a significant part of the time signal is ignored due to the fact that most windows exhibit small values near the boundaries. To avoid this loss of data, overlap analysis can be performed.

In 2032/34 standard overlap of 0%, 50%, 75% and maximum can be chosen.

The correlation as a function of fractional overlap, r can be calculated using the correlation coefficient.

$$c(r) = \frac{\int_0^T w(t) \cdot w\left(t + (1-r)T\right) dt}{\int_0^T w^2(t)\, dt} \tag{B.10}$$

Correlation Coefficient	25% Overlap	50% Overlap	75% Overlap	100% Overlap
Rectangular	0,25	0,5	0,75	1
Harming	0,0075	0,1667	0,6592	1
Kaiser-Bessel	0,0014	0,0735	0,5389	1
Flat Top	0,0005	-0,0153	0,0455	1

Table B.2. Correlation coefficients for 25%, 50%, 75% and 100% overlap for the various window functions

The correlation coefficients for 25%, 50%, 75% and 100% overlap are shown in Table B.2.

For an estimate based on the average of a number *n#d* of statistically independent records (or degrees of freedom) the BT-product (Bandwidth times Averaging Time) per filter is equal to the number of averages independent of the weighting function used

$$BT = n_d \qquad (B.11)$$

Thus the relative standard deviation, $\in_r$ for autospectra (RMS) of gaussian random signals is

$$\in_r = \frac{1}{2\sqrt{BT}} = \frac{1}{2\sqrt{n_d}} \qquad (B.12)$$

In an analysis with average of n_d records with 50% overlap the BT-product is given by (Refs. [2 and 3])

$$BT_{50\%} = [[1+2c^2(50\%)]/n_d - 2c^2(50\%)/n^2 d]^{-1} \qquad (B.13)$$

and for 75% overlap the BT-product is given by (Refs. [2 and 3]).

$$BT_{75\%} = [[1+2c^2(75\%) + 2c^2(50\%) + 2c^2(25\%)\}/n_d$$

$$- 2[c^2(75\%) + c^2(50\%) + 3c^2(25\%)]/n^2_d]^{-1} \qquad (B.14)$$

The negative terms in B.13 and B.14 are edge effects of the average and can be ignored if the number of averages, n_d is larger than ten. Also note that for most windows the correlation (squared) for 25 % overlap is small compared to 1 and can also be omitted from B.14 without significant error.

The effective BT-product per filter per record BT_{eff}. shown in Table 3 (in Part I of this article) is now calculated from

$$BT_{eff}\,(50\%) = BT_{50\%}/n_d \qquad \text{(B.15)}$$

and

$$BT_{eff}\,(75\%) = BT_{75\%}\,/n_d \qquad \text{(B.16)}$$

The theoretical values have been verified experimentally (see **Appendix D).**

An example: for a white noise gaussian random signal 123 spectra have been averaged using Hanning Weighting with 75% overlap. What is the difference in dB between the maximum and minimum values in the auto-spectrum estimate?

From Table 3 we have the effective BT-product to be 123 · 0,52 = 64. From (B.12) the relative standard deviation (68% confidence interval) is 1/16 or 0,5 dB. The 99% confidence interval is given by ± three times the standard deviation. Assuming that the maximum and minimum values of the spectral estimate will be the extremes of the 99% confidence interval we will have a difference between the maximum and minimum values of $2 \cdot 3 \cdot \in_r$, i.e. here 3 dB.

Appendix C

Effective Weighting of Overlapped Spectral Averaging

The effective weighting of an overlapped spectral average analysis can be defined as the variation of the spectral level from an impulse versus the impulse's position in time - that is the weight given to the data in the spectral average as a function of time. For example, for 50% overlap, linear averaging and Hanning window a weighting as shown in Fig. C.I is obtained. The Figure of interest here is the ripple on the spectral level, which can be defined as 10 log (Max/Min) - in the above example 3 dB.

The effective weighting is relatively easy to calculate numerically by summing a series of squared weighting functions with the specified overlap (see **Appendix A** eqn. (A.16)). The ripple periodicity must by symmetry be the same as the shift between spectra.

A case of interest is the effective weighting function obtained in overlap analysis with Hanning window applied. The ripple obtained as a function of shift between records is shown in Fig. C.2. As can be seen the ripple falls very rapidly from 3 dB for a shift of 0,5 to zero between shifts of 0,3 and 0,4. Additional zeroes are seen for smaller shifts. These actually lie in the series $^1/_3$, $^1/_4$, $^1/_5$, $^1/_6$ etc., i.e. $^1/_{(\text{integer}>2)}$.

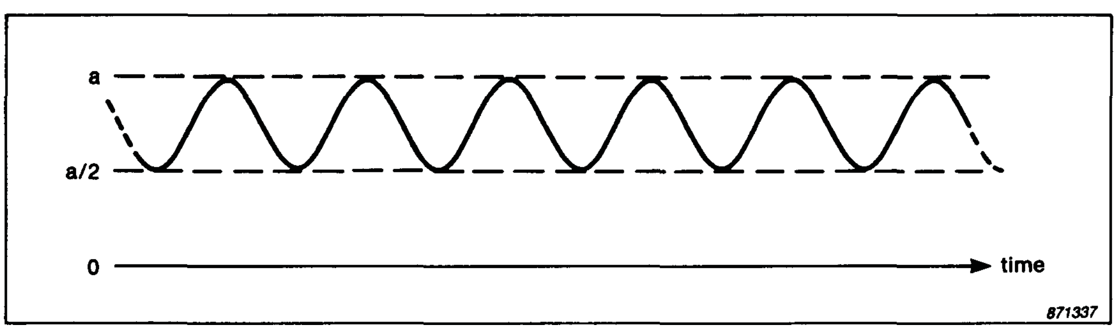

Fig.C.1. Ripple in the effective weighting of the time signal when using Hanning Weighting and 50% overlap

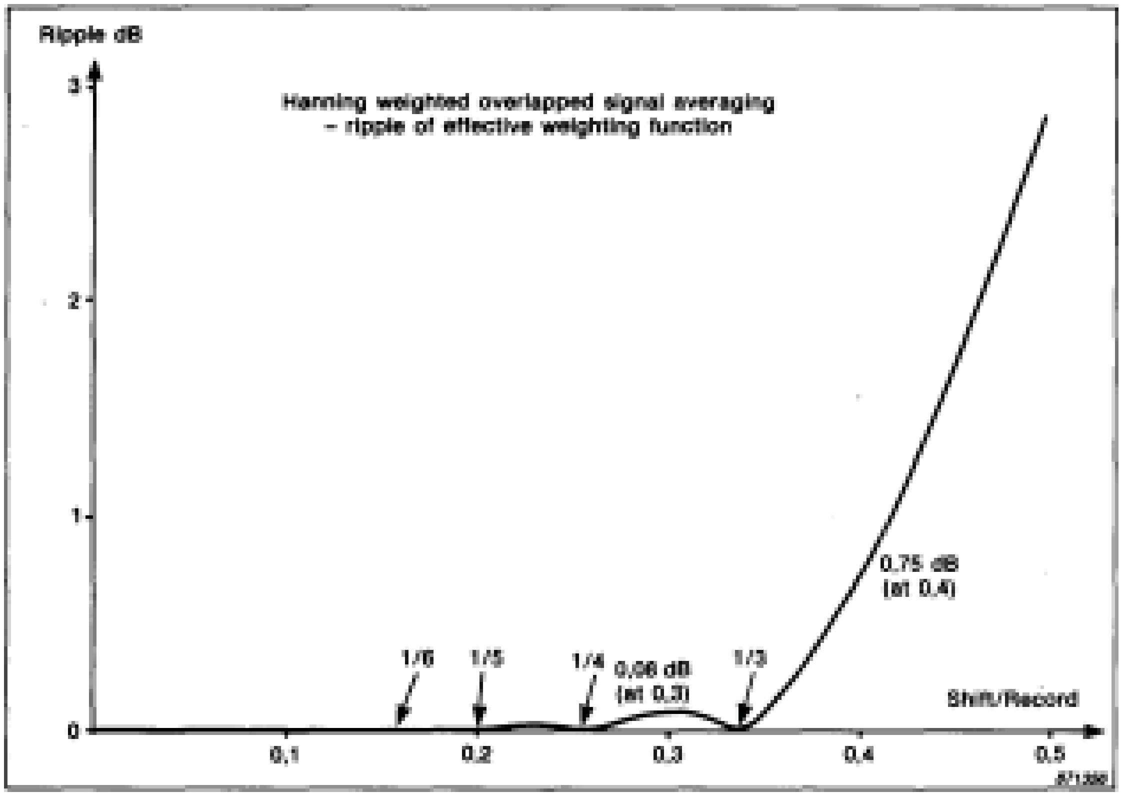

Fig.C.2. Ripple of effective weighting function using Hanning weighted overlapped signal averaging

Among other things this means that the widest analysis bandwidth for overlapped averaging to obtain a uniform weighting is found with an overlap of $^2/_3$. While $^2/3$ is not a practical shift given the normal FFT size the nearest value is quite good enough.

This situation comes about in the following manner. The squared Hanning has a form $[1 - \cos(2\pi\, {}^t/_T)]^2$ i.e. contains only a constant and the terms $\cos(2\pi\, t/T)$ and $\cos(4\pi\, t/T)$, where T is the window length. The shift of the window is equivalent to a phase shift of A for the $\cos(2\pi\, t/T)$ term and $2A$ for the $\cos(4\pi\, t/T)$ term. Considering the series of windows which affect a given impulse, the ripple is contained in these cos terms and the contribution for each term can be considered as the real part of a complex addition - the example for two windows separated by A is shown in Fig. C.3.a.

It is seen in Fig. C.3.b that when the shift is 0,5 of the window length, i.e. the phase shift $A = \pi$, the sum of only the terms with phase difference A is zero.

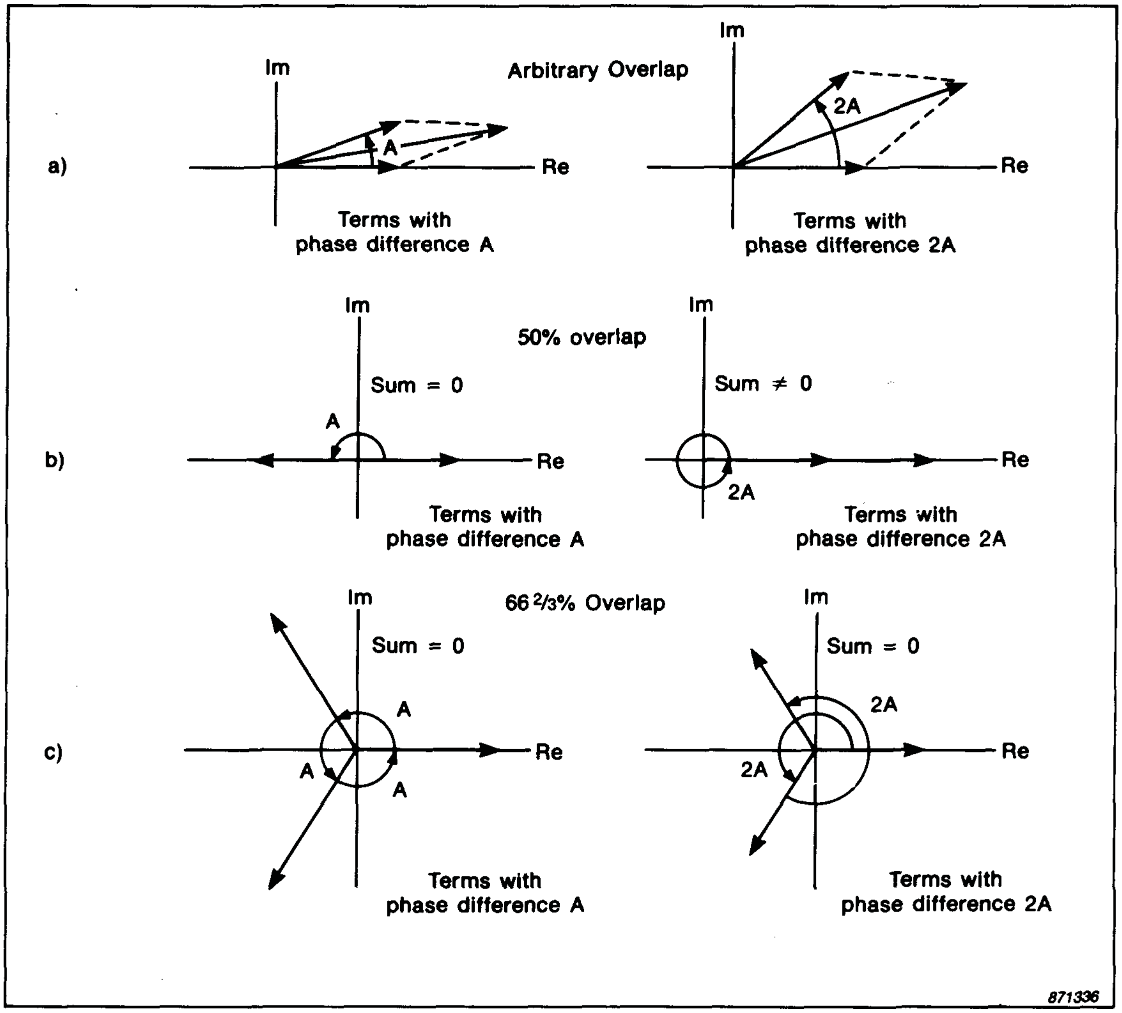

Fig.C.3. Addition (complex) of the terms with phase difference A and 2A in calculation of the ripple of the effective weighting function in situation with overlapping and Hanning

But when a shift of $^1/_3$ is used the sum of both the terms with phase difference A and $2\,A$ are zero and likewise for any shift of $^1/_{(\text{integer}>2)}$.

Thus the overlap must be $^2/_3$, $^3/_4$, $^4/_5$, $^5/_6$ etc. (see Fig. C.4) to obtain results equivalent to a true real-time analysis with parallel filters (Refs. [1,5 and 6] and **Appendix A**).

75% overlap is the most commonly used overlap, since it is an integer number of samples when the transform size is a power of two.

Using special parameter number 2 in 2032/34 an overlap of 1365 samples corresponding to nearly $^2/_3$ record length can be specified, thus giving a nearly flat weighting in the widest analysis bandwidth possible.

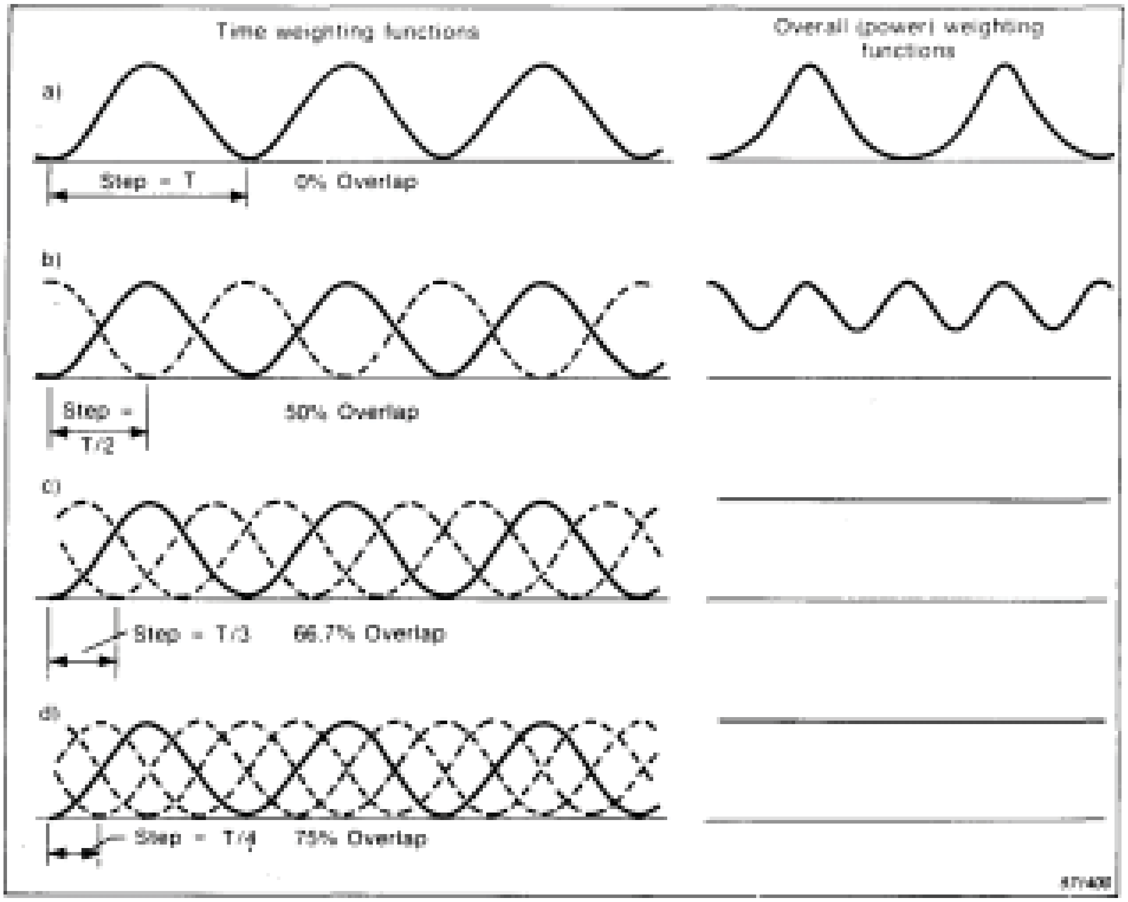

Fig. C.4. Overall weighting functions for overlapping Hanning windows

Appendix D

Experimental Determination of the BT-Product for FFT-Analysis using different weighting functions and overlap

The BT-product is determined from the relative standard deviation, $\in_r$ of the amplitude of auto-spectra estimates when analyzing a gaussian white noise random signal.

For RMS values we have

$$\in_r = \frac{1}{2 \cdot \sqrt{BT}} \Leftrightarrow BT = \frac{1}{4 \cdot \in_r^2} \qquad (D.1)$$

which means that we can determine the BT-product from experimentally determined standard deviations of autospectra estimates (measurements). The effective BT-product per record BT_{eff} is then given by

$$BT_{eff} = \frac{BT}{n_d} \qquad (D.2)$$

where n_d is number of linear averages.

The Measurement Setup is shown in Fig. D.1.

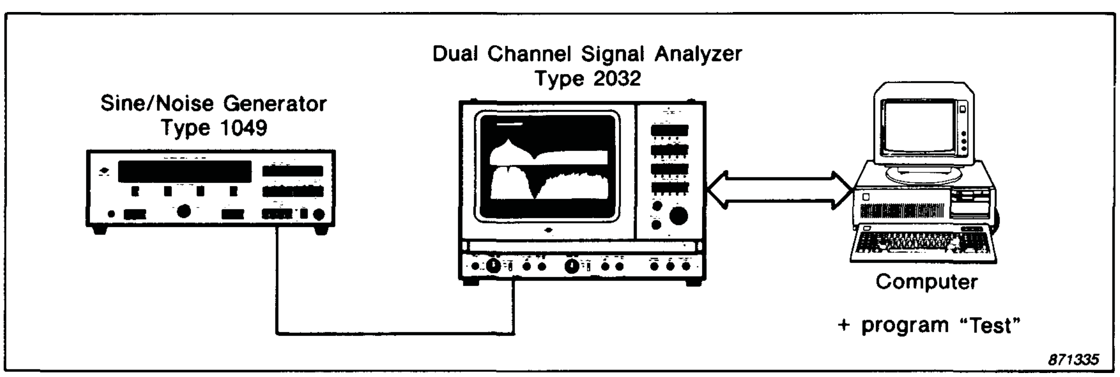

Fig. D.1. The instrumentation for experimental determination of the BT-product for FFT analysis

BT_{eff} per record	0% Overlap	50% Overlap	75% Overlap
Rectangular	0,954	0,674	0,368
Hanning	0,995	0,940	0,535
Kaiser-Bessel	1,009	0,996	0,628
Flat Top	0,990	1,000	0,994

Table D.1. Effective BT-product per record, when overlap analysis is performed (experimental values)

The number of averages (LIN), the overlap and the weighting function are chosen in the Measurement Setup of the 2032.

The readout of absolute (RMS) or relative (dB) values are chosen in the Display Setup.

The frequency interval (number of lines) and the number of estimates (measurements) are chosen in the programme.

Now the mean values and standard deviations from the autospectra at each frequency in the chosen frequency interval, as well as the mean value of these mean values and standard deviations are calculated in the computer.

A typical result is taken as the mean value of four experiments. In each experiment 100 estimates of autospectra, using 100 averages and 40 frequency lines, have been taken. Most of the results shown in Table D.I agree within 1 % of the theoretical values shown in Table 3 in Part I of this article.

Appendix E

Examples of User Defined Windows

The User Defined windows are implemented in the B & K Analyzers Types 2032/34 as

$$W(n) = \frac{2^E}{32768}\left[A_0 - A_1\cos(n\frac{2\pi}{N}) + A_2\cos(2n\frac{2\pi}{N}) - A_3\cos(3n\frac{2\pi}{N}) + A_4(4n\frac{2\pi}{N})\right] \quad \text{(E.1)}$$

$0 \leq n \leq N - 1$

N = 1024 if in Zero Pad Mode
N = 2048 if not in Zero Pad mode

Notice the slightly different formulation from the rest of this article with a common scaling factor for all the window coefficients.

In the design of User Defined windows the following criterion must be used:

The exponent E must be an integer as small as possible, however large enough to fulfil Equation (E.2).

$$2^E \geqq \sum_{i=0}^{n} a_i \quad \text{(E.2)}$$

The coefficients Ai (E.I) are now calculated

$$A_i = 2^{(15 - E)} \cdot a_i \quad \text{(E.3)}$$

Hamming Window

The Hamming window is defined as

$$w(t) = 1 - 0{,}84 \cos(2 \pi t) \quad \text{for } 0 \le t < T$$

$$w(t) = 0 \quad \text{elsewhere} \tag{E.4}$$

and has an Effective Noise Bandwidth of 1,3528 Δf.

The Hamming window can be implemented in the 2032 or 2034 using special parameters #6 to #12.

First the Noise Bandwidth is entered in special parameters #6 to #9 as

#6 and #8: 13528.
#7 and #9: -4.

Then the common exponent E in

#10: 1.

And finally the coefficients, here A_0 and A_1 in

#11: 2^{14} =16384 and
#12: $2^{14} \cdot 0{,}84$ = 13762.

This window is very similar to the Hanning Window, but has the special feature, that it suppresses the first sidelobe. However, the fall-off rate of the side-lobes is only 20 dB per decade compared to 60 dB per decade for the Hanning window. Fig. E.1 a) shows a "worst case" analysis of a sinusoid with Hamming weighting.

Blackman-Harris Window

The four term -92 dB Blackman-Harris window has the following coefficients:
$a_0 = 1$, $a_1 = 1{,}36...$, $a_2 = 0{,}39...$, $a_3 = 0{,}032....$ The Effective Noise Bandwidth is 2,00.. Δf.

The window is implemented in the 2032 or 2034 using the special parameters #6 to #14 as

#6 and #8: 2.
#7 and #9: 0.
#10: = 2.
#11: 2^{13} = 8192.
#12: $2^{13} \cdot 1{,}36$ = 11150.
#13: $2^{13} \cdot 0{,}39$ = 3226.
#10: $2^{13} \cdot 0{,}032$ = 267.

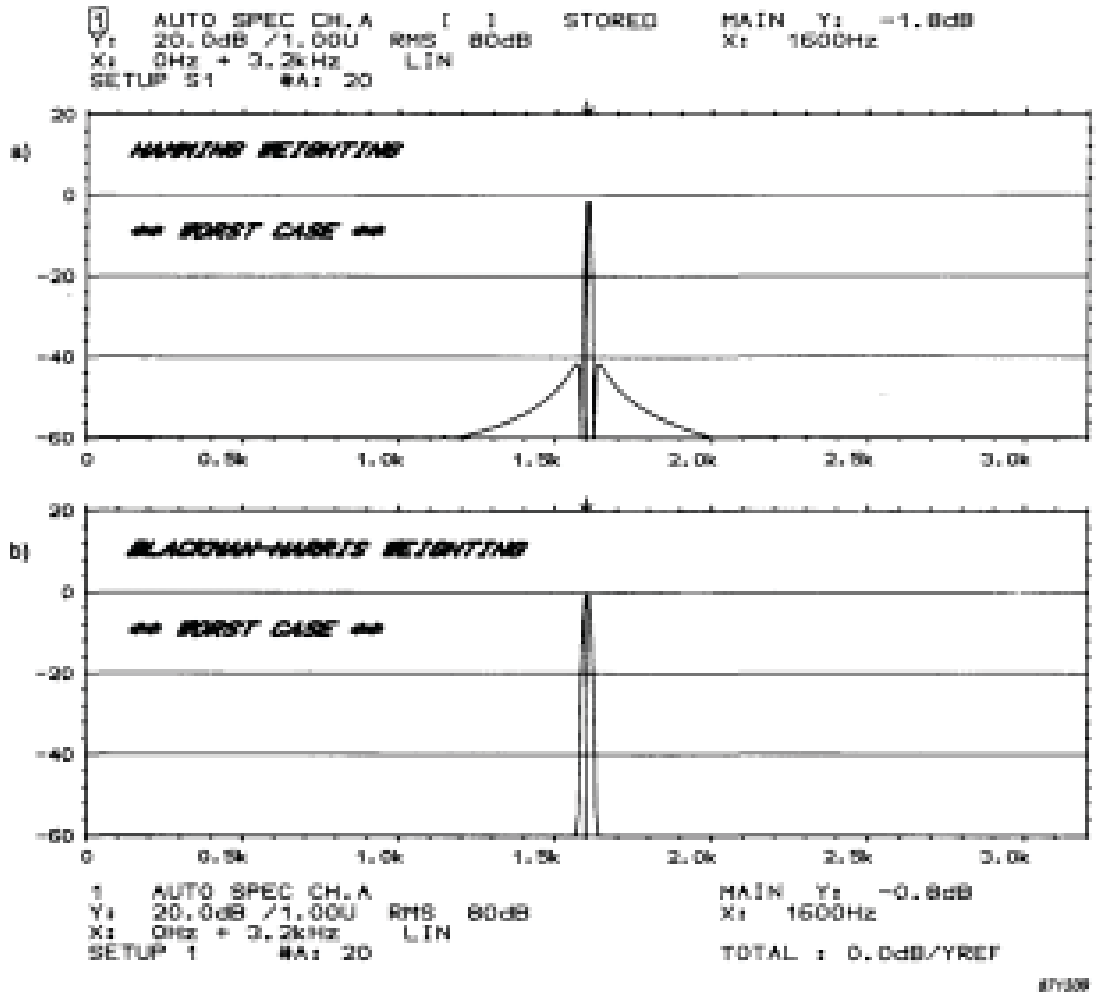

Fig. E.1. The "worst case", when analysing a sinusoid using a) Hamming window and b) Blackman-Harris window

The Blackman-Harris window has very much the same performance as the Kaiser-Bessel window Ref. [2] except that it suppresses the sidelobes more than 92 dB at a cost of an 11 % wider Noise Bandwidth. In Fig. E.1 b) a "worst case" analysis of a sinusoid with Blackman-Harris weighting is shown.

Appendix F

Picket Fence Effect

Whenever analysis with discrete fixed filters is performed, the spectrum is measured at the filter centre frequencies with a resolution given by the filter bandwidths. This is not only the case for DFT/FFT analysis, but in general when a bank of parallel filters or stepped filters are used for the analysis.

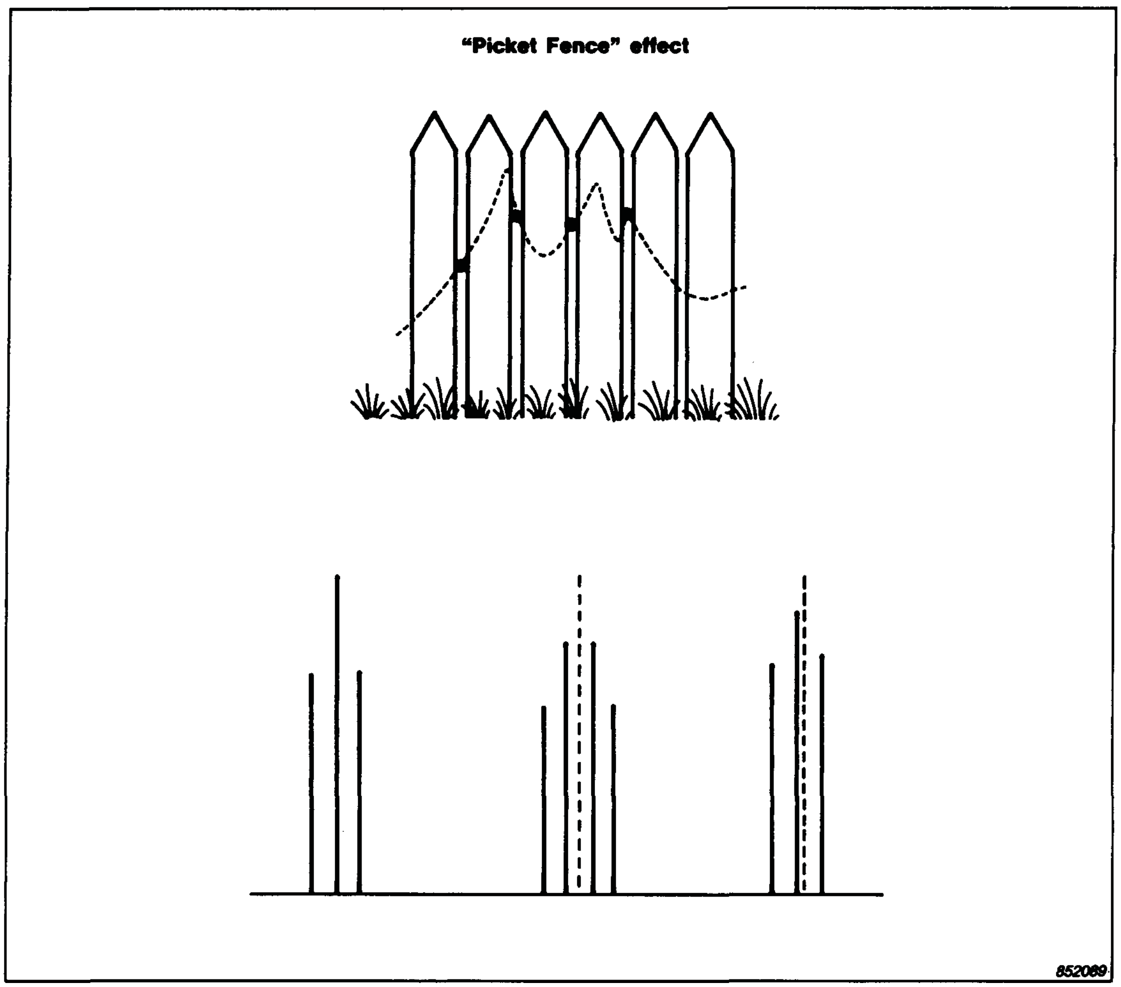

Fig. F.1. Illustration of Picket Fence Effect

The effect of only measuring the spectrum at discrete frequencies is referred to as the picket fence effect, since it is similar to viewing the continuous spectrum (measured with the given bandwidth) through a picket fence, see Fig. F.1.

As indicated in Figs. 7, 9, 12 and 16 (shown in Part I of this article) we will therefore in general get an error in both amplitude and frequency of the highest line in the spectrum of a frequency component. The amplitude error is limited by the ripple in the passband while the frequency error is limited by the line spacing Δf. The errors are referred to as picket fence effect errors. Only in the situation where the frequency component coincides with a centre frequency/line in the analysis both the amplitude and the frequency will be correct.

If we know or assume that it is a single and stable frequency component the errors can be compensated for by an interpolation technique on the well defined filter characteristics of the weighting functions, see Figs. 6, 8, 11 and 15 (in Part I of this article). The amplitude and frequency corrections can be calculated from the difference Δ, in dB, between the two highest lines around the peak. We will here limit the discussion to the Hanning window and Rectangular window, but similar formulae could be developed for other window functions.

The frequency correction, Δf_c Hz for Hanning Weighting is given by:

$$\Delta f_c = \frac{2 - 10\ \Delta^{dB/20dB}}{1 + 10^{\Delta dB/20dB}} \cdot \Delta f \qquad \text{(F.1)}$$

where Δf is the line spacing in the analysis.

The Equation F.1 is shown in graphical form in Fig. F.2 and is tabulated in Table F.1.

For Hanning Weighting, ΔdB has a maximum of 6 dB, when the frequency coincides exactly with an analysis line, and a minimum of zero dB, when it falls exactly between two lines.

The amplitude correction, ΔL dB for Hanning Weighting is given by

$$\Delta L = 20 \log \frac{\sin \pi\, \Delta f_c/\Delta f}{\pi\, \Delta f_c/\Delta f} \cdot \frac{1}{1-(\Delta f_c/\Delta f)^2} \qquad \text{(F.2)}$$

which is also shown in graphical forms in Fig. F.2 and is tabulated in Table F.1.

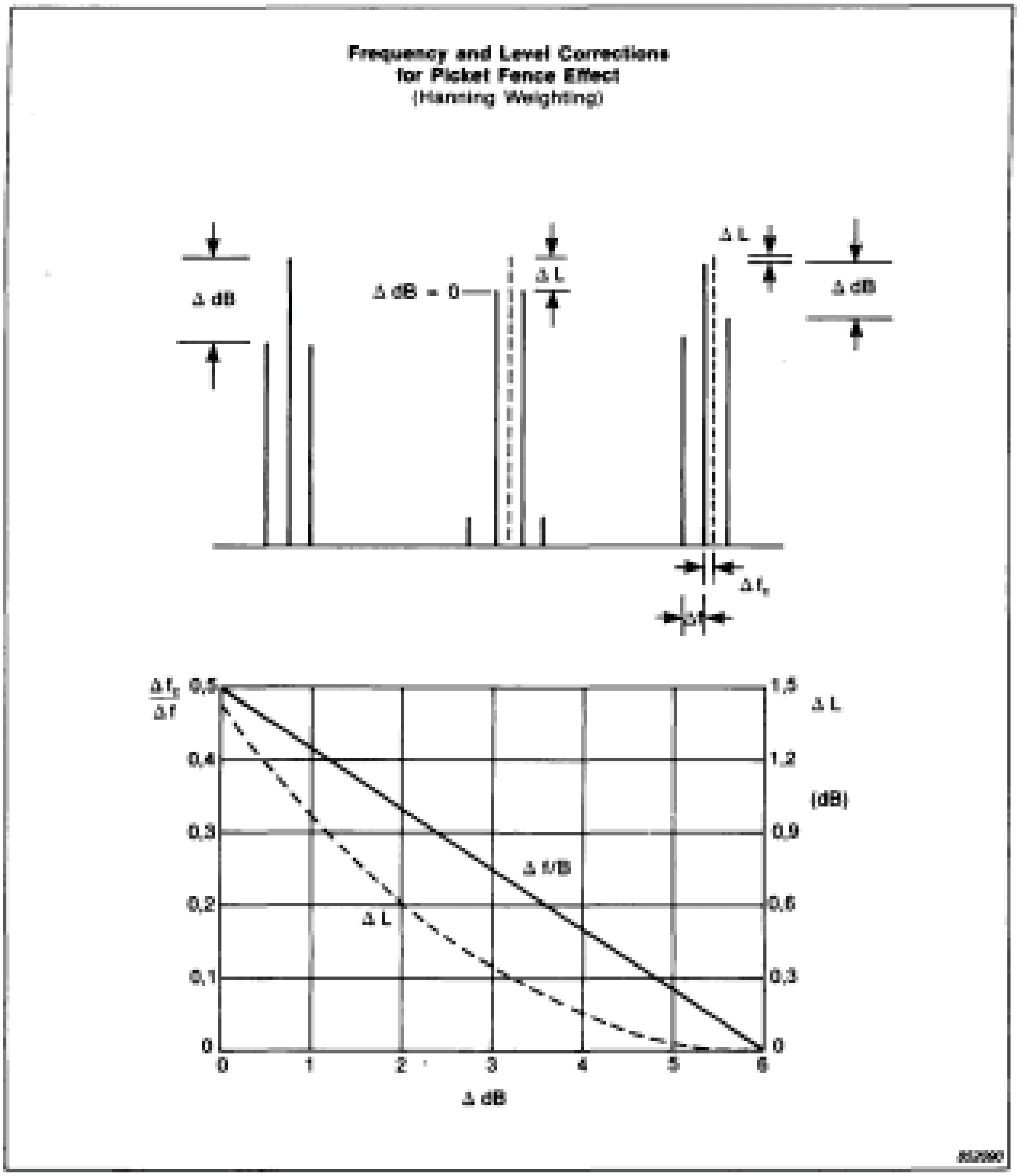

Fig. F.2. Amplitude and frequency compensation for picket fence effect with Hanning Weighting

For Hanning Weighting the amplitude correction, Δ*L* is 0 dB, when the frequency coincides exactly with an analysis line, which is indicated by a ΔdB equal to 6,0 dB. The amplitude correction is 1,42 dB, when ΔdB is equal to 0 dB, that is when the frequency of the signal is exactly between two lines.

ΔdB	ΔL	Δf_c
0.0	1.42	0.50
0.2	1.33	0.48
0.4	1.23	0.47
0.6	1.14	0.45
0.8	1.05	0.43
1.0	0.97	0.41
1.2	0.89	0.40
1.4	0.81	0.38
1.6	0.74	0.36
1.8	0.67	0.35
2.0	0.61	0.33
2.2	0.55	0.31
2.4	0.49	0.29
2.6	0.43	0.28
2.8	0.38	0.26

ΔdB	ΔL	Δf_c
3.0	0.33	0.24
3.2	0.29	0.23
3.4	0.25	0.21
3.6	0.21	0. 19
3.8	0. 18	0. 18
4.0	0. 14	0. 16
4.2	0. 12	0. 14
4.4	0.09	0. 13
4.6	0.07	0.11
4.8	0.05	0. 10
5.0	0.04	0.08
5.2	0.02	0.06
5.4	0.01	0.05
5.6	0.01	0.03
5.8	0.00	0.02
6.0	0.00	0.00

T01648GB0

Table F.1. Amplitude and frequency compensation for Picket Fence Effect with Hanning Weighting

Using this picket fence correction technique it is possible to achieve a frequency accuracy approximately 100 times finer than the line spacing. For cursor read out on 2032/34 the dB values used for these calculations can be found with two decimals rather than one in the Scratch Pad Memory octal addresses 1257 (the integer) and 1260 (the 10-exponent) for the upper graph, and 1357 (the integer) and 1360 (the 10-exponent) for the lower graph, see Fig. F.3.

For Rectangular Weighting the corresponding correction terms are for frequency

$$\Delta f_c = \frac{1}{1 + 10^{(\Delta dB / 20\ dB)}} \cdot \Delta f \qquad (F.3)$$

and for amplitude

$$\Delta L = 20 \log \frac{\left| \sin \pi \Delta f_c / \Delta f \right|}{\pi \Delta f_c / \Delta f} \qquad (F.4)$$

For system analysis where identification of resonance frequencies and dampings are essential similar techniques can be used. For lightly damped structures it is assumed that a resonance peak can be modelled by a single

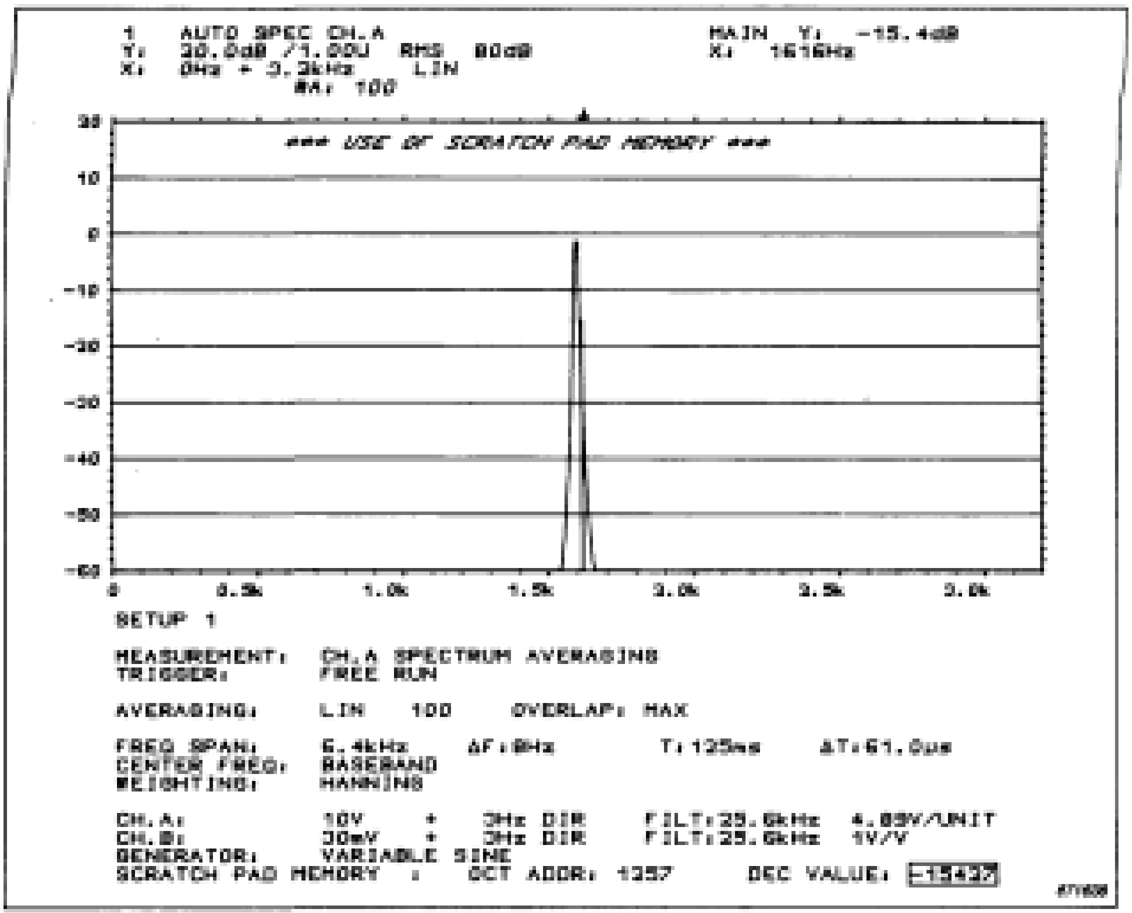

Fig. F.3. The use of scratch pad memory for readout of cursor values with higher accuracy

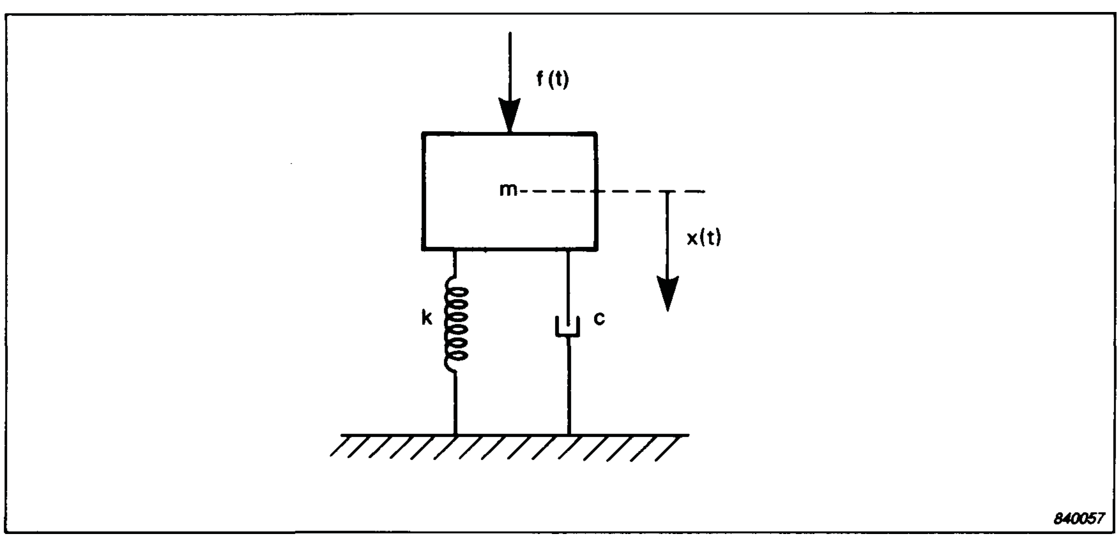

Fig. F.4. Mechanical Single Degree of Freedom (SDOF) model degree of freedom (SDOF) model, see Fig. 4. Such a model, consisting of a mass, spring and a damper (Refs. [9 and 10]) has a Frequency Response Function as shown in Fig. F.5.

Using a curvefit technique where the mathematical SDOF model is fitted to the measured Frequency Response Function using the method of least squares error, the resonance frequency, the peak amplitude and the damping can be estimated with a degree of accuracy much better than the resolution of the FFT analysis allows. The assumption is that the measurement is free of leakage.

An example is shown in Fig. F.6 where the resolution, i.e. the line spacing is 4 Hz. Pseudo-random excitation is here used to avoid leakage in the analysis. The curvefit calculates the resonance frequency with a resolution at least 100 times higher than the FFT analysis. A zoom measurement verifies the results.

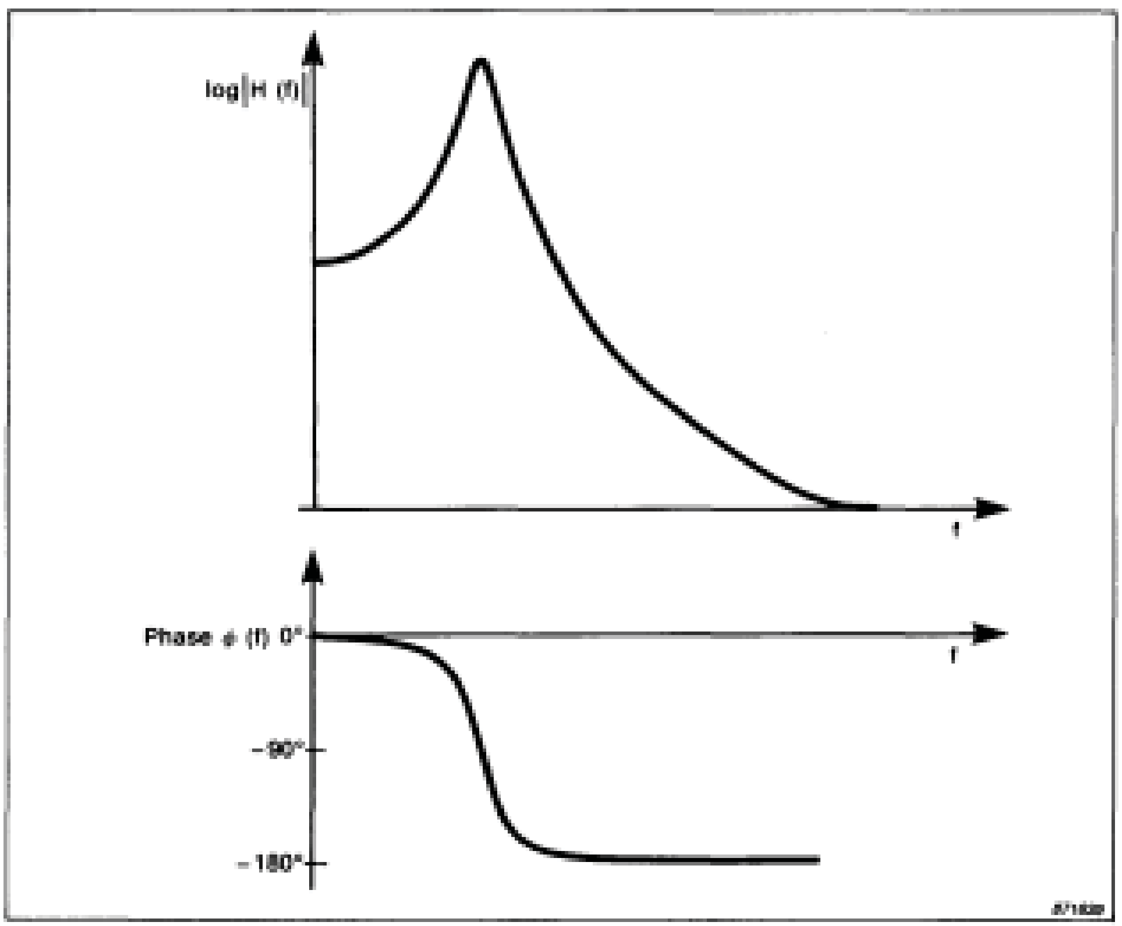

Fig. F.5. Logarithmic amplitude log |H(f)| and phase ϕ(f) of the Frequency Response Function of a Single Degree of Freedom model

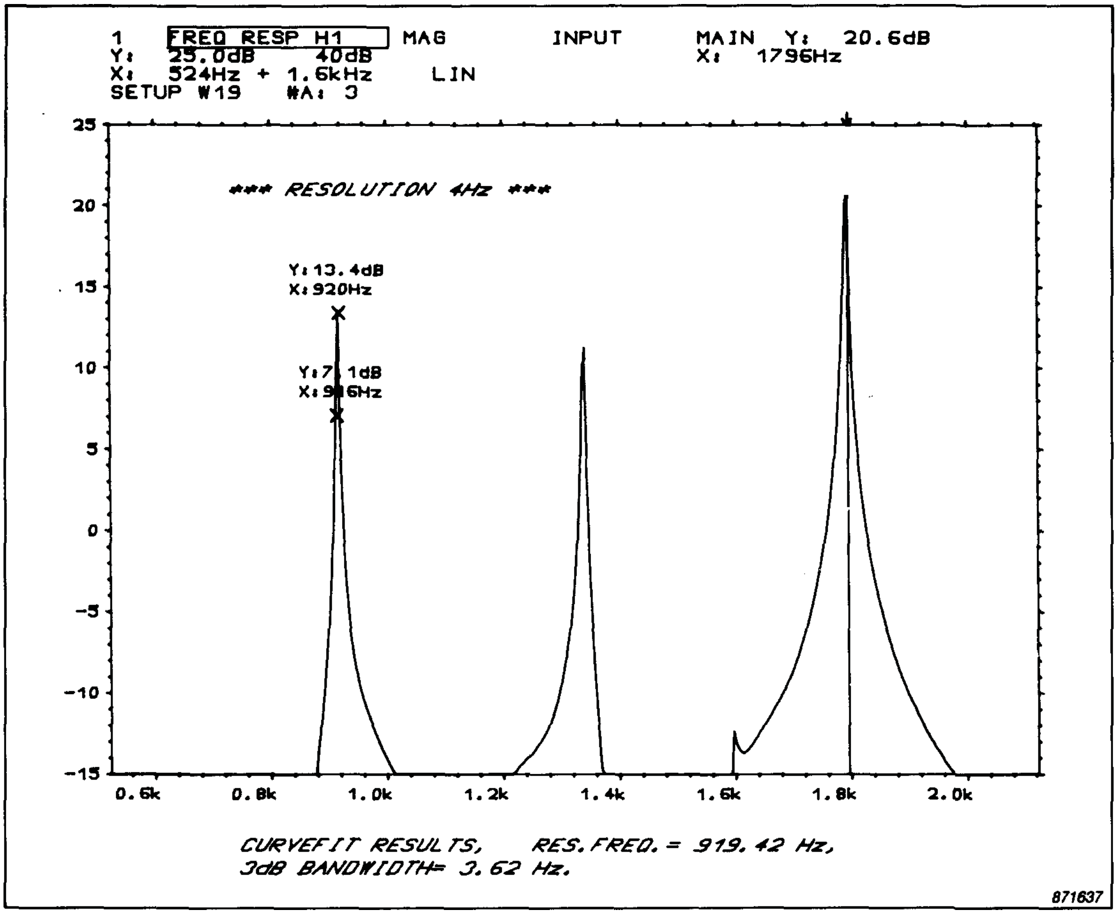

Fig. F.6. Estimation of resonance frequency and 3 dB bandwidth using a curvefit technique. Note that the line spacing in the analysis, Δf is *4 Hz*

References

[1] Randall, R.B. " *Frequency Analysis* ", Brüel & Kjær, 1987

[2] Harris, F.J. *"On the Use of Windows for Harmonic Analysis with the Discrete Fourier Transform",* Proceedings of the IEEE, Vol. 66, No.1, January 1978, pp. 51-83.

[3] Welch, P.D. "*The use of Fast Fourier Transform for the estimation of power spectra: A method based on time averaging over short, modified periodigrams",* IEEE Trans. Audio Electro Acoust., Vol. AU-15, June 1967, pp.70-73

[4] Thrane, N. "*The Discrete Fourier Transform and FFT Analyzers",* B & K Technical Review, No.1-1979

[5] Thrane, N. "Zoom *FFT",* B & K Technical Review, No.2-1980

[6] Boyes, J.D. *"Effective Weighting of Overlapped Spectral Averaging",* B & K Internal Paper, 1980

[7] Brigham, E.G. "*The Fast Fourier Transform",* Prentice Hall Inc., New Jersey, 1974

[8] Papoulis, A. "*The Fourier Integral and its Applications",* McGraw-Hill Inc., New York, 1962

[9] Herlufsen, H. *"Dual Channel FFT Analysis, Part 1",* B & K Technical Review, No. 1-1984

[10] Herlufsen, H. *"Dual Channel FFT Analysis, Part* 2", B & K Technical Review, No.2-1984

Footnote *(from page 7)*

The linear averaging algorithm used in the analyzers is:

$$\overline{|Y(i)|^2} = \frac{1}{i}|Y(i)|^2 + \frac{i-1}{i}\overline{|Y(i-1)|^2}$$

for $1 \leq i \leq N$

Thus the averaging can be stopped with correctly scaled result after any number of averages without having to wait for the predefined number of averages, N, to be performed.

Acoustic Calibrator for Intensity Measurement Systems *

by Erling Frederiksen

Abstract

A description is given of an acoustic calibrator for intensity measurement systems which use microphones of the pressure principle. The calibrator produces signals corresponding to those detected by intensity probe microphones when the probe is placed in a free progressive sound wave with either 0° or 90° incidence.

In the 90°-mode the signals of the calibrator are equal with respect to magnitude and phase. This mode can be used for pressure-sensitivity calibration of intensity systems and for measurement of residual intensity index. Calibrators supplying this type of signals have previously been described in the literature.

However, for a more rigorous calibration it should be verified that the system responds correctly also to a phase difference between the sound field signals when this differs from zero. Therefore this calibrator has also the 0°-incidence mode. In this mode the calibrator signals are equal to the signals at two points in space within a free progressive sound wave. The phase difference corresponds to a certain distance between the points which means that it is proportional to frequency. The signal magnitudes and the phase difference have revealed high stability and calibration accuracy of 0,1 dB is possible. The calibrator can also be used for particle velocity calibration.

Sommaire

Tout d'abord la description d'une source sonore étalon pour les systèmes de mesure d'intensité acoustique par microphones sensibles à la pression

* First published in Internoise 1987

est donnée. Cette source produit des signaux correspondant à ceux qui sont détectés par les microphones des sondes, lorsque la sonde est exposée à une onde sonore progressive libre avec une incidence de 0 ou de 90°.

Dans le mode 90°, les signaux de la source sont identiques en amplitude et phase. Ce mode peut être utilise pour l'étalonnage de sensibilité en pression des systèmes d'intensité et pour les mesures d'index d'intensité résiduelle. Des sources délivrant ce type de signal ont déjà été décrites dans la littérature.

Cependant, pour un étalonnage plus rigoureux, il faut vérifier que le système répond correctement lorsqu'il y a une différence de phase entre les deux signaux. C'est pour cela que la source dispose d'un mode 0°, où les signaux provenant de la source sont identiques aux signaux engendrés en deux points de l'espace par une onde sonore progressive libre. La différence de phase correspond à une distance donnée entre les points, et elle est donc proportionnelle à la fréquence. L'amplitude des signaux et les différences de phase ont révélé qu'une très grande stabilité et qu'une précision de 0,1 dB sont possibles. La source peut aussi être utilisée pour les étalonnages de vitesse particulaire.

Zusammenfassung

Es wird ein akustischer Kalibrator für Intensitätsmeßsysteme mit Druckmikrofonen beschrieben. Das vom Kalibrator erzeugte Signal entspricht dem von einer Intensitätssonde aufgenommenen, wenn sich dieses in einem freien Schallfeld mit 0°- oder 90°- Einfall befindet.

Beim 90°-Betrieb erzeugt der Kalibrator Signale, die nach Betrag und Phase gleich sind. Hiermit läßt sich der Druckübertragungsfaktor des Intensitätsme#systems kalibrieren sowie der Remanenz-Intensitätsindex bestimmen. Kalibratoren, die diese Signalart erzeugen, wurden bereits früher in der Literatur beschrieben.

Für eine strengere Überprüfung der Kalibrierung sollte auch das Verhalten bei Signalen, die eine unterschiedliche Phasenlage besitzen, untersucht werden. Hierfür besitzt der Kalibrator den 0°-Betrieb. Hier erzeugt der Kalibrator Signale, die den Signalen an zwei räumlich verschiedenen Stellen einer sich frei fortpflanzenden Schallwelle entsprechen. Die Phasendifferenz entspricht einem gegebenen Abstand im Raum, d.h. sie ist frequenzproportional. Der Betrag und die Phasendifferenz der Signale sind hochstabil und eine Kalibriergenauigkeit von 0,1 dB ist möglich. Der Kalibrator läßt sich auch zur Teilchenschnelle-Kalibrierung einsetzen.

Introduction

Today measurement of sound intensity has proved its usefulness for noise analysis. Instruments are constantly improving, but as they are quite complex many users have desired means of calibration to gain further confidence in their measurement results.

Most systems use pressure microphones and practically all field calibrations made today are pressure calibrations of the system channels. In fewer cases the channels are also tested for equality of their phase responses - usually at one frequency only.

An acoustical calibrator for a far more extended calibration has been developed. According to known principles it can be used for pressure level calibration at 250 Hz and for phase check by measurement of residual intensity index between 10 Hz and 5 kHz.

In addition to these features the calibrator has an extra operation mode in which it produces signals for calibration of intensity and particle velocity sensitivity of instruments operated in these modes. This new mode is the main theme of this paper.

Operation Principle of Intensity System with Pressure Microphones

Most measurement systems which employ pressure microphones determine the instantaneous values of particle velocity, $u(t)$ and of the sound intensity, $I(t)$ in accordance with the following expressions:

$$u(t) = \int \frac{p_1(t) - p_2(t)}{\rho_o \Delta r_o} dt \, ; \quad I(t) = \frac{p_1(t) + p_2(t)}{2} \int \frac{p_1(t) - p_2(t)}{\rho_o \Delta r_o} dt$$

$P_1(t), p_2(t)$: instantaneous values of the pressure signals
$\Delta r_o, \rho_o$: system parameters for microphone distance and air density

For sinusoidal signals the measured values of the particle velocity, u [rms] and of the time average value of sound intensity, $\bar{I}$ become:

$$u[\text{rms}] = \frac{\left(\left[(P_1 + P_2) \sin \phi/2\right]^2 + \left[(P_1 - P_2) \cos \phi/2\right]^2\right)^{0,5}}{\omega \rho_o \Delta r_o}$$

$$\bar{I} = \frac{P_1 P_2 \sin \phi}{\omega \rho_o \Delta r_o}$$

P_1, P_2: rms-values of the sinusoidal pressure signals

ϕ, ω: phase angle between the pressure signals and angular frequency

Operation of the Sound Intensity Calibrator

The formulae above show that the measurement results are functions of four signal parameters. Therefore a calibrator has to produce signals for which these parameters are stable as functions of time and perform in a predictable way under common environmental conditions.

A calibrator which statisfies these requirements has been developed. It consists of a sound source and of a special coupler with two cavities, (a) and (b), see Fig. 1. The cavities have ports (1, 2 and 3) for connection of intensity probe microphones. One of the cavities (a) is directly connected to the source while the second cavity (b) is coupled to (a) via an acoustical coupling element which contains a resistance and a mass in series connection.

At low frequencies the acoustical network formed by the coupling element and by the compliance of cavity (b) creates cavity signals with a phase difference which is proportional to frequency and with magnitudes which are nearly equal. These properties exactly comply with the pressure at two points in a space where a plane sound wave is propagating. Thus for a pressure microphone probe the calibrator can simulate a free field wave with definable levels of sound pressure, particle velocity and intensity.

The coupler has been designed to create a phase difference corresponding to that valid for 50 mm microphone distance with an angle of zero degrees between the probe axis and the wave's propagation direction. The coupler properties are independent of the choice of sound source but a well defined source is needed for sensitivity calibration, therefore a piston-

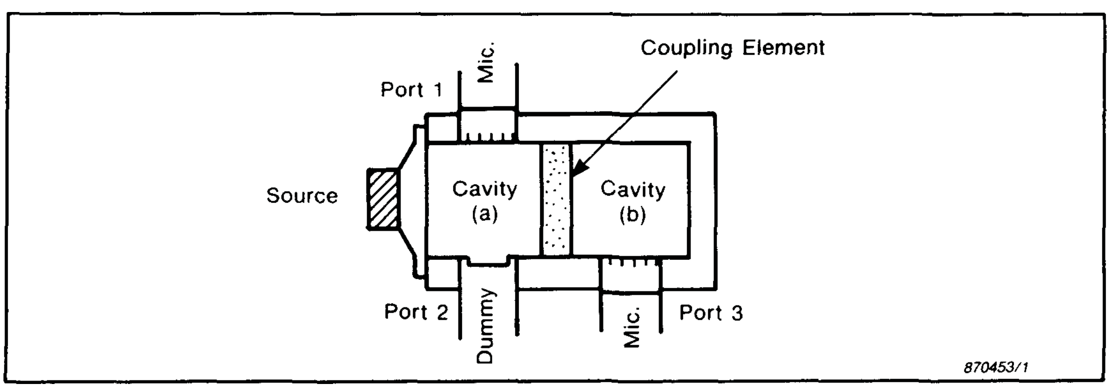

Fig.1. Principle of the intensity calibrator. The microphones are placed in the ports (1) and (3) for calibration of intensity sensitivity

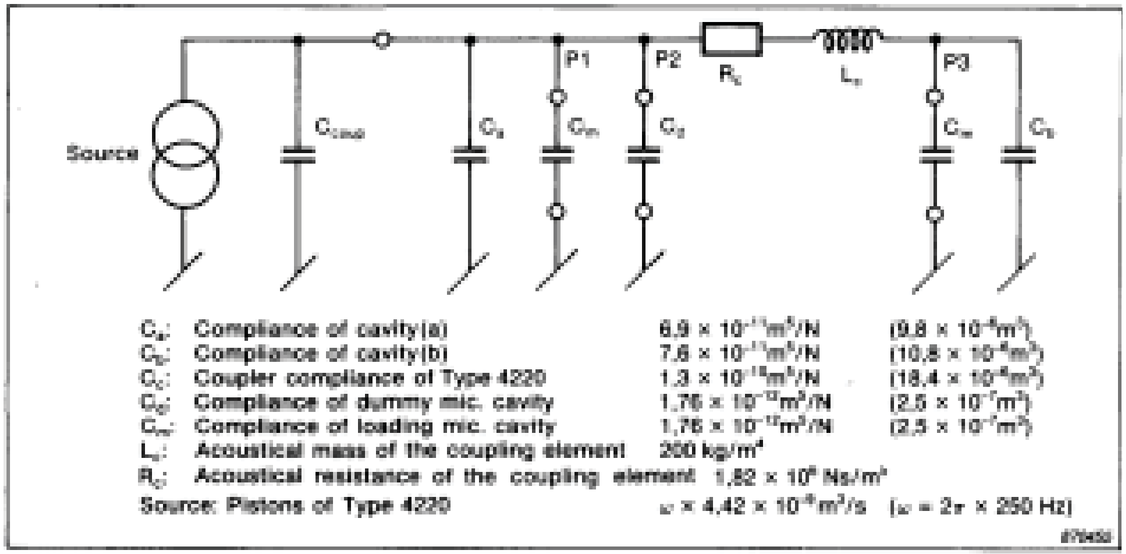

Fig.2. Model of the calibrator driven by the pistonphone with values valid at 1013 mbar and 20° C. The microphones are placed in the ports (1) and (3) for intensity or velocity calibration

phone, B & K Type 4220 was chosen for operations of this mode. See a model of the calibrator in Fig. 2.

The magnitude and phase differences between the pressure of the cavities, (b)-(a) have been measured and calculated, see Fig. 3 which also shows that within the range from a few Hz to about 500 Hz the phase difference between the ports is nearly equal to the free-field phase lag for points 50 mm apart. When driven by a pistonphone at 250 Hz the sound

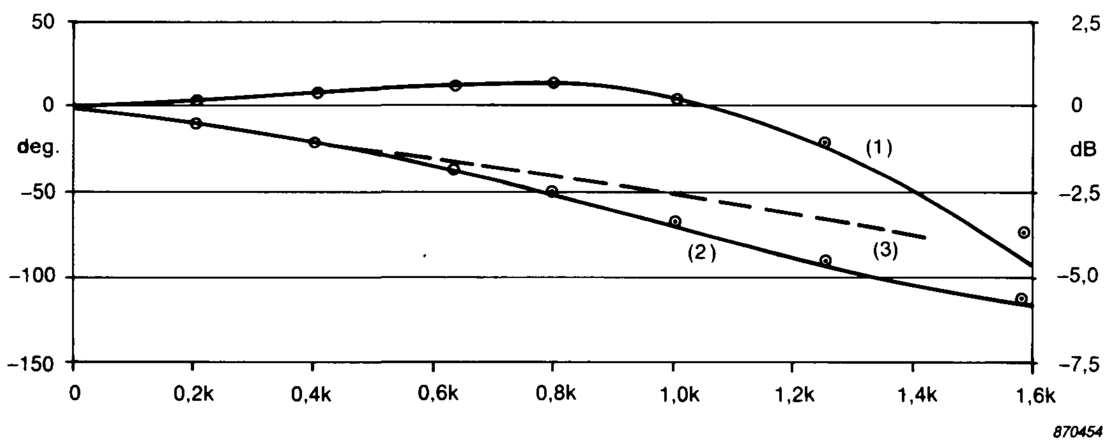

Fig. 3 Magnitude difference (1) and phase difference (2) between the pressure of the calibrator cavities, (b)-(a) were measured (curves) and calculated (points). The dotted line (3) shows the free-field phase lag for points 50 mm apart at 20° C

pressure levels of the cavities are nominally 118 dB therefore the particle velocity and intensity levels are also close to this value.

Due to the phase linearity with frequency the levels are not critical with respect to frequency. At 250 Hz the slopes are as small as + 0,7 x 10^{-3} dB/Hz for intensity and + 1,5 x 10^{-3} dB/Hz for velocity.

Environmental Influences

The pressure and intensity levels as functions of the ambient pressure were measured with an FFT-analyzer and together with the particle velocity level they were also calculated by use of the model. The results are listed in the table below.

Attention should be paid to the agreement between the measured and the calculated results and to the fact that the intensity level is practically independent of the ambient pressure. Notice that the pressure level follows the ambient pressure (last line of the table) while the particle velocity level shows the same changes but in the opposite direction.

By measurement and calculation the temperature coefficient of the intensity level has been found to be + 0,024 dB/°C.

Amb. pressure, p_a	mbar	700	800	900	994	1000	1013
L_I measured	dB	-0,12	-0,07	-0,02	0	+0,01	-
L_I calculated	dB	-0,06	-0,03	-0,01	0	0	0
L_p cav.(a) measured	dB	-2,89	-1,80	-0,82	0	+0,05	-
L_p cav.(a) calculated	dB	-2,87	-1,79	-0,82	0	+0,05	+0,16
L_v calculated	dB	+2,93	+1,82	+0,83	0	-0,05	-0,15
20 log (P_a/994)	dB	-3,05	-1,89	-0,86	0	+0,05	+0,16

Notes for Application of the Calibrator

The calibrator is designed for laboratory as well as field use. The calibrator supplies sound pressure to the microphone diaphragms only. The calibrator works correctly with the newly introduced microphone types which are especially designed for intensity measurements and which have extremely low vent-sensitivity.

In the calibration mode for intensity sensitivity only very small errors will occur with ordinary measurement microphones while significant errors might occur in the mode for measurement of residual intensity index, especially at low frequencies.

Accuracy and Calibration of the Intensity Calibrator

Determination of the calibrator's intensity and particle velocity levels requires calibration of sound pressure, frequency and of the phase difference between the cavities which is more simple to measure than might be expected as microphones with known phase characteristics are not needed.

Calibration can be made with any two microphones which load the coupler correctly, i.e. with 250 mm^3. During the first phase measurement the microphones are inserted arbitrarily in the ports (1) and (3) while they are interchanged before the second measurement. The difference between the results is twice the phase difference between the cavities. The method eliminates a possible phase difference between the channels of the applied phase meter. The resulting calibration levels are found by inserting the measured values in the formulae given under the discussion of the measurement principle.

An accuracy of the intensity calibration level better than 0,15 dB is rather easy to obtain and seems relevant in practice as artificial stability tests have given very promising results for the calibrator.

Conclusion

An intensity calibrator with a possible accuracy of 0,1 dB has been developed. The calibrator can simulate two angles of sound incidence on the intensity probe, 0° or 90°. In the 0°-mode sensitivity of measurement systems can be calibrated while in the 90°-mode the residual intensity index can be measured.

It might be necessary to correct the calibrator's intensity level for the temperature but the ambient pressure has practically no influence at all.

The principle is new but the properties of the calibrator have been measured under different environmental conditions and a model has been worked out. The good agreement between the behaviour of the calibrator and the model shows that all significant physical effects are known.

For assistance with the experiments the author wishes to thank A. Halfdaner.

References

[1] Rasmussen, G., Brock, M. "*Transducers for intensity measurements*", ICA, Paris 83

[2] Frederiksen E. *"Pressure microphones for intensity measurements with significantly improved phase properties"*, ICA, Toronto, '86

Previously issued numbers of Brüel & Kjær Technical Review

(Continued from cover page 2)

4-1982	Sound Intensity (Part II Instrumentation and Applications) Flutter Compensation of Tape Recorded Signals for Narrow Band Analysis
3-1982	Sound Intensity (Part I Theory).
2-1982	Thermal Comfort.
1-1982	Human Body Vibration Exposure and its Measurement.
4-1981	Low Frequency Calibration of Acoustical Measurement Systems. Calibration and Standards. Vibration and Shock Measurements.
3-1981	Cepstrum Analysis.
2-1981	Acoustic Emission Source Location in Theory and in Practice.
1-1981	The Fundamentals of Industrial Balancing Machines and Their Applications.
4-1980	Selection and Use of Microphones for Engine and Aircraft Noise Measurements.
3-1980	Power Based Measurements of Sound Insulation. Acoustical Measurement of Auditory Tube Opening.
2-1980	Zoom-FFT.
1-1980	Luminance Contrast Measurement.
4-1979	Prepolarized Condenser Microphones for Measurement Purposes. Impulse Analysis using a Real-Time Digital Filter Analyzer.
3-1979	The Rationale of Dynamic Balancing by Vibration Measurements. Interfacing Level Recorder Type 2306 to a Digital Computer.
2-1979	Acoustic Emission.

Special technical literature

Brüel & Kjær publishes a variety of technical literature which can be obtained from your local Brüel & Kjær representative.
The following literature is presently available:

○ Mechanical Vibration and Shock Measurements (English), 2nd edition
○ Modal Analysis of Large Structures-Multiple Exciter Systems (English)
○ Acoustic Noise Measurements (English), 3rd edition
○ Architectural Acoustics (English)
○ Noise Control (English, French)
○ Frequency Analysis (English)
○ Electroacoustic Measurements (English, German, French, Spanish)
○ Catalogues (several languages)
○ Product Data Sheets (English, German, French, Russian)

Furthermore, back copies of the Technical Review can be supplied as shown in the list above. Older issues may be obtained provided they are still in stock.

Brüel & Kjær

DK-2850 Nærum · Denmark · Telephone: +45 2 80 05 00 · Telex: 37316 bruka dk · Fax.: 02 80 14 05

ISSN 007-2621

BV 0032-11

Printed in Denmark by Nærum Offset